

MOUNTAIN-PLAINS CONSORTIUM

MPC 19-372 | P. Dahal, M. Tazarv and N. Wehbe

Mechanical Bar Splices for
Accelerated Construction
of Bridge Columns



A University Transportation Center sponsored by the U.S. Department of Transportation serving the Mountain-Plains Region. Consortium members:

Colorado State University
North Dakota State University
South Dakota State University

University of Colorado Denver
University of Denver
University of Utah

Utah State University
University of Wyoming

Mechanical Bar Splices for Accelerated Construction of Bridge Columns

**Puskar Dahal
Mostafa Tazarv
Nadim Wehbe**

Department of Civil and Environmental Engineering
South Dakota State University
Brookings, South Dakota

February 2019

Acknowledgements

The work presented in this report conducted with support from South Dakota State University and the Mountain-Plains Consortium (MPC), a University Transportation Center (UTC) funded by the U.S. Department of Transportation. The contents of this paper reflect the views of the authors, who are responsible for the facts and accuracy of the information presented.

The project objectives could not be accomplished without the support of several industry partners. The authors are indebted to Bar Splice Company, Dayton Superior Corp., Dextra America, Erico International Corp., Epsilon Technology, Headed Reinforcement Corp., and Splice Sleeve North America for in-kind material donations and technical feedback throughout the entire project. The authors would like to thank Mr. Zach Gutzmer, manager of the Lohr Structures Laboratory, and graduate students Sandip Rimal, Abdullah Boudaqa, Heath Pederson, Abdullah Al Hashib, Lucas Bohn, and Zachary Carnahan for their efforts and input during this project.

Disclaimer

The contents of this report reflect the views of the authors, who are responsible for the facts and the accuracy of the information presented. This document is disseminated under the sponsorship of the Department of Transportation, University Transportation Centers Program, in the interest of information exchange. The U.S. Government assumes no liability for the contents or use thereof.

NDSU does not discriminate in its programs and activities on the basis of age, color, gender expression/identity, genetic information, marital status, national origin, participation in lawful off-campus activity, physical or mental disability, pregnancy, public assistance status, race, religion, sex, sexual orientation, spousal relationship to current employee, or veteran status, as applicable. Direct inquiries to: Vice Provost, Title IX/ADA Coordinator, Old Main 201, 701-231-7708, ndsueoaa@ndsu.edu.

ABSTRACT

Compared with conventional lap splicing, mechanical splicing is an alternative method of connecting bars in reinforced concrete (RC) structures, and is used mainly to reduce bar congestion in joints. Recently, mechanical bar splices, which are also referred to as bar couplers, have been used in laboratories as a new type of precast column connection to accelerate bridge construction. Nevertheless, current codes prohibit the use of bar couplers in the plastic hinge regions of bridge columns in high seismic zones. This may be due to a lack of systematic test data on the coupler performance, limited experimental studies on mechanically spliced bridge columns, and engineering precautions. The present experimental and analytical studies were performed to (1) generate the first-of-its-kind experimental database of the bar coupler performance, (2) quantify the coupler stress-strain relationship, and (3) quantify the seismic performance of mechanically spliced bridge columns. All U.S. manufacturers of mechanical bar splices were contacted to collect couplers that could potentially be incorporated into bridge columns. Ten different coupler products were selected, and more than 160 mechanical bar splices were tested under uniaxial monotonic and cyclic loading to failure. Properties of the couplers were established, and a coupler material model adopted from the literature was verified. Furthermore, a parametric study was carried out to investigate the seismic performance of mechanically spliced bridge columns utilizing the verified coupler models. More than 240 pushover analyses were performed. It was found that bridge columns incorporating couplers may exhibit 43% lower displacement ductility capacity compared with conventional RC columns, and the force capacity of these columns is slightly higher than that of the RC columns. Columns spliced with rigid and long couplers will show the lowest displacement capacities. Finally, new standard testing methods for mechanical bar splices were proposed based on the findings of the present study, and it was shown that consistent and reliable results could be achieved using the proposed testing methods.

TABLE OF CONTENTS

1. INTRODUCTION.....	1
1.1 Introduction.....	1
1.2 Objectives and Scope.....	1
1.3 Document Outline.....	1
2. LITERATURE REVIEW	2
2.1 Introduction.....	2
2.2 Mechanical Bar Splice Types	2
2.3 Mechanical versus Lap Splicing	3
2.4 Mechanical Bar Splices in Design Codes	3
2.4.1 Mechanical Bar Splices in Codes.....	3
2.4.2 Coupler Load Transfer Mechanism	4
2.5 Bar Splice Testing Methods and Results from Previous Studies.....	7
2.5.1 Testing Methods for Mechanical Bar Splices	7
2.5.2 Acceptance Criteria for Couplers.....	9
2.5.3 Past Studies	9
2.6 References.....	12
3. TEST MATRIX, TEST SETUP, AND LOADING PROTOCOLS FOR MECHANICAL BAR SPLICES.....	14
3.1 Introduction.....	14
3.2 Test Matrix for Mechanical Bar Splices	14
3.2.1 Selection of Coupler Test Specimens.....	14
3.2.2 Test Matrix.....	15
3.2.3 Test Specimen Nomenclature System.....	22
3.3 Test Setup for Mechanical Bar Splices	22
3.3.1 Instrumentation	24
3.4 Mechanical Bar Splice Preparation.....	25
3.5 Loading Protocols for Mechanical Bar Splices.....	29
3.5.1 Monotonic Loading.....	29
3.5.2 Cyclic Loading.....	29
3.6 References.....	30
4. RESULTS OF EXPERIMENTAL STUDIES ON MECHANICAL BAR SPLICES.....	32
4.1 Introduction.....	32
4.2 Coupler Monotonic Test Results	32
4.2.1 Headed Reinforcement Couplers	32
4.2.2 Threaded Couplers	34
4.2.3 Swaged Couplers.....	39
4.2.4 Grouted Sleeve Couplers.....	41
4.2.5 Hybrid Couplers.....	45
4.3 Summary of Coupler Monotonic Test Results.....	49
4.3.1 Measured Coupler Rigid Length Factors	50
4.3.2 Recommended Coupler Rigid Length Factors (β)	57
4.3.3 Coupler Material Model Verification.....	59
4.4 Coupler Cyclic Test Results.....	61
4.4.1 Headed Reinforcement Couplers	61

4.4.2 Threaded Couplers	63
4.4.3 Swaged Couplers.....	69
4.4.4 Grouted Sleeve Couplers.....	71
4.4.5 Hybrid Couplers.....	75
4.5 Summary of Coupler Cyclic Test Results.....	79
4.6 References.....	81
5. ANALYTICAL STUDY ON MECHANICALLY SPLICED BRIDGE COLUMNS.....	82
5.1 Introduction.....	82
5.2 Modeling Method for Mechanically Spliced Bridge Columns.....	82
5.2.1 Expected Mechanical Properties for Couplers.....	84
5.3 Parametric Study.....	85
5.3.1 Reference Conventional Reinforced Concrete Columns.....	85
5.3.2 Parameters of Mechanically Spliced Columns.....	86
5.4 Parametric Study Results	87
5.4.1 Low-Ductile Columns.....	87
5.4.2 Medium-Ductile Columns.....	91
5.4.3 High-Ductile Columns	95
5.4.4 Summary of Parametric Study	99
5.5 Summary	101
5.6 References.....	101
6. MECHANICAL BAR SPLICES FOR ACCELERATED CONSTRUCTION OF BRIDGE COLUMNS.....	102
6.1 Introduction.....	102
6.2 Proposed Acceptance Criteria for Mechanical Bar Splices	102
6.2.1 General Requirements.....	102
6.3 Proposed Material Model for Mechanical Bar Splices	103
6.4 Proposed Method of Testing for Mechanical Bar Splices	104
6.4.1 Scope.....	105
6.4.2 Referenced Documents	105
6.4.3 Apparatus	105
6.4.4 Definitions.....	105
6.4.5 Physical Properties and Preparation.....	106
6.4.6 Monotonic Test	107
6.4.7 Cyclic Test	111
6.4.8 Dynamic Test.....	111
6.4.9 Report.....	112
6.4.10 Hazards	112
6.4.11 Safety	112
6.5 Summary	112
6.6 References.....	112
6.7 Appendix.....	115
7. SUMMARY AND CONCLUSIONS.....	116
7.1 Summary.....	116
7.2 Conclusions.....	116
APPENDIX A. CALTRANS AUTHORIZED LIST OF COUPLERS.....	117

ABBREVIATIONS

AASHTO	American Association of State Highway and Transportation Officials
ASTM	American Society of Testing and Materials
ABC	Accelerated Bridge Construction
ACI	American Concrete Institute
DOT	Department of Transportation
ft	Feet
GS	Grouted Sleeve Coupler
HR	Headed Reinforcement Coupler
HY	Hybrid Coupler
in.	Inch
kip	1000 pounds
ksi	kip per square inch
SDSU	South Dakota State University
SH	Shear Screw Coupler
SW	Swaged Coupler
TH	Threaded Coupler

LIST OF TABLES

Table 2.1	Mechanical bar splices in design codes	4
Table 3.1	Selected couplers for uniaxial testing	15
Table 3.2	Test matrix for headed reinforcement couplers	16
Table 3.3	Test matrix for threaded couplers	17
Table 3.3	continued	18
Table 3.4	Test matrix for swaged couplers.....	19
Table 3.5	Test matrix for grouted sleeve couplers.....	20
Table 3.6	Test matrix for hybrid couplers	21
Table 4.1	Measured compressive strength for grout used in grouted sleeve couplers (NMB).....	43
Table 4.2	Measured compressive strength for grout used in grouted sleeve coupler (by Dayton).....	45
Table 4.3	Measured compressive strength for grout used in grouted-threaded hybrid couplers	49
Table 4.4	Measured coupler rigid length factors	51
Table 4.4	continued	52
Table 4.4	continued	53
Table 4.5	Coupler failure modes under monotonic loading.....	56
Table 4.6	Recommended coupler rigid length factors (β)	57
Table 4.7	Coupler failure modes under cyclic loading	80
Table 5.1	Modeling method for mechanically spliced bridge columns	83
Table 5.2	Coupler mechanical properties splicing ASTM A706 Grade 60 reinforcing steel bars	84
Table 5.3	RC column general design parameters	85
Table 5.4	RC column transverse reinforcement, drift ratio, and displacement ductility capacity	86
Table 5.5	Coupler products used in analytical study	87
Table 5.6	Summary of parametric study on mechanically spliced bridge columns.....	100

LIST OF FIGURES

Figure 2.1	Different mechanical bar splice products and types	2
Figure 2.2	Compression-only and tension-only mechanical bar splices	4
Figure 2.3	One sample of threaded couplers.....	5
Figure 2.4	One sample of headed reinforcement couplers.....	5
Figure 2.5	One sample of shear screw couplers.....	5
Figure 2.6	One sample of swaged couplers.....	6
Figure 2.7	Samples of grouted sleeve couplers.....	6
Figure 2.8	Samples of hybrid couplers	7
Figure 2.9	Mechanical splice low-cycle loading protocols according to ISO/DIS 15835 (2017)	9
Figure 2.10	Stress-strain model for mechanical bar splices (Tazarv and Saiidi, 2016).....	10
Figure 2.11	Different types of mechanical bar splices studies by Bompa and Elghazouli (2017).....	11
Figure 2.12	Typical stress-strain relationships for bar couplers (Bompa and Elghazouli, 2017)	11
Figure 2.13	Comparative performance of mechanical bar splices (Bompa and Elghazouli, 2017)	12
Figure 3.1	Coupler test specimen name guide	22
Figure 3.2	Test setup for mechanical bar splices	23
Figure 3.3	Geometry of unspliced and spliced test specimens.....	24
Figure 3.4	Extensometers used for unspliced and spliced specimens	25
Figure 3.5	Preparation of headed reinforcement couplers	26
Figure 3.6	Preparation of Dayton grouted sleeve couplers	26
Figure 3.7	Preparation of NMB grouted sleeve couplers.....	26
Figure 3.8	Preparation of Dextra Type-A threaded couplers	27
Figure 3.9	Preparation of Dextra Type-B threaded couplers	27
Figure 3.10	Preparation of Erico threaded couplers.....	27
Figure 3.11	Preparation of swaged couplers	28
Figure 3.12	Preparation of hybrid couplers (swaged and threaded).....	28
Figure 3.13	Preparation of hybrid couplers (threaded and grouted)	28
Figure 3.14	Target strains in cyclic testing of mechanical bar splices.....	30
Figure 3.15	Sample of cyclic loading history for mechanical bar splices.....	30
Figure 4.1	Monotonic test results for No. 5 (16-mm) headed reinforcement couplers	33
Figure 4.2	Monotonic test results for No. 8 (25-mm) headed reinforcement couplers	33

Figure 4.3	Monotonic test results for No. 10 (32-mm) headed reinforcement couplers	34
Figure 4.4	Monotonic test results for No. 5 (16-mm) threaded couplers (Type A)	35
Figure 4.5	Monotonic test results for No. 8 (24-mm) threaded couplers (Type A)	35
Figure 4.6	Monotonic test results for No. 10 (32-mm) threaded couplers (Type A)	36
Figure 4.7	Monotonic test results for No. 5 (16-mm) threaded couplers (Type B)	36
Figure 4.8	Monotonic test results for No. 8 (24-mm) threaded couplers (Type B)	37
Figure 4.9	Monotonic test results for No. 10 (32-mm) threaded couplers (Type B)	37
Figure 4.10	Monotonic test results for No. 5 (16-mm) tapered threaded couplers	38
Figure 4.11	Monotonic test results for No. 8 (25-mm) tapered threaded couplers	38
Figure 4.12	Monotonic test results for No. 10 (32-mm) tapered threaded couplers	39
Figure 4.13	Monotonic test results for No. 5 (16-mm) swaged couplers.....	40
Figure 4.14	Monotonic test results for No. 8 (24-mm) swaged couplers.....	40
Figure 4.15	Monotonic test results for No. 10 (32-mm) swaged couplers.....	41
Figure 4.16	Monotonic test results for No. 5 (16-mm) grouted sleeve couplers (NMB).....	42
Figure 4.17	Monotonic test results for No. 8 (25-mm) grouted sleeve couplers (NMB).....	42
Figure 4.18	Monotonic test results for No. 10 (32-mm) grouted sleeve couplers (NMB).....	43
Figure 4.19	Monotonic test results for No. 5 (16-mm) grouted sleeve couplers (Dayton Superior)	44
Figure 4.20	Monotonic test results for No. 8 (24-mm) grouted sleeve couplers (Dayton Superior)	44
Figure 4.21	Monotonic test results for No. 10 (32-mm) grouted sleeve couplers (Dayton Superior)	45
Figure 4.22	Monotonic test results for No. 5 (16-mm) threaded-swaged hybrid couplers	46
Figure 4.23	Monotonic test results for No. 8 (24-mm) threaded-swaged hybrid couplers	46
Figure 4.24	Monotonic test results for No. 10 (32-mm) threaded-swaged hybrid couplers	47
Figure 4.25	Monotonic test results for No. 5 (16-mm) grouted-threaded hybrid couplers	48
Figure 4.26	Monotonic test results for No. 8 (24-mm) grouted-threaded hybrid couplers	48
Figure 4.27	Monotonic test results for No. 10 (32-mm) grouted-threaded hybrid couplers	49
Figure 4.28	Calculation of coupler rigid length factor using measured strain data	50
Figure 4.29	Calculated and measured stress-strain relationships for No.10 (32-mm) couplers using different Beta	54
Figure 4.30	Calculated stress-strain relationships for spliced and unspliced No.10 (32-mm) ASTM A706 reinforcing steel bars.....	58
Figure 4.31	Calculated and measured stress-strain relationships for No.10 (32-mm) couplers using recommended Beta	60

Figure 4.32	Cyclic test results for No. 5 (16-mm) headed reinforcement couplers	62
Figure 4.33	Cyclic test results for No. 8 (24-mm) headed reinforcement couplers	62
Figure 4.34	Cyclic test results for No. 10 (32-mm) headed reinforcement couplers	62
Figure 4.35	Failure of headed reinforcement couplers under cyclic loading	63
Figure 4.36	Cyclic test results for No. 5 (16-mm) threaded couplers (Type A)	64
Figure 4.37	Cyclic test results for No. 8 (24-mm) threaded couplers (Type A)	64
Figure 4.38	Cyclic test results for No. 10 (32-mm) threaded couplers (Type A)	64
Figure 4.39	Failure of threaded couplers (Type A) under cyclic loading	65
Figure 4.40	Cyclic test results for No. 5 (16-mm) threaded couplers (Type B).....	66
Figure 4.41	Cyclic test results for No. 8 (24-mm) threaded couplers (Type B).....	66
Figure 4.42	Cyclic test results for No. 10 (32-mm) threaded couplers (Type B).....	66
Figure 4.43	Failure of threaded couplers (Type B) under cyclic loading	67
Figure 4.44	Cyclic test results for No. 5 (16-mm) tapered threaded couplers	68
Figure 4.45	Cyclic test results for No. 8 (24-mm) tapered threaded couplers	68
Figure 4.46	Cyclic test results for No. 10 (32-mm) tapered threaded couplers	68
Figure 4.47	Failure of tapered threaded couplers under cyclic loading	69
Figure 4.48	Cyclic test results for No. 5 (16-mm) swaged couplers.....	70
Figure 4.49	Cyclic test results for No. 8 (24-mm) swaged couplers.....	70
Figure 4.50	Cyclic test results for No. 10 (32-mm) swaged couplers.....	70
Figure 4.51	Failure of swaged couplers under cyclic loading.....	71
Figure 4.52	Cyclic test results for No. 5 (16-mm) grouted sleeve couplers (NMB).....	72
Figure 4.53	Cyclic test results for No. 8 (24-mm) grouted sleeve couplers (NMB).....	72
Figure 4.54	Cyclic test results for No. 10 (32-mm) grouted sleeve couplers (NMB).....	72
Figure 4.55	Failure of NMB grouted sleeve couplers under cyclic loading	73
Figure 4.56	Cyclic test results for No. 5 (16-mm) grouted sleeve couplers (Dayton Superior)	74
Figure 4.57	Cyclic test results for No. 8 (24-mm) grouted sleeve couplers (Dayton Superior)	74
Figure 4.58	Cyclic test results for No. 10 (32-mm) grouted sleeve couplers (Dayton Superior).....	74
Figure 4.59	Failure of grouted sleeve couplers (Dayton Superior) under cyclic loading	75
Figure 4.60	Cyclic test results for No. 5 (16-mm) threaded-swaged hybrid couplers	76
Figure 4.61	Cyclic test results for No. 8 (24-mm) threaded-swaged hybrid couplers	76
Figure 4.62	Cyclic test results for No. 10 (32-mm) threaded-swaged hybrid couplers	76

Figure 4.63	Failure of swaged-threaded hybrid couplers under cyclic loading	77
Figure 4.64	Cyclic test results for No. 5 (16-mm) grouted-threaded hybrid couplers	78
Figure 4.65	Cyclic test results for No. 8 (24-mm) grouted-threaded hybrid couplers	78
Figure 4.66	Cyclic test results for No. 10 (32-mm) grouted-threaded hybrid couplers	78
Figure 4.67	Failure of grouted-threaded hybrid couplers under cyclic loading.....	79
Figure 5.1	Analytical model details for columns with couplers at base.....	83
Figure 5.2	Coupler model parameters splicing ASTM A706 Grade 60 reinforcing steel bars	84
Figure 5.3	Pushover analysis results for AR4-ALI5-D3	88
Figure 5.4	Pushover analysis results for AR6-ALI5-D3	88
Figure 5.5	Pushover analysis results for AR8-ALI5-D3	88
Figure 5.6	Pushover analysis results for AR4-ALI10-D3	89
Figure 5.7	Pushover analysis results for AR6-ALI10-D3	89
Figure 5.8	Pushover analysis results for AR8-ALI10-D3	89
Figure 5.9	Pushover analysis results for AR4-ALI15-D3	90
Figure 5.10	Pushover analysis results for AR6-ALI15-D3	90
Figure 5.11	Pushover analysis results for AR8-ALI15-D3	90
Figure 5.12	Pushover analysis results for AR4-ALI5-D5	92
Figure 5.13	Pushover analysis results for AR6-ALI5-D5	92
Figure 5.14	Pushover analysis results for AR8-ALI5-D5	92
Figure 5.15	Pushover analysis results for AR4-ALI10-D5	93
Figure 5.16	Pushover analysis results for AR6-ALI10-D5	93
Figure 5.17	Pushover analysis results for AR8-ALI10-D5	93
Figure 5.18	Pushover analysis results for AR4-ALI15-D5	94
Figure 5.19	Pushover analysis results for AR6-ALI15-D5	94
Figure 5.20	Pushover analysis results for AR8-ALI15-D5	94
Figure 5.21	Pushover analysis results for AR4-ALI5-D7	96
Figure 5.22	Pushover analysis results for AR6-ALI5-D7	96
Figure 5.23	Pushover analysis results for AR8-ALI5-D7	96
Figure 5.24	Pushover analysis results for AR4-ALI10-D7	97
Figure 5.25	Pushover analysis results for AR6-ALI10-D7	97
Figure 5.26	Pushover analysis results for AR8-ALI10-D7	97

Figure 5.27	Pushover analysis results for AR4-ALI15-D7	98
Figure 5.28	Pushover analysis results for AR6-ALI15-D7	98
Figure 5.29	Pushover analysis results for AR8-ALI15-D7	98
Figure 6.1	Coupler and bar regions	103
Figure 6.2	Generic stress-strain model for mechanical bar splices (Tazarv and Saiidi, 2016)	104
Figure 6.3	Stress-strain relationships for mechanically spliced No. 10 (32 mm) bars	104
Figure 6.4	Coupler and bar regions	106
Figure 6.5	Test setup and minimum length requirements for unspliced and spliced specimens	108
Figure 6.6	Measured stress-strain relationships for unspliced and spliced specimens	109
Figure 6.7	Calculation of coupler rigid length factor based on stress-strain relationships	110
Figure 6.8	Different strain measuring devices for mechanical bar splices	115

EXECUTIVE SUMMARY

Introduction

In reinforced concrete structures, splicing of reinforcing bars is inevitable due to bar length limitations. The conventional method of splicing, lap splicing, is done by placing a sufficient length of connecting bars side-by-side and usually tying them with steel wires. An alternative method is the use of mechanical devices, which are commonly referred to as “mechanical bar splices” or “bar couplers.” Lap splicing has historically been the most common splice type. Nevertheless, the use of bar couplers is increasing since they reduce bar congestion and may result in a cost-competitive construction.

Accelerated bridge construction (ABC) is a new paradigm in the United States with an ultimate goal of faster bridge construction. ABC heavily relies on prefabricated bridge elements. However, the main challenge of ABC, especially in seismic regions, is how to connect precast elements with sufficient strength and deformability.

Objectives

The main objectives of the present study were to establish the behavior of mechanical bar splices suited for bridge columns, to generate an experimental database for seismic couplers, and to quantify the effect of such couplers on the seismic performance of bridge columns.

Literature Review

A literature review was conducted to identify knowledge gaps regarding bar couplers to be used in bridge columns. Available standard testing methods, coupler acceptance criteria for ductile members, and past experimental studies were reviewed. Table ES.1 presents the coupler type classification based on different design codes. It can be inferred that couplers cannot be used in the plastic hinge regions of ductile members in high seismic zones.

Tazarv and Saiidi (2016) proposed minimum requirements for mechanical bar splices to be incorporated in plastic hinge regions of bridge columns as the following:

1. The total length of a mechanical bar splice (L_{sp}) should not exceed $15d_b$ (d_b is the diameter of the smaller of the two spliced bars).
2. A spliced bar should fracture outside coupler regions regardless of the loading type (monolithic, cyclic, or dynamic). Only ASTM A706 reinforcement should be used in mechanically spliced bridge columns.

Figure ES.1 presents the coupler stress-strain model proposed by Tazarv and Saiidi (2016), which was adopted in the present study to establish the coupler behavior and to generate the experimental database. Couplers tend to reduce the strain capacity of the splice compared with that of the unspliced bar with minimal effect on the strength (if couplers are stronger than the splicing bars). Therefore, a shift in the stress-strain relationship can be assumed for a mechanically spliced bar, as shown in Figure ES.1b. The key parameter in this model is the “coupler rigid length factor, β ” in which a higher beta results in a lower strain capacity for the splice.

Table ES.1 Mechanical bar splices in design codes

Code	Splice Type	Stress Limit	Strain Limit	Max Slip	Location Restriction
AASHTO (2013 & 2011)	Full Mechanical Connection ^(a)	$\geq 1.25f_y$	None	No. 3-14: 0.01 in. No. 18: 0.03 in.	Shall not be used in plastic hinge of columns in SDC C and D (AASHTO SGS 2011, Article 8.8.3)
ACI 318 (2014)	Type 1	$\geq 1.25f_y$	None	None	Shall not be used in the plastic hinge of ductile members of special moment frames neither in longitudinal nor in transvers bars (Article 18.2.7)
	Type 2	$\geq 1.0f_u$	None	None	Shall not be used within one-half of the beam depth in special moment frames but are allowed in any other members at any location (Articles 18.2.7 & 25.5.7)
Caltrans SDC (2013)	Service	None	$> 2\%$	None	No splicing is allowed in "No-Splice Zone" of ductile members, which is the plastic hinge region. Ultimate splices are permitted outside of the "No-Splice Zone" for ductile members. Service splices are allowed in capacity protected members (Ch. 8)
	Ultimate	None	$> 9\%$ for No. 10 (32 mm) and smaller ^(b) $> 6\%$ for No. 11 (36 mm) and larger ^(b)	None	
Eurocode 8 (2004)	N.A.	None	None	None	Cannot be used if couplers are not covered by appropriate testing under conditions compatible with the selected ductility class (Sec. 5.6.3)
NZS 3101-1 (2006)	Mechanical Connections	\geq breaking strength of spliced reinforcing bar	None	At $0.95f_y$ bar stress, the coupler elongation should not exceed 1.1 times the unspliced bar elongation w/ the same length	Shall not be located within the beam/column joint regions, or within one effective depth of the member from the critical section. Shall be located within the middle quarter of columns (Sec. 8.9)

Note:

^a AASHTO LRFD (2013) Article 5.11.5.2.2.

^b For ASTM A706 Reinforcing Steel Bars. There is also a maximum strain demand limit (e.g., 2% for ultimate splices and 0.2% (the bar yield strain) for service splices) [Caltrans Memo to Designers 20-9].

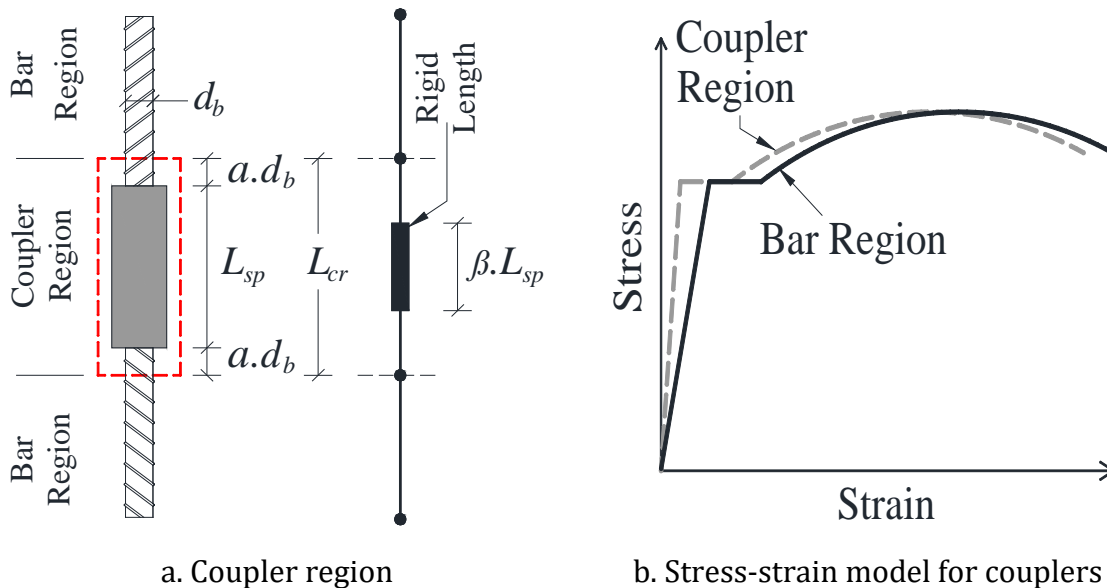


Figure ES.1 Stress-strain model for mechanical bar splices (Tazarv and Saiddi, 2016)

Experimental Programs

All U.S. coupler manufacturers were contacted, and based on the expected performance (Table ES.2) and availability, more than 270 coupler samples, including nine different products, were collected from six manufacturers. Subsequently, more than 160 of which were tested under uniaxial tensile monotonic and cyclic loading to failure in the Lohr Structures laboratory at South Dakota State University to determine their mechanical properties. A test matrix, test setup (Figure ES.2), and loading protocols were prepared before testing.

Table ES.2 Selected couplers for uniaxial testing

Coupler Type	Coupler Manufacturer	Coupler Model	ACI Coupler Types		Caltrans Coupler Types		AASHTO Coupler Type Full Mechanical Connection (FMC)
			Type 1	Type 2	Service Splice	Ultimate Splice	
Shear Screw Coupler	Erico International Corp.	LENTON® LOCK (B1 Series)		X		X	N.A.
Headed Bar Coupler	Headed Reinforcement Corp.	Xtender® 500/510 Standard Coupler		X		X	N.A.
Grouted Sleeve Coupler	Dayton Superior	D410 Sleeve-Lock® Grout Sleeve		X		X	X
	Splice Sleeve North America	NMB		X	X		N.A.
Threaded Coupler	Dextra America, Inc.	Bartec Standard Splice (type A)		X		X	N.A.
	Dextra America, Inc.	Bartec Position Splices (Type B)		X		X	N.A.
	Erico International Corp.	LENTON® PLUS, Standard Coupler, (A12)		X		X	X
Swaged Coupler	Bar Splice	BarGrip® XL		X		X	N.A.
Hybrid Coupler	Dextra America, Inc.	Griptec®		X		X	N.A.
	Erico International Corp.	Lenton Interlock		X	X		N.A.

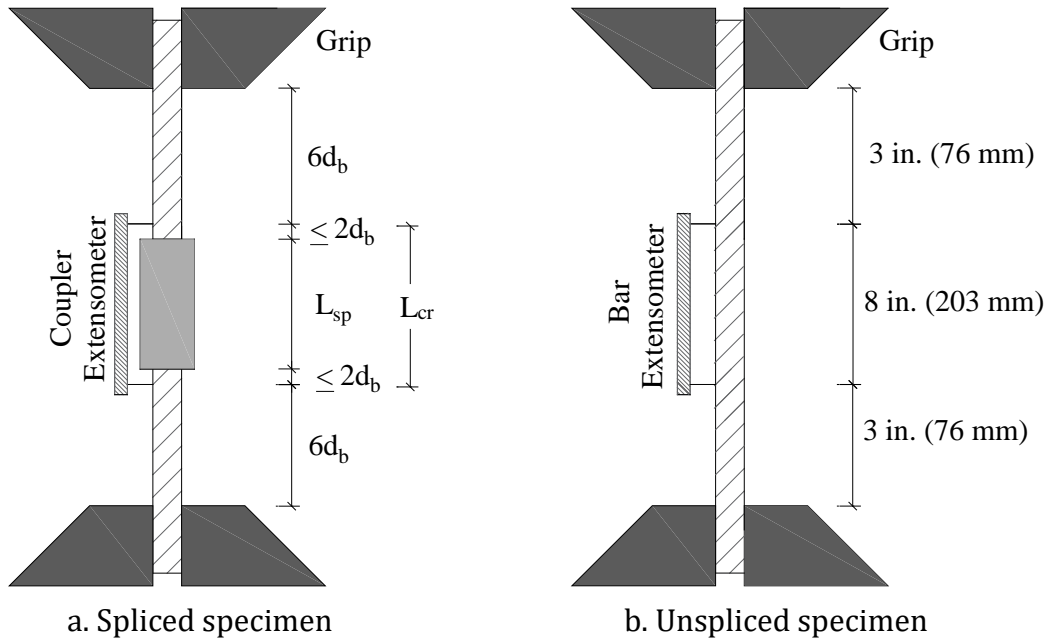
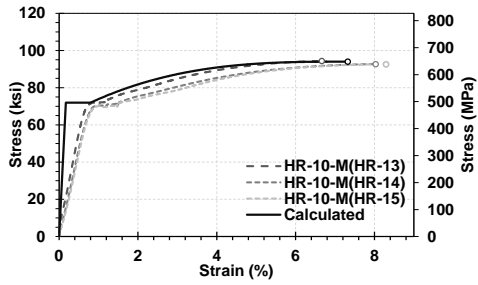


Figure ES.2 Geometry of spliced and unspliced specimens

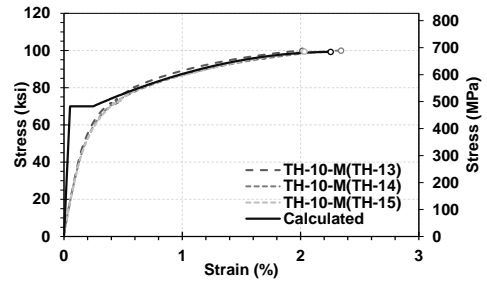
Results of Experimental Studies on Mechanical Bar Splices

The experimental results indicate that different couplers exhibit different stress-strain behavior depending on their size, type, and product. For example, Figure ES.3 shows the measured stress-strain relationships for nine different No. 10 (32-mm) couplers tested in the present study. Based on the monotonic test data for each coupler type, and using the coupler material model proposed by Tazarv and Saiidi (2016), the rigid length factors for different coupler types and sizes were proposed, as summarized in Table ES.3. These values were based on the average of three measured β_u rounded up to the nearest 0.05.

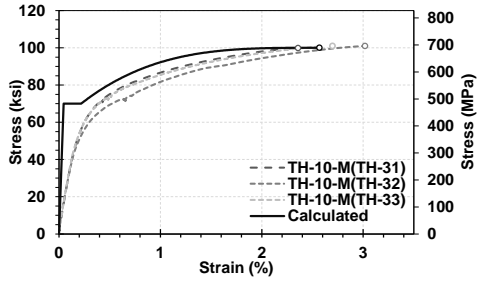
Figure ES. 3 also includes the calculated stress-strain relationships using the proposed coupler rigid length factor. It can be seen that the coupler material model can reasonably capture the actual behavior of different couplers using only one parameter, which is beta. The overestimation of the initial stiffness using this model is not necessarily a concern, especially when couplers are used in bridge columns. The coupler length is negligible with respect to the bridge column length, thus it will have minimal effects on the column initial stiffness. Furthermore, previous column test data showed that couplers mainly affect the displacement capacity of bridge columns. Therefore, a reliable material model for couplers should capture the ultimate strain of a coupler, which is achieved using Tazarv's model.



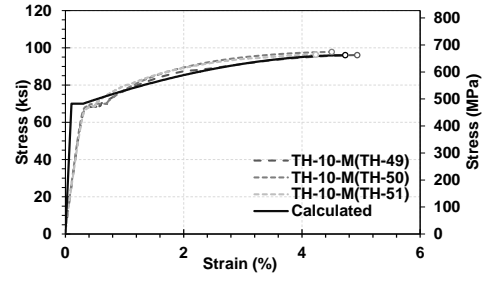
a. Headed Reinforcement



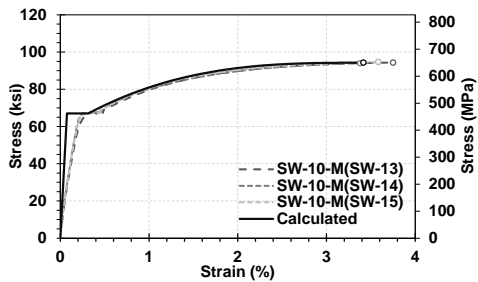
b. Threaded Type A by Dextra



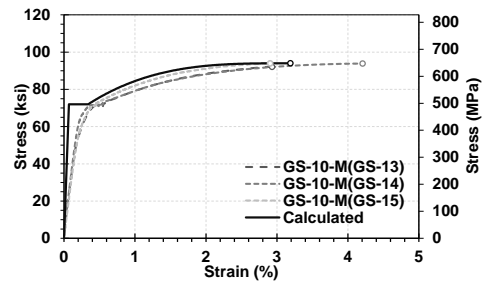
c. Threaded Type B by Dextra



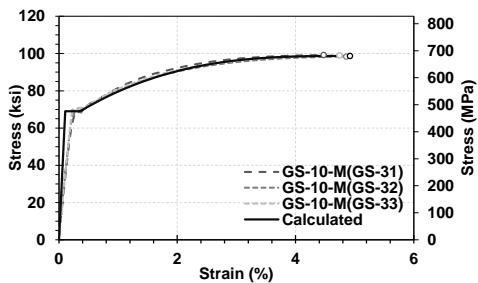
d. Taper Threaded Erico



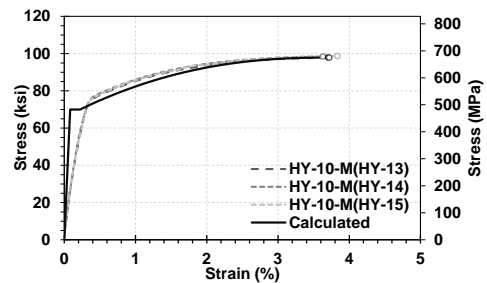
e. Swaged



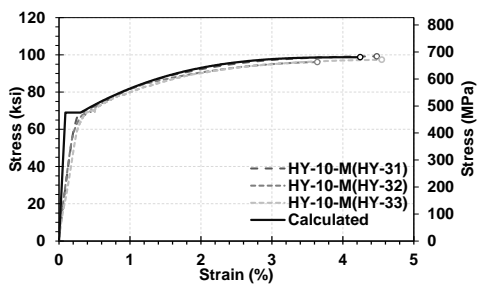
f. Grouted Sleeve by NMB



g. Grouted Sleeve by Dayton



h. Hybrid by Dextra



i. Hybrid by Erico

Figure ES.3 Measured and calculated stress-strain relationships for No.10 (32-mm) splices

Table ES.3 Recommended rigid length factors (β)

Coupler Type	No. 5 (16 mm)	No. 8 (24 mm)	No. 10 (32 mm)
Headed Reinforcement	0.80	0.75	0.55
Threaded (Dextra-Type A)	1.70	1.5	1.60
Threaded (Dextra-Type B)	1.60	1.5	1.65
Threaded (Erico)	0.95	1.10	1.05
Swaged	0.90	0.90	0.95
Grouted Sleeve (NMB)	0.95	0.65	0.85
Grouted Sleeve (Dayton)	0.70	0.70	0.65
Hybrid (Dextra)	0.80	0.90	0.85
Hybrid (Erico)	0.80	0.80	0.80

Tables ES.4 and ES.5, respectively, present a summary of the coupler failure modes tested under monotonic and cyclic loads. It can be inferred that all No. 8 (24-mm) and No. 10 (32-mm) couplers tested in the present study can be categorized as the seismic coupler. Nevertheless, No. 5 (16-mm) grouted sleeve couplers provided by the two manufacturers failed by the bar pullout, thus they are not seismic couplers. Furthermore, it can be concluded that different test regimes do not change the coupler performance since the couplers failed in a similar fashion under monotonic and cyclic loads.

Table ES.4 Coupler failure modes under monotonic loading

Coupler Type	Size	Failure Mode			Remarks
		Bar Fracture	Bar Pullout	Coupler Failure	
Headed Bar Coupler	No. 5 (16 mm)	XXX			Seismic Coupler
	No. 8 (24 mm)	XXX			Seismic Coupler
	No. 10 (32 mm)	XXX			Seismic Coupler
Swaged Coupler	No. 5 (16 mm)	XXX			Seismic Coupler
	No. 8 (24 mm)	XX		X	Seismic Coupler
	No. 10 (32 mm)	XXX			Seismic Coupler
Threaed Coupler (Type A)	No. 5 (16 mm)	XXX			Seismic Coupler
	No. 8 (24 mm)	XXX			Seismic Coupler
	No. 10 (32 mm)	XXX			Seismic Coupler
Threaed Coupler (Type B)	No. 5 (16 mm)	XXX			Seismic Coupler
	No. 8 (24 mm)	XXX			Seismic Coupler
	No. 10 (32 mm)	XXX			Seismic Coupler
Threaded Coupler (Taper)	No. 5 (16 mm)	XXX			Seismic Coupler
	No. 8 (24 mm)	XXX			Seismic Coupler
	No. 10 (32 mm)	XXX			Seismic Coupler
Grouted Coupler (NMB)	No. 5 (16 mm)		XXX		
	No. 8 (24 mm)	XXX			Seismic Coupler
	No. 10 (32 mm)	XXX			Seismic Coupler
Grouted Coupler (Dayton)	No. 5 (16 mm)	X	XX		
	No. 8 (24 mm)	XXX			Seismic Coupler
	No. 10 (32 mm)	XXX			Seismic Coupler
Hybrid Coupler (Thredad and Swaged)	No. 5 (16 mm)	XXX			Seismic Coupler
	No. 8 (24 mm)	XXX			Seismic Coupler
	No. 10 (32 mm)	XXX			Seismic Coupler
Hybrid Coupler (Grouted and Thredad)	No. 5 (16 mm)	XXX			Seismic Coupler
	No. 8 (24 mm)	XXX			Seismic Coupler
	No. 10 (32 mm)	XX		X	Seismic Coupler

X = one sample

Table ES.5 Coupler failure modes under cyclic loading

Coupler Type	Size	Failure Mode			Remarks
		Bar Fracture	Bar Pullout	Coupler Failure	
Headed Bar Coupler	No. 5 (16 mm)	XXX			Seismic Coupler
	No. 8 (24 mm)	XXX			Seismic Coupler
	No. 10 (32 mm)	XXX			Seismic Coupler
Swaged Coupler	No. 5 (16 mm)	XXX			Seismic Coupler
	No. 8 (24 mm)	XXX			Seismic Coupler
	No. 10 (32 mm)	XXX			Seismic Coupler
Threaded Coupler (Type A)	No. 5 (16 mm)	XXX			Seismic Coupler
	No. 8 (24 mm)	XXX			Seismic Coupler
	No. 10 (32 mm)	XXX			Seismic Coupler
Threaded Coupler (Type B)	No. 5 (16 mm)	XXX			Seismic Coupler
	No. 8 (24 mm)	XXX			Seismic Coupler
	No. 10 (32 mm)	XXX			Seismic Coupler
Threaded Coupler (Taper)	No. 5 (16 mm)	XXX			Seismic Coupler
	No. 8 (24 mm)	XXX			Seismic Coupler
	No. 10 (32 mm)	XXX			Seismic Coupler
Grouted Coupler (NMB)	No. 5 (16 mm)	X	XX		
	No. 8 (24 mm)	XXX			Seismic Coupler
	No. 10 (32 mm)	XXX			Seismic Coupler
Grouted Coupler (Dayton)	No. 5 (16 mm)		XXX		
	No. 8 (24 mm)	XXX			Seismic Coupler
	No. 10 (32 mm)	XXX			Seismic Coupler
Hybrid Coupler (Threaded and Swaged)	No. 5 (16 mm)	XXX			Seismic Coupler
	No. 8 (24 mm)	XXX			Seismic Coupler
	No. 10 (32 mm)	XXX			Seismic Coupler
Hybrid Coupler (Grouted and Threaded)	No. 5 (16 mm)	XXX			Seismic Coupler
	No. 8 (24 mm)	XXX			Seismic Coupler
	No. 10 (32 mm)	XX		X	Seismic Coupler

X = one sample

Analytical Study on Mechanically Spliced Bridge Columns

A parametric study was carried out to investigate the seismic performance of bridge columns incorporating different mechanical bar splices. More than 240 pushover analyses were performed on 27 bridge columns spliced with eight different coupler products. Table ES.6 presents a summary of all analyses, Figure ES.4 illustrates the analytical model, and Figure ES.5 shows sample pushover relationships for mechanically spliced bridge columns.

The parametric study showed that the size, type, and length of couplers can significantly affect the ductility of bridge columns. Longer couplers and couplers with higher “rigid length factors” may reduce the column displacement ductility capacity by 43%. Furthermore, it was found that the lateral load carrying capacity of mechanically spliced bridge columns is slightly higher than that for conventional unspliced columns (but no more than 10%).

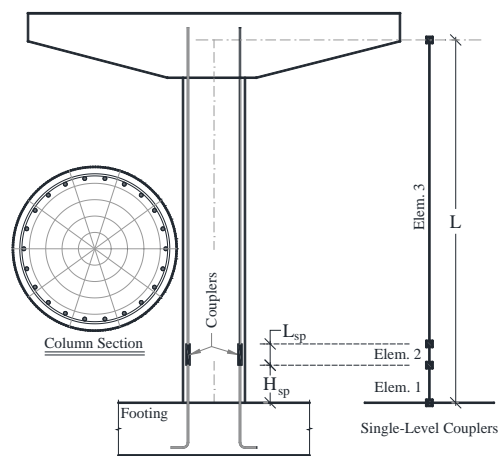
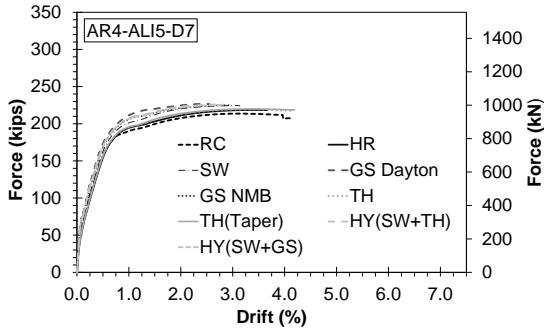
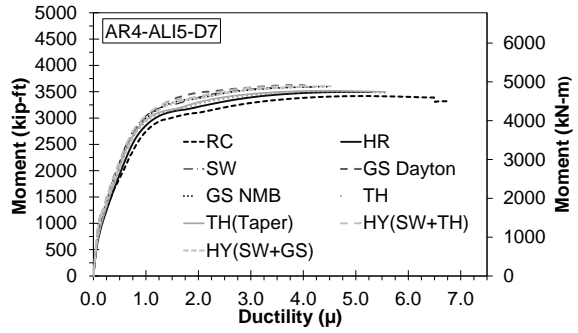


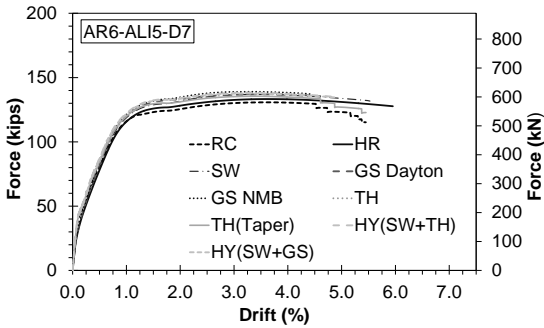
Figure ES.4 Analytical model details for columns with couplers at base



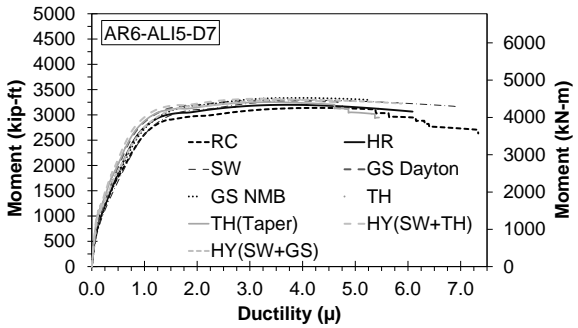
a. Force-drift relationship for AR=4, ALI=5%, & D=7



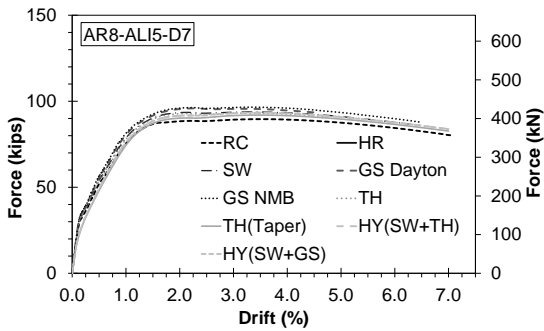
b. Moment-ductility relationship for AR=4, ALI=5%, & D=7



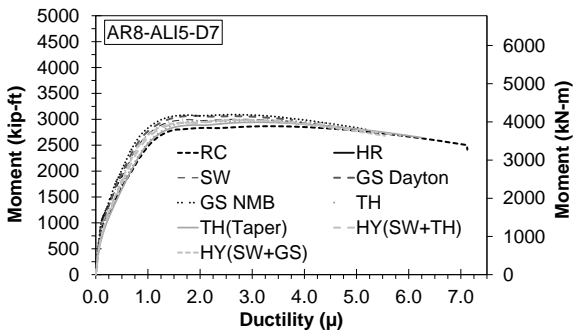
c. Force-drift relationship for AR=6, ALI=5%, & D=7



d. Moment-ductility relationship for AR=6, ALI=5%, & D=7



e. Force-drift relationship for AR=8, ALI=5%, & D=7



f. Moment-ductility relationship for AR=8, ALI=5%, & D=7

Figure ES.5 Pushover relationships for mechanically spliced bridge columns

Table ES.6 Summary of parametric study on mechanically spliced bridge columns

Column ID	Ductility (Ductility Reduction Compared to RC in %)								
	RC	HR $L_{sp} = 3.88$ in. $\beta = 0.55$	TH $L_{sp} = 3.06$ in. $\beta = 1.65$	TH-Taper $L_{sp} = 4.20$ in. $\beta = 1.05$	SW $L_{sp} = 9.50$ in. $\beta = 0.95$	GS-NMB $L_{sp} = 18$ in. $\beta = 0.85$	GS-Dayton $L_{sp} = 18$ in. $\beta = 0.65$	HY-Dextra $L_{sp} = 10.63$ in. $\beta = 0.85$	HY-Erico $L_{sp} = 10.75$ in. $\beta = 0.80$
AR4-ALI5-D3	3.0	2.8 (7.6)	2.6 (15.0)	2.5 (16.9)	2.4 (19.9)	2.6 (14.0)	2.6 (6.6)	2.5 (15.6)	2.6 (14.0)
AR4-ALI5-D5	4.9	4.9 (0.2)	4.4 (10.8)	4.2 (14.6)	4.0 (18.2)	3.2 (36.0)	3.4 (30.4)	4.5 (8.5)	4.5 (8.7)
AR4-ALI5-D7	7.0	5.3 (24.8)	6.2 (12.2)	5.6 (21.1)	4.2 (40.7)	4.5 (36.4)	4.0 (42.8)	4.1 (41.4)	4.5 (35.7)
AR4-ALI10-D3	2.9	2.9 (1.0)	2.5 (13.7)	2.5 (16.1)	2.3 (21.6)	2.7 (6.2)	2.7 (6.2)	2.5 (13.7)	2.6 (11.3)
AR4-ALI10-D5	5.0	5.0 (0.0)	4.5 (10.7)	4.4 (12.3)	3.8 (24.7)	3.9 (20.9)	4.0 (20.1)	2.6 (47.6)	4.0 (19.9)
AR4-ALI10-D7	6.9	5.8 (16.4)	6.3 (9.0)	5.6 (18.6)	4.3 (38.3)	4.1 (41.3)	4.6 (33.4)	4.4 (35.8)	4.6 (34.0)
AR4-ALI15-D3	3.0	2.9 (4.0)	2.7 (11.7)	2.6 (13.3)	2.6 (15.0)	2.6 (14.3)	2.7 (11.7)	2.9 (4.7)	2.9 (4.3)
AR4-ALI15-D5	5.0	4.9 (2.1)	4.6 (9.5)	4.5 (10.3)	4.6 (8.5)	3.2 (37.1)	3.7 (26.6)	3.9 (23.4)	3.9 (22.8)
AR4-ALI15-D7	7.1	6.0 (16.3)	5.0 (29.8)	6.7 (5.5)	5.1 (28.1)	4.6 (34.9)	4.9 (30.9)	4.1 (42.1)	5.3 (25.5)
AR6-ALI5-D3	3.1	2.9 (8.5)	2.6 (15.3)	2.6 (17.8)	2.4 (22.3)	2.6 (16.9)	2.8 (10.1)	2.6 (18.2)	2.6 (18.2)
AR6-ALI5-D5	5.1	4.9 (4.5)	4.5 (11.9)	4.3 (17.0)	4.1 (19.9)	3.7 (28.1)	5.0 (3.3)	4.2 (17.2)	4.4 (14.3)
AR6-ALI5-D7	7.3	6.5 (11.6)	4.8 (34.7)	6.2 (15.8)	5.0 (31.8)	4.3 (41.2)	4.8 (34.7)	4.7 (35.5)	5.1 (31.0)
AR6-ALI10-D3	3.3	2.8 (14.0)	2.6 (21.9)	2.5 (24.0)	2.3 (29.2)	2.5 (22.8)	2.8 (16.4)	2.5 (24.3)	2.5 (22.8)
AR6-ALI10-D5	5.1	4.9 (3.7)	4.3 (14.4)	4.2 (16.9)	4.0 (20.7)	4.7 (7.8)	4.5 (10.2)	4.5 (11.6)	4.7 (8.0)
AR6-ALI10-D7	6.7	6.3 (6.1)	5.8 (14.3)	5.6 (16.8)	5.4 (20.2)	4.9 (26.9)	4.8 (28.1)	5.2 (23.0)	4.7 (29.6)
AR6-ALI15-D3	2.9	2.8 (3.1)	2.6 (9.6)	2.6 (12.7)	2.4 (17.1)	2.6 (10.3)	2.9 (2.1)	2.6 (12.7)	2.6 (10.6)
AR6-ALI15-D5	4.9	4.8 (2.2)	4.3 (11.8)	4.3 (13.4)	4.6 (6.3)	4.3 (13.4)	4.0 (17.7)	4.6 (7.1)	4.7 (4.5)
AR6-ALI15-D7	6.6	6.4 (1.7)	6.0 (8.2)	5.9 (10.2)	5.9 (10.7)	5.4 (18.3)	4.3 (34.5)	6.0 (8.4)	6.0 (8.1)
AR8-ALI5-D3	3.0	2.8 (7.9)	2.6 (14.5)	2.5 (17.5)	2.4 (22.4)	2.5 (19.1)	2.7 (10.9)	2.5 (18.2)	2.5 (18.2)
AR8-ALI5-D5	5.1	4.5 (11.9)	5.3 (-2.7)	5.1 (0.8)	3.8 (26.0)	4.5 (11.7)	4.3 (16.4)	5.2 (-1.0)	3.5 (32.3)
AR8-ALI5-D7	7.1	4.3 (40.2)	6.1 (14.5)	6.3 (12.2)	5.3 (26.1)	5.2 (27.4)	5.0 (30.2)	5.8 (18.0)	5.5 (22.2)
AR8-ALI10-D3	3.1	2.8 (8.7)	2.6 (17.1)	2.5 (19.7)	2.6 (15.8)	2.6 (17.7)	2.8 (11.3)	2.5 (19.7)	2.5 (18.1)
AR8-ALI10-D5	5.2	4.5 (12.8)	4.2 (19.0)	4.3 (17.3)	4.4 (15.3)	4.1 (19.6)	4.3 (17.1)	4.1 (19.6)	4.0 (22.1)
AR8-ALI10-D7	7.0	4.8 (31.2)	4.6 (35.2)	4.4 (36.9)	4.5 (35.3)	4.6 (35.2)	4.5 (35.3)	4.7 (33.0)	4.6 (34.6)
AR8-ALI15-D3	3.1	2.9 (6.2)	2.6 (18.3)	2.5 (20.8)	2.4 (25.0)	2.5 (20.2)	2.9 (6.2)	2.5 (20.5)	2.6 (18.6)
AR8-ALI15-D5	5.1	3.8 (25.0)	3.5 (30.5)	3.4 (32.9)	3.3 (35.8)	3.4 (32.5)	3.5 (30.5)	3.4 (33.5)	3.4 (32.5)
AR8-ALI15-D7	6.0	3.9 (35.4)	3.6 (40.1)	3.6 (40.7)	3.5 (42.4)	3.5 (42.7)	3.7 (38.9)	3.5 (42.7)	3.5 (41.9)

Note: "AR" refers to the aspect ratio, "ALI" refers to the column axial load index, "D" refers to the displacement ductility capacity, "RC" refers to the reference columns, "HR" refers to the headed reinforcement couplers, " L_{sp} " is the coupler length, " β " is the coupler rigid length factor, "TH" refers to the threaded couplers, "SW" refers to the swaged couplers, "GS" refers to the grouted couplers, and "HY" refers to the hybrid couplers; 1 in. = 25.4 mm.

Proposed Method of Testing for Mechanical Bar Splices

Mechanical bar splices can be incorporated in bridge columns to accelerate construction. For ABC, couplers most likely will be used at the ends of the precast columns either inside the column or in the column adjoining member. In either case, couplers might affect the column seismic performance by mainly reducing the displacement capacity. Not all mechanical bar splices can be used in bridge columns because they may prematurely fail. The current design codes ban the use of couplers in plastic hinge regions. Nevertheless, establishing a standard testing method for couplers, providing acceptance criteria for couplers, and quantifying coupler effects on the column behavior may relax this ban and may allow deployment of mechanically spliced precast columns in high seismic regions.

Based on the findings of the experimental and analytical studies and the literature, acceptance criteria, a material model, and standard testing methods for mechanical bar splices were proposed to facilitate the use of couplers in bridge columns. The proposed standard includes monotonic, cyclic, and dynamic testing procedures. The proposed testing methods can be used for spliced bars conforming to either ASTM A706 or ASTM A615.

Conclusions

The following conclusions can be drawn based on the experimental and analytical studies:

- The test data showed that the coupler length, size, and type significantly affect the coupler performance. The general trend was that longer couplers exhibited lower strain capacities compared with shorter couplers. Couplers with higher rigid length factors showed the lowest strain capacities.
- The coupler acceptance criteria and the coupler stress-strain model proposed by Tazarv and Saiidi (2016) were found viable to identify couplers that are suited for bridge columns. These couplers were labeled as “seismic couplers.”
- The test data showed that monotonic testing is sufficient to establish a coupler behavior using only one parameter, “coupler rigid length factor.” No significant change was seen in the behavior of couplers under monotonic and cyclic loads. Nevertheless, cyclic loading is needed to verify the coupler performance under simulated seismic actions.
- Consistent results can be achieved using the proposed standard testing method for couplers.
- The parametric study showed that the size, type, and length of couplers can significantly affect the ductility of bridge columns. Longer couplers and couplers with higher “rigid length factors” may reduce the column displacement ductility capacity by 43%.
- The analytical study showed that the lateral load carrying capacity of mechanically spliced bridge columns are slightly higher than that for conventional RC columns (no more than 10%).

1. INTRODUCTION

1.1 Introduction

In reinforced concrete structures, splicing of reinforcing steel bars is inevitable due to bar length limitations. The conventional method of splicing, lap splicing, is done by placing a sufficient length of connecting bars side-by-side and usually tying them with steel wires. An alternative method is the use of mechanical devices, which are commonly referred to as “mechanical bar splices” or “bar couplers.” Lap splicing has historically been the most common splice type. Nevertheless, the use of bar couplers is increasing since they reduce bar congestion and may result in a cost-competitive construction.

Accelerated bridge construction (ABC) is a new paradigm in the United States with an ultimate goal of faster bridge construction. ABC heavily relies on prefabricated bridge elements. However, the main challenge of ABC, especially in seismic regions, is how to connect precast elements with sufficient strength and deformability.

Even though a few ABC column connections have been developed and proof tested in laboratories, the use of precast bridge columns incorporating mechanical bar splices are rare in actual bridges. This is because (1) current codes prohibit the use of bar couplers in plastic hinge regions of bridge columns; (2) there is a lack of unified standard testing methods, acceptance criteria, and material models for couplers; (3) there is no systematic experimental work in which the behavior of different coupler types and sizes was established and compared; and (4) there are a few studies on the seismic performance of mechanically spliced bridge bridges.

1.2 Objectives and Scope

The main objectives of the present study were to establish the behavior of mechanical bars splices suited for bridge columns, to generate an experimental database for such couplers, and to quantify the effect of such couplers on the seismic performance of bridge columns.

To achieve these objectives, the following experimental and analytical programs were completed: (1) all U.S. mechanical bar coupler manufacturers were contacted to collect test samples; (2) a test matrix, a setup, and loading protocols were prepared; (3) more than 160 bar couplers were tested under unified monotonic and cyclic loading to failure; (4) a comprehensive database of coupler behavior was established; and (5) more than 240 pushover analyses were carried out to quantify the effect of bar couplers on the seismic performance of bridge columns.

1.3 Document Outline

Section 1 presents an introduction of the study and the scope of the work done. A literature review on mechanical bar splices was conducted, and a summary is presented in Section 2. Section 3 discusses the experimental program (including the test setup, loading protocols, and instrumentation plans) executed in this study on three sizes of nine different mechanical bar splices. Section 4 presents the results of the bar coupler experimental study, including monotonic and cyclic tests. Furthermore, coupler properties were established, and a coupler material model adopted from the literature was verified in this section. The results of an analytical study on the seismic performance of mechanically spliced bridge columns are presented in Section 5. A standard testing method was developed for bar couplers, which is presented in Section 6. Finally, the summary and conclusions of the study are presented in Section 7.

2. LITERATURE REVIEW

2.1 Introduction

The process of transferring the load from one reinforcing bar to other in concrete structures may be done through lap splicing or using mechanical devices. The main advantages of utilizing mechanical bar splices, which are commonly referred to as bar couplers, are to reduce bar congestion and to minimize the splice length. Furthermore, mechanical bar splicing is a better alternative to lap splicing, which is more susceptible to splitting failure in flexural members (Hurd, 1998).

Mechanical bar splices are the focus of this section, which includes a review of different coupler types, couplers in the U.S. codes, and past studies on couplers.

2.2 Mechanical Bar Splice Types

Figure 2.1 shows nine different products of tension-compression mechanical bar splices. Other products, such as shear-screw couplers, are also available but not shown in the figure. Based on the anchoring mechanism, couplers can be categorized in six general types: threaded, headed, swaged, grouted, shear-screw, and hybrid (combination of two types). Note different manufacturers produce these coupler types with different commercial names and usually with minor differences in size and detailing. However, the load-transfer mechanism of any tension-compression coupler is through one of these six types.



Figure 2.1 Different mechanical bar splice products and types

In threaded couplers, bar ends are threaded and are connected through a long nut. Bar ends are headed in headed couplers and then are connected using a male-female threaded connection locking the heads in-place. Steel bars and a steel sleeve are pressed together using a hydraulic jack to anchor bars in a swaged coupler. In grouted couplers, bars are inserted in a steel sleeve and then a high-strength grout is poured to complete the connection through bond. Bars are connected to a steel sleeve using screws in a shear screw

coupler. Finally, a hybrid coupler connects bars through at least two of the above mentioned mechanisms. More discussion on the coupler types can be found in Section 2.4.2.

2.3 Mechanical versus Lap Splicing

The performance of a mechanical bar splice mostly depends on the configuration and performance of the splice itself while a lap splice entirely depends on the bond strength between concrete and steel to transfer loads. Some advantages of mechanical splicing compared with lap splicing can be summarized as:

- **Strength:** Mechanical splices can fully develop bars to their fracture.
- **Congestion:** Mechanical splices reduce bar congestion especially at the joints.
- **Economic:** Mechanical splices may reduce the cost since a lower amount of steel is used.
- **Time:** Mechanical splices may reduce engineering design time since development length calculations may not be needed.

2.4 Mechanical Bar Splices in Design Codes

Mechanical bar splices are usually classified in design codes based on their performance and the strength they can develop. The definition and requirements of couplers in five design codes are summarized herein.

2.4.1 Mechanical Bar Splices in Codes

Table 2.1 presents a summary of five different code requirements on mechanical bar splices. ACI 318 (2014) classifies bar couplers as either Type 1 or Type 2. This classification is based on the strength that the coupler can develop. For example, a coupler that can withstand more than 1.25 times the yield strength is Type 1. Caltrans SDC (2013) allows “service” and “ultimate” couplers, which are classified based on their strain capacity. AASHTO LRFD (2014) only allows couplers that can develop a minimum strength of 1.25 times the yield strength of the bar. Even though couplers are generally allowed, current bridge and building design codes prohibit the use of mechanical bar splices in the plastic hinge regions of ductile members in high seismic regions (Table 2.1).

Table 2.1 Mechanical bar splices in design codes

Code	Splice Type	Stress Limit	Strain Limit	Max Slip	Location Restriction
AASHTO (2013 & 2011)	Full Mechanical Connection ^(a)	$\geq 1.25f_y$	None	No. 3-14: 0.01 in. No. 18: 0.03 in.	Shall not be used in plastic hinge of columns in SDC C and D (AASHTO SGS 2011, Article 8.8.3)
ACI 318 (2014)	Type 1	$\geq 1.25f_y$	None	None	Shall not be used in the plastic hinge of ductile members of special moment frames neither in longitudinal nor in transverse bars (Article 18.2.7)
	Type 2	$\geq 1.0f_u$	None	None	Shall not be used within one-half of the beam depth in special moment frames but are allowed in any other members at any location (Articles 18.2.7 & 25.5.7)
Caltrans SDC (2013)	Service	None	> 2%	None	No splicing is allowed in “No-Splice Zone” of ductile members, which is the plastic hinge region. Ultimate splices are permitted outside of the “No-Splice Zone” for ductile members. Service splices are allowed in capacity protected members (Ch. 8)
	Ultimate	None	> 9% for No. 10 (32 mm) and smaller ^(b) > 6% for No. 11 (36 mm) and larger ^(b)	None	
Eurocode 8 (2004)	N.A.	None	None	None	Cannot be used if couplers are not covered by appropriate testing under conditions compatible with the selected ductility class (Sec. 5.6.3)
NZS 3101-1 (2006)	Mechanical Connections	\geq breaking strength of spliced reinforcing bar	None	At $0.95f_y$ bar stress, the coupler elongation should not exceed 1.1 times the unspliced bar elongation w/ the same length	Shall not be located within the beam/column joint regions, or within one effective depth of the member from the critical section. Shall be located within the middle quarter of columns (Sec. 8.9)

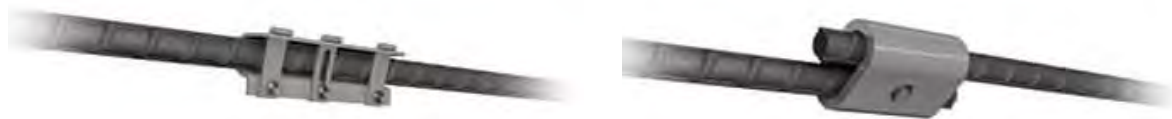
Note:

(a) AASHTO LRFD (2013) Article 5.11.5.2.2.

(b) For ASTM A706 Reinforcing Steel Bars. There is also a maximum strain demand limit (e.g., 2% for ultimate splices and 0.2% (the bar yield strain) for service splices) [Caltrans Memo to Designers 20-9].

2.4.2 Coupler Load Transfer Mechanism

Couplers were categorized based on their anchoring mechanism and also their performance in the previous sections. In addition to these variations, some couplers resist only compressive loads (Figure 2.2a), some resist only tensile loads (Figure 2.2b), and some can withstand both compressive and tensile loads (all couplers in Figure 2.1). Since couplers suitable for bridge columns are the focus of this study, the load transfer mechanism of tension-compression couplers is discussed in this section.



a) Compression coupler
(source: www.theconstructor.org)

b) Tension coupler
(source: www.theconstructor.org)

Figure 2.2 Compression-only and tension-only mechanical bar splices

2.4.2.1 Threaded Couplers

Figure 2.3 shows one sample of the threaded couplers in which bar ends are threaded and are engaged with the coupler internal threads to complete the splice. Threads can have different orientations and lengths. For example, regular threaded couplers have straight threads (running parallel). However, tapered threaded couplers have non-parallel threads in which bar diameter is reduced from the coupler ends toward the middle of the coupler. In some products, bar ends may be forged to be bigger in diameter; thus, after threading, the ends are not the weak link. Threaded couplers can be used in new construction or in the repair of reinforced concrete structures.



Figure 2.3 One sample of threaded couplers

2.4.2.2 Headed Reinforcement Couplers

Figure 2.4 shows one sample of the headed couplers, which consists of male and female components with threads on the male component to be fit in the internal threads of the female component. Bar ends are headed using a hydraulic jack. Headed reinforcement couplers can be used in new construction or in the repair of reinforced concrete structures.



Figure 2.4 One sample of headed reinforcement couplers

2.4.2.3 Shear-Screw Couplers

Figure 2.5 shows one example of shear-screw couplers in which bars are connected to the steel sleeve using screws. Since these couplers do not need bar end preparation, they can be installed quickly using simple tools. These couplers are usually used in new construction due to their large sizes. However, Yang et al. (2014) used these couplers in an experimental study to replace column fractured longitudinal bars with new ones.



(source: www.bar-us.com)

Figure 2.5 One sample of shear screw couplers

2.4.2.4 Swaged Couplers

Figure 2.6 shows a swaged coupler (prior to assembly), which consists of a seamless steel sleeve that is pressed to the splicing bars to provide mechanical interlock. Similar to shear-screw couplers, these couplers are usually used in new construction due to their large sizes. Nevertheless, Yang et al. (2014) used these couplers to replace fractured longitudinal bars of a bridge column.



Figure 2.6 One sample of swaged couplers

2.4.2.5 Grouted Sleeve Couplers

Grouted sleeve couplers are made of grout filled steel sleeves to connect bars through bond (Figure 2.7). Grouted sleeve couplers are usually used in precast structures to connect precast elements.



a. Grouted sleeve coupler by Dayton Superior



b. Grouted sleeve coupler by NMB

Figure 2.7 Samples of grouted sleeve couplers

2.4.2.6 Hybrid Couplers

Couplers that simultaneously use at least two of the above mentioned anchoring mechanisms are categorized as hybrid couplers. Figure 2.8 shows two samples of hybrid couplers: threaded-grouted (thread on one end of the coupler, grouted sleeve on another end), and threaded-swaged (two swaged pieces connected at the middle using a threaded mechanism).



a. Threaded-grouted hybrid coupler



b. Threaded-swaged hybrid coupler

Figure 2.8 Samples of hybrid couplers

2.5 Bar Splice Testing Methods and Results from Previous Studies

A summary of standard testing methods for mechanical bar splices, coupler acceptance criteria for ductile members, and a review of past experimental studies on couplers are presented in this section.

2.5.1 Testing Methods for Mechanical Bar Splices

Three testing standards are currently available for mechanical bar splices: ASTM A1034 (2016), California Test 670 (2004), and ISO/DIS 15835 (2009). The following sections discuss the testing methods specified in these standards.

2.5.1.1 ASTM A1034 (2016)

ASTM A1034 (2016) includes testing procedures for monotonic, full cyclic, high-cycle fatigue, slip, differential elongation, and low temperature tests. Nevertheless, this ASTM standard does not offer any acceptance criteria for couplers. A summary of coupler monotonic and cyclic testing is presented herein.

2.5.1.1.1 Monotonic Tensile Testing

This test measures the performance of mechanical bar splices under increasing tensile loads. A specimen is placed in a testing machine and pulled to failure.

2.5.1.1.2 Full-Cycle Testing

This test is used to investigate how mechanical bar splices perform under alternating tensile and compressive loads. A specimen is placed in a testing machine and loaded in tension, then in compression, and loaded again in tension until a specified number of cycles is reached. Each cycle may exceed the yield strain of the bar and is intended to simulate the demands of earthquake loading on the specimen.

2.5.1.2 California Test 670 (2004)

California Test 670 (2004) includes testing procedures for slip, tensile, cyclic, and fatigue tests. Similar to the ASTM standard, this standard does not specify any acceptance criteria for couplers. Coupler monotonic tensile and cyclic testing procedures according to this standard are briefly discussed in this section.

2.5.1.2.1 Monotonic Tensile Testing

Monotonic tensile testing must be performed in accordance with ASTM A370 Section 13 and A9:

- a. Apply an axial tensile load to the sample sufficient to cause failure.
- b. Document the maximum load obtained.
- c. Calculate the ultimate tensile strength by dividing the maximum load by the sample's nominal cross-sectional area. Record the ultimate tensile strength on the Test Form.
- d. Check for necking.

2.5.1.2.2 Cyclic Testing

- a. Cyclically load the sample from 5% to 90% of the specified yield strength (f_y) of the sample for 100 cycles. Use a haversine waveform at 0.5 cps for No. 10 (32-mm) bars and larger, and a haversine waveform at 0.7 cps for smaller bars. Record whether or not the sample fractures.
- b. If sample does not fracture during the cyclic test, increase the axial tensile load until the sample fractures.
- c. On the Test Form, record whether the sample passed the cyclical testing and, if applicable, the ultimate tensile strength, location of failure, and any necking.

2.5.1.3 ISO/DIS 15835 (2017)

International Organization for Standardization (ISO) specifies testing procedures for tensile, slip, high-cycle fatigue, and low-cycle reverse loading. Similar to other documents, this standard does not offer any acceptance criteria for couplers. A summary of coupler tensile and fatigue tests is presented.

2.5.1.3.1 Tensile Testing

The testing equipment and the testing procedure shall conform to ISO 15630-1. The A_g in the spliced bar shall be measured according to ISO 15630-1 outside the length of the mechanical splice (as defined in ISO 15835-1) on both sides of the connection.

2.5.1.3.2 Fatigue Testing

The high-cycle fatigue test measures the performance of mechanical bar splices under sinusoidal waveform tensile loads. The test piece shall be gripped in the testing equipment in such a way that the force is transmitted axially and, as much as possible, free of any bending moment on the whole test piece. The frequency of load cycles shall be constant during the test and also during the test series. The frequency shall be between 1 Hz to 200 Hz. If the frequency is higher than 60 Hz, it shall be checked that the temperature of the test sample does not exceed 40°C during the test. The test is terminated upon fracture of the test piece or upon reaching the specified number of cycles without fracture.

Low-cycle loading test is to simulate seismic actions. Figure 2.9 shows the low-cycle loading protocol in which the specimen is pulled to $0.9f_y$ in tension and then the load is reversed to $0.5f_y$ in compression for 20 cycles. Subsequently, the specimen is pulled to two times the tensile yield strain and the load is reversed to $0.5f_y$ in compression for four cycles. Four more cycles are completed, but with a tensile strain target of five times the yield strain. Finally, the splice is pulled to failure.

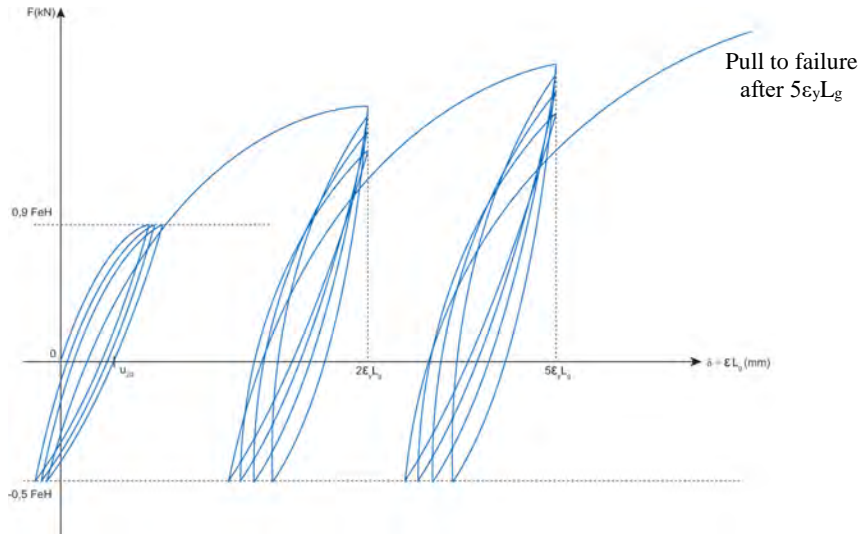


Figure 2.9 Mechanical splice low-cycle loading protocols according to ISO/DIS 15835 (2017)

2.5.2 Acceptance Criteria for Couplers

It was discussed that current standard testing methods do not provide acceptance criteria for mechanical bars splices. Furthermore, current design codes (Table 2.1) do not usually allow the use of couplers in plastic hinge regions of ductile members. Therefore, the current coupler requirements in these design codes are mainly force-based not displacement-based. New acceptance criteria are needed for successful incorporation of couplers in ductile members. One set of displacement-based requirements was proposed by Tazarv and Saiidi (2016), which is discussed in the following section.

2.5.3 Past Studies

Tazarv and Saiidi (2016) performed a state-of-the-art review of mechanical bar splices and mechanically spliced columns. They also proposed acceptance criteria, a material model, and design methods for couplers and columns with couplers. A summary of their findings is presented first. Then new coupler studies became available after Tazarv and Saiidi (2016) were reviewed.

2.5.3.1 Study by Tazarv and Saiidi (2016)

2.5.3.1.1 Acceptance Criteria for Mechanical Bar Splices

Tazarv and Saiidi (2016) proposed minimum requirements for mechanical bar splices to be incorporated in plastic hinge regions of bridge columns as:

1. The total length of a mechanical bar splice (L_{sp}) should not exceed $15d_b$ (d_b is the diameter of the smaller of the two spliced bars).
2. A spliced bar should fracture outside coupler region regardless of the loading type (e.g., monolithic, cyclic, or dynamic). Only ASTM A706 reinforcement should be used in mechanically spliced bridge columns.

2.5.3.1.2 Coupler Stress-Strain Material Model

Figure 2.10a shows a mechanical bar splice and regions defined in Tazarv and Saiidi (2016). When a spliced bar is in tension, it can be assumed that only a portion of the coupler contributes to the overall elongation and the remaining portion of the coupler (βL_{sp}) is rigid due to its anchoring mechanism. The rigid portion of the coupler does not contribute to the total elongation of the splice and can be represented using the “coupler rigid length factor (β).” This factor should be determined through experiments and might be different for different coupler sizes and types.

The coupler and bar regions can be identified for each mechanical bar splice, as shown in Figure 2.10a. The coupler region (L_{cr}) includes the coupler length (L_{sp}) plus α times the bar diameter ($\alpha \cdot d_b$) from each end of the coupler. For the same tensile force, the coupler region axial deformation will be lower, resulting in a lower strain in the coupler region (ε_{sp}) compared with the strain of the connecting reinforcing bar (ε_s) due to the coupler rigidity (Figure 2.10b). Equation 2.1 or 2.2 relates the coupler strains to a reference unspliced bar strains as:

$$\frac{\varepsilon_{sp}}{\varepsilon_s} = \frac{L_{cr} - \beta L_{sp}}{L_{cr}} \quad (\text{Eq. 2.1})$$

or

$$\frac{\varepsilon_{sp}}{\varepsilon_s} = \frac{(1 - \beta)L_{sp} + 2\alpha d_b}{L_{sp} + 2\alpha d_b} \quad (\text{Eq. 2.2})$$

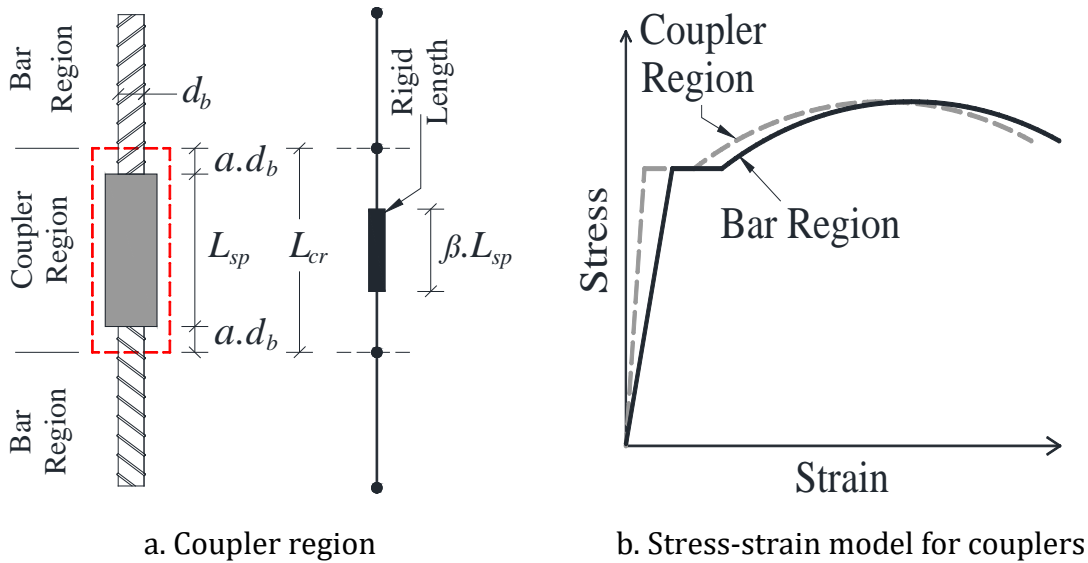


Figure 2.10 Stress-strain model for mechanical bar splices (Tazarv and Saiidi, 2016)

It can be assumed that the bar stress is independent of the presence of the coupler or its size, stiffness, and anchoring mechanism as long as the coupler is stronger than the connecting bars. It should be noted that couplers not at least as strong as the connecting bars are unacceptable.

Overall, the stress-strain relationship of any type of mechanical bar splices can be determined by knowing only the coupler rigid length factor (β). The condition in which $\beta = 0$ is similar to an unspliced connection in which the stress-strain of the coupler region is the same as that for the anchoring bar. Larger β indicates that the coupler region strains are lower than those for unspliced bars at any given stress.

2.5.3.2 Study by Bompa and Elghazouli (2017)

Bompa and Elghazouli (2017) compared tensile and cyclic response of more than 350 mechanical bar splices (Figure 2.11), which were tested under monotonic and cyclic loading to failure (Figure 2.12) conforming to the requirements of ISO 15835 (2009). The test data were collected from the literature.

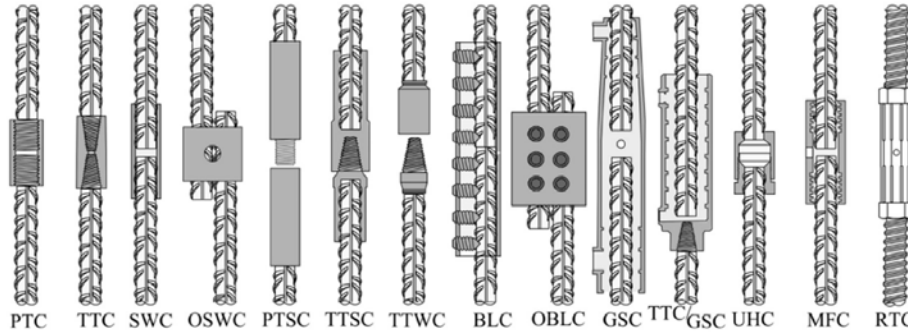


Figure 2.11 Different types of mechanical bar splices studies by Bompa and Elghazouli (2017)

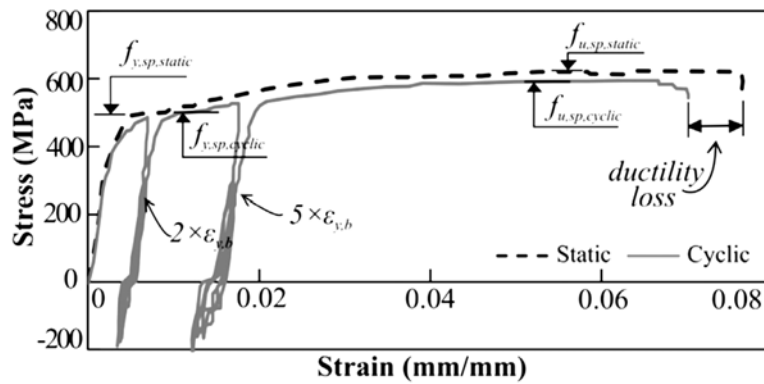


Figure 2.12 Typical stress-strain relationships for bar couplers (Bompa and Elghazouli, 2017)

A summary of the collated data is shown in Figure 2.13. The “ductility” in this study was defined as the ratio of the coupler region ultimate strain to the bar ultimate strain. Note that ductility in the U.S. design codes is based on displacements not strains. It can be seen that coupler strains were up to 50% lower than unspliced bar strains (Figure 2.13c). The study concluded that a detailed experimental study is needed to investigate the strain capacity of couplers.

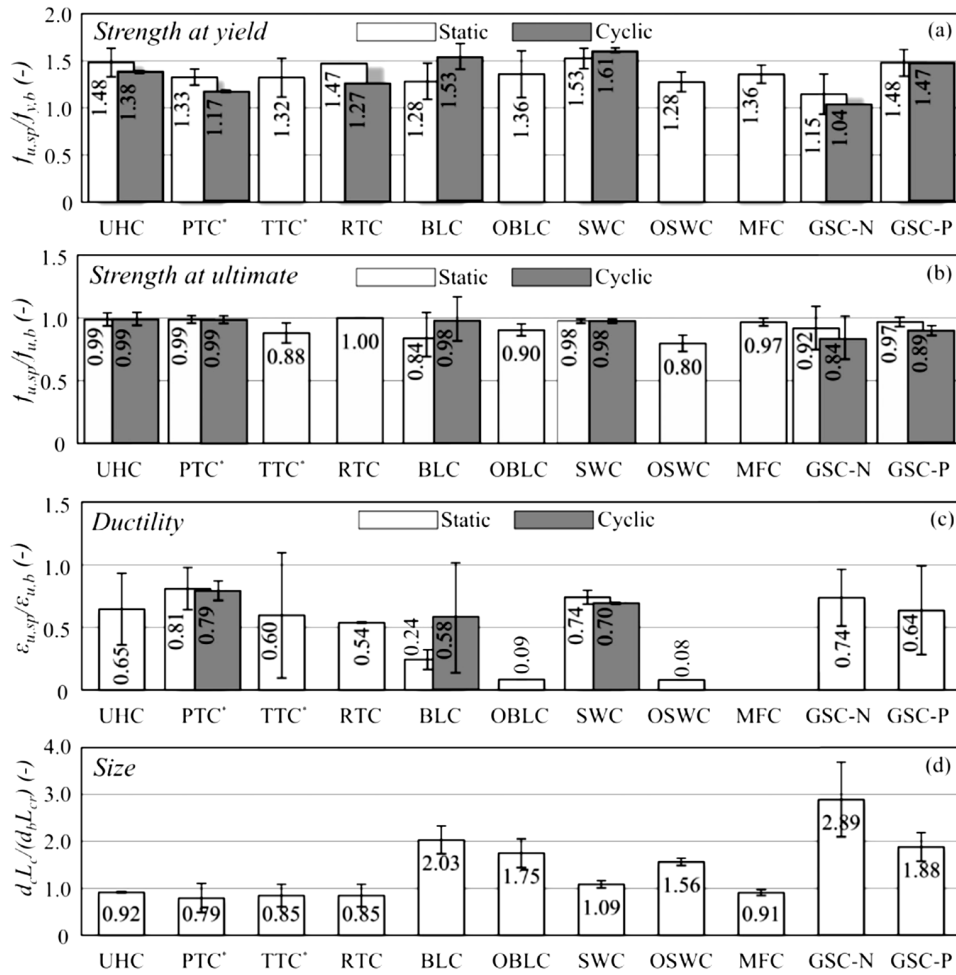


Figure 2.13 Comparative performance of mechanical bar splices (Bompa and Elghazouli, 2017)

2.6 References

- AASHTO LRFD. (2014). "AASHTO Guide Specifications for LRFD Seismic Bridge Design," Washington, D.C., American Association of State Highway and Transportation Officials.
- AASHTO SGS. (2011) "AASHTO Guide Specifications for Seismic Bridge Design," Washington, D.C., American Association of State Highway and Transportation Officials.
- ACI 439.3R-07. (2007). "Types of Mechanical Splices for Reinforcing Bars," American Concrete Institute Committee 439, 24 pp.
- ACI 318-14. (2014). "Building Code Requirement for Structural Concrete and Commentary," American Concrete Institute Committee.
- ASTM A1034. (2016). "Standard Test Methods for Testing Mechanical Splices for Steel Reinforcing Bars," ASTM International, West Conshohocken, PA.
- ASTM A706. (2009). "Standard Specification for Low-Alloy Steel Deformed and Plain Bars for Concrete Reinforcement," West Conshohocken, PA, 6 pp.
- Bompa, D.V., and Elghazouli, A.Y. (2017). "Ductility Considerations for Mechanical Reinforcement Couplers," *Structures*, Vol. 12, Nov. Issue, pp.115-119.

- California Test 670. (2004). "Method of Tests for Mechanical and Welded Reinforcing Steel Splices," Sacramento, CA, California Department of Transportation, 7 pp.
- Caltrans SDC. (2013). "Seismic Design Criteria," Version 1.7. Sacramento, CA, California Department of Transportation.
- Caltrans. (2015). "Authorized List of Couplers for Reinforcing Steel." Sacramento, CA, California Department of Transportation, September 21.
- Caltrans Memo to Designers. (2016). "20-9 Splices in Bar Reinforcing Steel," Sacramento, CA, California Department of Transportation, 9 pp., <<http://www.dot.ca.gov/des/techpubs/manuals/bridge-memo-to-designer/page/section-20/20-9.pdf>>.
- Eurocode 8. (2004). "Design of Structures for Earthquake Resistance - part 1: General Rules, Seismic Actions and Rules for Buildings," London, UK.
- Haber, Z.B., Saiidi, M.S., and Sanders, D.H. (2015), "Behavior and Simplified Modeling of Mechanical Reinforcing Bar Splices," *ACI Structural Journal*, Vol. 112, No. 2, pp. 179-88
- Haber, Z.B., Saiidi, M.S., and Sanders, D.H. (2013). "Precast Column Footing Connections for Accelerated Bridge Construction in Seismic Zones," Rep. No. CCEER 13-08 Center for Civil Engineering Earthquake Research, Dept. of Civil and Environmental Engineering, Univ. of Nevada, Reno. NV.
- Hurd, M.K. (1998). "Mechanical vs. Lap Splicing," The Aberdeen Group, Publication No. C980683, 3 pp., <https://www.concreteconstruction.net/_view-object?id=00000153-8c4e-dbf3-a177-9c7f8a4e0000>.
- NZS 3101-1. (2006). "Concrete Structures Standard - The Design of Concrete Structures," Standards New Zealand, 600 pp.
- Taskin, K., and Peker, K. (2015). "Assessing and Evaluation of the Mechanical Properties of Reinforcement Coupler Systems in Turkey," *SMAR2015*, The Third Conference on Smart Monitoring Assessment and Rehabilitation of Civil Structures, Antalya, Turkey, Sept. 7-9.
- ISO 15835. (2009). "Steels for the Reinforcement of Concrete - Reinforcement Couplers for Mechanical Splices of Bars (Parts 1)," International Organization for Standardization, Geneva, Switzerland.
- ISO/DIS 15835. (2017). "Steels for the Reinforcement of Concrete - Reinforcement Couplers for Mechanical Splices of Bars (Parts 1 to 3)," International Organization for Standardization, Geneva, Switzerland.
- Scott, M., and Fenves, G. (2006). "Plastic Hinge Integration Methods for Force-Based Beam-Column Elements," *Journal of Structural Engineering*, ASCE, 10.1061/ (ASCE) 0733-9445(2006)132:2(244), 244–252.
- Tazarv, M. and Saiidi, M.S. (2015). "Design and Construction of Bridge Columns Incorporating Mechanical Bar Splices in Plastic Hinge Zones," Center for Civil Engineering Earthquake Research, Department of Civil and Environmental Eng., University of Nevada; 2014. P. 400. Report No. CCEER-14-06.
- Tazarv, M. and Saiidi, M.S. (2016). "Seismic Design of Bridge Columns Incorporating Mechanical Bar Splices in Plastic Hinge Regions," *Engineering Structures*, DOI: 10.1016/j.engstruct.2016.06.041, Vol. 124, pp. 507-520.
- Yang, Y., Sneed, L.H., Morgan, A., Saiidi, M.S., Belarbi, A. (2014). "Repair of Earthquake-Damaged Bridge Columns with Interlocking Spirals and Fractured Bars," California Department of Transportation Report No. CA 14-2179, 211 pp.

3. TEST MATRIX, TEST SETUP, AND LOADING PROTOCOLS FOR MECHANICAL BAR SPLICES

3.1 Introduction

Different mechanical bar splices, their splicing mechanism, minimum code requirements, and acceptance criteria for bar couplers were discussed in Section 2. Based on the minimum requirements and their availability, more than 270 couplers, including nine different products, were collected from six manufacturers. Subsequently, more than 160 of which were tested under uniaxial tensile monotonic and cyclic loading to failure in the Lohr Structures laboratory at South Dakota State University to determine their mechanical properties. This section discusses the test matrix, test setup, specimen preparations, and loading protocols for mechanical bar splices. The test results are presented in the following section.

3.2 Test Matrix for Mechanical Bar Splices

The procedure followed to select coupler test specimens and the test matrix is discussed herein.

3.2.1 Selection of Coupler Test Specimens

At the time of this writing, there were more than 10 U.S. coupler manufacturers producing more than 60 coupler products. Furthermore, some of these manufacturers produce the same coupler types with some variations and sometimes with different performance. Therefore, a set of selection criteria was needed to identify couplers that could potentially be used in plastic hinge regions of ductile members.

The minimum requirements of the U.S. codes on mechanical bar splices and the results from previous studies were used to select coupler test specimens in the present work. Different coupler types were categorized in Section 2.4. The U.S. codes' requirements on couplers were presented in Section 2.4.1. Only those couplers that could potentially fracture bars were selected for testing in the present study. Such couplers are usually labeled in the manufacturer's datasheet as ACI Type 2 coupler and Caltrans Ultimate coupler.

All coupler types in the U.S. market were reviewed, and a list of couplers meeting the above mentioned selection criteria was developed, as presented in Table 3.1. Note Caltrans has a list of pre-approved couplers (Appendix A), and manufacturers usually include the code certificates in their brochures. Code compliance information in the table was extracted from the Caltrans pre-approved list or the product datasheet. The AASHTO Full Mechanical Connection is also included in the table for completeness.

Table 3.1 Selected couplers for uniaxial testing

Coupler Type	Coupler Manufacturer	Coupler Model	ACI Coupler Types		Caltrans Coupler Types		AASHTO Coupler Type
			Type 1	Type 2	Service Splice	Ultimate Splice	Full Mechanical Connection (FMC)
Shear Screw Coupler	Erico International Corp.	LENTON® LOCK (B1 Series)		X		X	N.A.
Headed Bar Coupler	Headed Reinforcement Corp.	Xtender® 500/510 Standard Coupler		X		X	N.A.
Grouted Sleeve Coupler	Dayton Superior	D410 Sleeve-Lock® Grout Sleeve		X		X	X
	Splice Sleeve North America	NMB		X	X		N.A.
Threaded Coupler	Dextra America, Inc.	Bartec Standard Splice (type A)		X		X	N.A.
	Dextra America, Inc.	Bartec Position Splices (Type B)		X		X	N.A.
	Erico International Corp.	LENTON® PLUS, Standard Coupler, (A12)		X		X	X
Swaged Coupler	Bar Splice	BarGrip® XL		X		X	N.A.
Hybrid Coupler	Dextra America, Inc.	Griptec®		X		X	N.A.
	Erico International Corp.	Lenton Interlock		X	X		N.A.

3.2.2 Test Matrix

Tables 3.2 to 3.6 present the coupler test matrixes, which include the coupler information, the specimen name, the specimen identification (ID), bar sizes, and loading types. The right column of the tables presents the geometry of the test specimen. The specimen naming guide is presented in the following section. Note that for each spliced specimen at least one unspliced bar was tested as the reference sample.

During the period of this study, the selected shear screw coupler (Table 3.1) was not available in the market due to a change or shortage in the supply chain. Therefore, no test was performed on shear screw couplers. Other available shear screw couplers cannot develop the full strength of the splicing bars.

Table 3.2 Test matrix for headed reinforcement couplers

Product Details	Specimen Name	Specimen ID	Bar Size	Loading Type	Specimen Geometry (in.)
Coupler Type: Headed Bar Manufacturer: Headed Reinforcement Corp Model No: Xtender® 500/510 Standard Coupler	HR-1	HR-5-M(HR-2)	No.5 (16 mm)	Monotonic	$L_{sp} = 2.4$
	HR-2	HR-5-M(HR-2)			$L_{cr} = 4.9$
	HR-3	HR-5-M(HR-3)			$L_{tot} = 20$
	HR-4	HR-5-C(HR-4)		Cyclic	$L_{sp} = 2.4$
	HR-5	HR-5-C(HR-5)			$L_{cr} = 4.9$
	HR-6	HR-5-C(HR-6)			$L_{tot} = 20$
	HR-7	HR-8-M(HR-7)	No.8 (25 mm)	Monotonic	$L_{sp} = 3.25$
	HR-8	HR-8-M(HR-8)			$L_{cr} = 5.75$
	HR-9	HR-8-M(HR-9)			$L_{tot} = 31.25$
	HR-10	HR-8-C(HR-10)		Cyclic	$L_{sp} = 3.25$
	HR-11	HR-8-C(HR-11)			$L_{cr} = 5.75$
	HR-12	HR-8-C(HR-12)			$L_{tot} = 31.25$
	HR-13	HR-10-M(HR-13)	No.10 (32 mm)	Monotonic	$L_{sp} = 3.88$
	HR-14	HR-10-M(HR-14)			$L_{cr} = 7.0$
	HR-15	HR-10-M(HR-15)			$L_{tot} = 31.88$
	HR-16	HR-10-C(HR-16)		Cyclic	$L_{sp} = 3.88$
	HR-17	HR-10-C(HR-17)			$L_{cr} = 7.0$
	HR-18	HR-10-C(HR-18)			$L_{tot} = 31.88$

Note: L_{sp} is the coupler length, L_{cr} is the coupler region length, and L_{tot} is the grip-to-grip length of the test specimen; 1 in. = 25.4 mm

Table 3.3 Test matrix for threaded couplers

Product Details	Specimen Name	Specimen ID	Bar Size	Loading Type	Specimen Geometry (in.)
<p>Coupler Type: Threaded</p> <p>Manufacturer: Dextra America, Inc.</p> <p>Model No: Bartec Standard Splice (Type A)</p>	TH-1	TH-5-M(TH-1)	No.5 (16 mm)	Monotonic	L _{sp} = 1.75 L _{cr} = 4.25 L _{tot} = 21.25
	TH-2	TH-5-M(TH-2)			
	TH-3	TH-5-M(TH-3)			
	TH-4	TH-5-C(TH-4)		Cyclic	L _{sp} = 1.75 L _{cr} = 4.25 L _{tot} = 21.25
	TH-5	TH-5-C(TH-5)			
	TH-6	TH-5-C(TH-6)			
	TH-7	TH-8-M(TH-7)	No.8 (25 mm)	Monotonic	L _{sp} = 2.63 L _{cr} = 5.13 L _{tot} = 30.63
	TH-8	TH-8-M(TH-8)			
	TH-9	TH-8-M(TH-9)			
	TH-10	TH-8-C(TH-10)		Cyclic	L _{sp} = 2.63 L _{cr} = 5.13 L _{tot} = 30.63
	TH-11	TH-8-C(TH-11)			
	TH-12	TH-8-C(TH-12)			
	TH-13	TH-10-M(TH-13)	No.10 (32 mm)	Monotonic	L _{sp} = 3.06 L _{cr} = 6.03 L _{tot} = 31.0
	TH-14	TH-10-M(TH-14)			
	TH-15	TH-10-M(TH-15)			
	TH-16	TH-10-C(TH-16)		Cyclic	L _{sp} = 3.06 L _{cr} = 6.03 L _{tot} = 31.0
	TH-17	TH-10-C(TH-17)			
	TH-18	TH-10-C(TH-18)			
<p>Coupler Type: Threaded</p> <p>Manufacturer: Dextra America, Inc.</p> <p>Model No: Bartec Standard Splice (Type B)</p>	TH-19	TH-5-M(TH-19)	No.5 (16 mm)	Monotonic	L _{sp} = 1.75 L _{cr} = 4.25 L _{tot} = 21.25
	TH-20	TH-5-M(TH-20)			
	TH-21	TH-5-M(TH-21)			
	TH-22	TH-5-C(TH-22)		Cyclic	L _{sp} = 1.75 L _{cr} = 4.25 L _{tot} = 21.25
	TH-23	TH-5-C(TH-23)			
	TH-24	TH-5-C(TH-24)			
	TH-25	TH-8-M(TH-25)	No.8 (25 mm)	Monotonic	L _{sp} = 2.63 L _{cr} = 5.13 L _{tot} = 30.63
	TH-26	TH-8-M(TH-26)			
	TH-27	TH-8-M(TH-27)			
	TH-28	TH-8-C(TH-28)		Cyclic	L _{sp} = 2.63 L _{cr} = 5.13 L _{tot} = 30.63
	TH-29	TH-8-C(TH-29)			
	TH-30	TH-8-C(TH-30)			
	TH-31	TH-10-M(TH-31)	No.10 (32 mm)	Monotonic	L _{sp} = 3.06 L _{cr} = 6.03 L _{tot} = 31.0
	TH-32	TH-10-M(TH-32)			
	TH-33	TH-10-M(TH-33)			
	TH-34	TH-10-C(TH-34)		Cyclic	L _{sp} = 3.06 L _{cr} = 6.03 L _{tot} = 31.0
	TH-35	TH-10-C(TH-35)			
	TH-36	TH-10-C(TH-36)			

Note: L_{sp} is the coupler length, L_{cr} is the coupler region length, and L_{tot} is the grip-to-grip length of the test specimen; 1 in. = 25.4 mm

Table 3.3 continued

Product Details	Specimen Name	Specimen ID	Bar Size	Loading Type	Specimen Geometry (in.)			
Coupler Type: Threaded	TH-37	TH-5-M(TH-37)	No.5 (16 mm)	Monotonic	$L_{sp} = 2.38$			
	TH-38	TH-5-M(TH-38)			$L_{cr} = 4.88$			
	TH-39	TH-5-M(TH-39)			$L_{tot} = 35.5$			
	TH-40	TH-5-C(TH-40)		Cyclic	$L_{sp} = 2.38$			
	TH-41	TH-5-C(TH-41)			$L_{cr} = 4.88$			
	TH-42	TH-5-C(TH-42)			$L_{tot} = 21.25$			
	Manufacturer: Erico International Corp.	TH-43	TH-8-M(TH-43)	No.8 (25 mm)	Monotonic	$L_{sp} = 3.75$		
		TH-44	TH-8-M(TH-44)			$L_{cr} = 6.25$		
		TH-45	TH-8-M(TH-45)			$L_{tot} = 33.5$		
		TH-46	TH-8-C(TH-46)		Cyclic	$L_{sp} = 3.75$		
TH-47		TH-8-C(TH-47)	$L_{cr} = 6.25$					
TH-48		TH-8-C(TH-48)	$L_{tot} = 33.5$					
Model No: LENTON® PLUS Standard Coupler (A12)		TH-49	TH-10-M(TH-49)			No.10 (32 mm)	Monotonic	$L_{sp} = 4.20$
		TH-50	TH-10-M(TH-50)					$L_{cr} = 7.38$
	TH-51	TH-10-M(TH-51)	$L_{tot} = 37.0$					
	TH-52	TH-10-C(TH-52)	Cyclic	$L_{sp} = 4.20$				
	TH-53	TH-10-C(TH-53)		$L_{cr} = 7.38$				
	TH-54	TH-10-C(TH-54)		$L_{tot} = 37.0$				

Note: L_{sp} is the coupler length, L_{cr} is the coupler region length, and L_{tot} is the grip-to-grip length of the test specimen; 1in. = 25.4 mm

Table 3.4 Test matrix for swaged couplers

Product Details	Specimen Name	Specimen ID	Bar Size	Loading Type	Specimen Geometry (in.)
Coupler Type: Swaged Coupler Manufacturer: Bar Splice Model No: BarGrip® XL	SW-1	SW-5-M(SW-1)	No.5 (16 mm)	Monotonic	$L_{sp} = 5.25$
	SW-2	SW-5-M(SW-2)			$L_{cr} = 7.75$
	SW-3	SW-5-M(SW-3)			$L_{tot} = 21.25$
	SW-4	SW-5-C(SW-4)		Cyclic	$L_{sp} = 5.25$
	SW-5	SW-5-C(SW-5)			$L_{cr} = 7.75$
	SW-6	SW-5-C(SW-6)			$L_{tot} = 21.25$
	SW-7	SW-8-M(SW-7)	No.8 (25 mm)	Monotonic	$L_{sp} = 7.90$
	SW-8	SW-8-M(SW-8)			$L_{cr} = 10.4$
	SW-9	SW-8-M(SW-9)			$L_{tot} = 39.0$
	SW-10	SW-8-C(SW-10)		Cyclic	$L_{sp} = 7.90$
	SW-11	SW-8-C(SW-11)			$L_{cr} = 10.40$
	SW-12	SW-8-C(SW-12)			$L_{tot} = 39.0$
	SW-13	SW-10-M(SW-13)	No.10 (32 mm)	Monotonic	$L_{sp} = 9.50$
	SW-14	SW-10-M(SW-14)			$L_{cr} = 12.68$
	SW-15	SW-10-M(SW-15)			$L_{tot} = 40.0$
	SW-16	SW-10-C(SW-16)		Cyclic	$L_{sp} = 9.50$
	SW-17	SW-10-C(SW-17)			$L_{cr} = 12.68$
	SW-18	SW-10-C(SW-18)			$L_{tot} = 40.0$

Note: L_{sp} is the coupler length, L_{cr} is the coupler region length, and L_{tot} is the grip-to-grip length of the test specimen; 1in. = 25.4 mm

Table 3.5 Test matrix for grouted sleeve couplers

Product Details	Specimen Name	Specimen ID	Bar Size	Loading Type	Specimen Geometry (in.)
<p>Coupler Type: Splice Sleeve North America</p> <p>Manufacturer: Splice Sleeve North America</p> <p>Model No: NMB</p>	GS-1	GS-5-M(GS-1)	No.5 (16 mm)	Monotonic	L _{sp} = 9.63 L _{cr} = 12.13 L _{tot} = 36.50
	GS-2	GS-5-M(GS-2)			
	GS-3	GS-5-M(GS-3)			
	GS-4	GS-5-C(GS-4)		Cyclic	L _{sp} = 9.63 L _{cr} = 12.13 L _{tot} = 36.50
	GS-5	GS-5-C(GS-5)			
	GS-6	GS-5-C(GS-6)			
	GS-7	GS-8-M(GS-7)	No.8 (25 mm)	Monotonic	L _{sp} = 14.50 L _{cr} = 17.0 L _{tot} = 38.50
	GS-8	GS-8-M(GS-8)			
	GS-9	GS-8-M(GS-9)			
	GS-10	GS-8-C(GS-10)		Cyclic	L _{sp} = 14.50 L _{cr} = 17.0 L _{tot} = 38.50
	GS-11	GS-8-C(GS-11)			
	GS-12	GS-8-C(GS-12)			
	GS-13	GS-10-M(GS-13)	No.10 (32 mm)	Monotonic	L _{sp} = 18.0 L _{cr} = 21.20 L _{tot} = 43.0
	GS-14	GS-10-M(GS-14)			
	GS-15	GS-10-M(GS-15)			
	GS-16	GS-10-C(GS-16)		Cyclic	L _{sp} = 18.0 L _{cr} = 21.2 L _{tot} = 43.0
	GS-17	GS-10-C(GS-17)			
	GS-18	GS-10-C(GS-18)			
<p>Coupler Type: Splice Sleeve North America</p> <p>Manufacturer: Dayton Superior</p> <p>Model No: D410 Sleeve-Lock® Grout Sleeve</p>	GS-19	GS-5-M(GS-19)	No.5 (16 mm)	Monotonic	L _{sp} = 9.50 L _{cr} = 12.0 L _{tot} = 36.50
	GS-20	GS-5-M(GS-20)			
	GS-21	GS-5-M(GS-21)			
	GS-22	GS-5-C(GS-22)		Cyclic	L _{sp} = 9.50 L _{cr} = 12.0 L _{tot} = 36.50
	GS-23	GS-5-C(GS-23)			
	GS-24	GS-5-C(GS-24)			
	GS-25	GS-8-M(GS-25)	No.8 (25 mm)	Monotonic	L _{sp} = 16.5 L _{cr} = 19.0 L _{tot} = 39.50
	GS-26	GS-8-M(GS-26)			
	GS-27	GS-8-M(GS-27)			
	GS-28	GS-8-C(GS-28)		Cyclic	L _{sp} = 16.5 L _{cr} = 19.00 L _{tot} = 39.50
	GS-29	GS-8-C(GS-29)			
	GS-30	GS-8-C(GS-30)			
	GS-31	GS-10-M(GS-31)	No.10 (32 mm)	Monotonic	L _{sp} = 18.0 L _{cr} = 21.2 L _{tot} = 43.0
	GS-32	GS-10-M(GS-32)			
GS-33	GS-10-M(GS-33)				
GS-34	GS-10-C(GS-34)	Cyclic		L _{sp} = 18.0 L _{cr} = 21.2 L _{tot} = 43.0	
GS-35	GS-10-C(GS-35)				
GS-36	GS-10-C(GS-36)				

Note: L_{sp} is the coupler length, L_{cr} is the coupler region length, and L_{tot} is the grip-to-grip length of the test specimen; 1in. =25.4 mm

Table 3.6 Test matrix for hybrid couplers

Product Details	Specimen Name	Specimen ID	Bar Size	Loading Type	Specimen Geometry (in.)
Coupler Type: Hybrid Manufacturer: Dextra America, Inc Model No: Griptec®	HY-1	HY-5-M(HY-1)	No.5 (16 mm)	Monotonic	$L_{sp} = 8.13$
	HY-2	HY-5-M(HY-2)			$L_{cr} = 10.63$
	HY-3	HY-5-M(HY-3)			$L_{tot} = 32.12$
	HY-4	HY-5-C(HY-4)		Cyclic	$L_{sp} = 8.13$
	HY-5	HY-5-C(HY-5)			$L_{cr} = 10.63$
	HY-6	HY-5-C(HY-6)			$L_{tot} = 32.12$
	HY-7	HY-8-M(HY-7)	No.8 (25 mm)	Monotonic	$L_{sp} = 9.31$
	HY-8	HY-8-M(HY-8)			$L_{cr} = 11.81$
	HY-9	HY-8-M(HY-9)			$L_{tot} = 39.25$
	HY-10	HY-8-C(HY-10)		Cyclic	$L_{sp} = 9.31$
	HY-11	HY-8-C(HY-11)			$L_{cr} = 11.81$
	HY-12	HY-8-C(HY-12)			$L_{tot} = 39.25$
	HY-13	HY-10-M(HY-13)	No.10 (32 mm)	Monotonic	$L_{sp} = 10.63$
	HY-14	HY-10-M(HY-14)			$L_{cr} = 13.8$
	HY-15	HY-10-M(HY-15)			$L_{tot} = 40.0$
	HY-16	HY-10-C(HY-16)		Cyclic	$L_{sp} = 10.63$
	HY-17	HY-10-C(HY-17)			$L_{cr} = 13.8$
	HY-18	HY-10-C(HY-18)			$L_{tot} = 40.0$
Coupler Type: Hybrid Manufacturer: Erico International Corp. Model No: Lenton Interlock	HY-19	HY-5-M(HY-19)	No.5 (16 mm)	Monotonic	$L_{sp} = 7.88$
	HY-20	HY-5-M(HY-20)			$L_{cr} = 10.38$
	HY-21	HY-5-M(HY-21)			$L_{tot} = 40.0$
	HY-22	HY-5-C(HY-22)		Cyclic	$L_{sp} = 7.88$
	HY-23	HY-5-C(HY-23)			$L_{cr} = 10.38$
	HY-24	HY-5-C(HY-24)			$L_{tot} = 40.0$
	HY-25	HY-8-M(HY-25)	No.8 (25 mm)	Monotonic	$L_{sp} = 8.75$
	HY-26	HY-8-M(HY-26)			$L_{cr} = 11.25$
	HY-27	HY-8-M(HY-27)			$L_{tot} = 39.25$
	HY-28	HY-8-C(HY-28)		Cyclic	$L_{sp} = 8.75$
	HY-29	HY-8-C(HY-29)			$L_{cr} = 11.25$
	HY-30	HY-8-C(HY-30)			$L_{tot} = 39.25$
	HY-31	HY-10-M(HY-31)	No.10 (32 mm)	Monotonic	$L_{sp} = 10.75$
	HY-32	HY-10-M(HY-32)			$L_{cr} = 13.93$
	HY-33	HY-10-M(HY-33)			$L_{tot} = 40.0$
	HY-34	HY-10-C(HY-34)		Cyclic	$L_{sp} = 10.75$
	HY-35	HY-10-C(HY-35)			$L_{cr} = 13.93$
	HY-36	HY-10-C(HY-36)			$L_{tot} = 40.0$

Note: L_{sp} is the coupler length, L_{cr} is the coupler region length, and L_{tot} is the grip-to-grip length of the test specimen; 1in. =25.4 mm

3.2.3 Test Specimen Nomenclature System

A naming system including the coupler type, bar size, loading protocol, and a specific ID was developed to quickly identify each test specimen. Figure 3.1 illustrates the naming system for a coupler specimen.

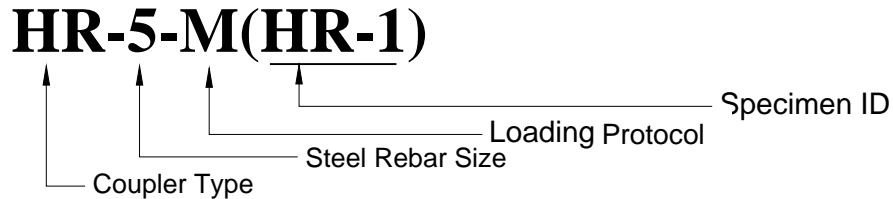


Figure 3.1 Coupler test specimen name guide

The following describes each portion of the specimen name:

- The first term indicates the coupler type as:
 - SS: Shrew screw coupler
 - HR: Headed reinforcement coupler
 - SW: Swaged coupler
 - TH: Threaded coupler
 - GS: Grouted sleeve coupler
 - HY: Hybrid coupler
- The second term refers to the bar size, which can be No. 5 (16 mm), No. 8 (25 mm), or No. 10 (32 mm).
- The third term indicates the loading type, which can be monotonic (M) or cyclic (C).
- The term in the parentheses is a specific ID assigned to each coupler specimen, as presented in Tables 3.2 to 3.6.

Note for each spliced specimen at least one unspliced bar was tested as the reference sample, which was named the same as the corresponding coupler but adding “-Ref.” at the end (e.g., HR-5-M(HR-1)-Ref).

3.3 Test Setup for Mechanical Bar Splices

Figure 3.2 shows the test setup for mechanical bar splices, including a static universal testing machine, its hydraulic system and controller, and one test specimen with an extensometer specifically developed for couplers.

The universal testing machine could accommodate samples with a maximum length of 43 in. (1092 mm). The total stroke of the machine was 7 in. (178 mm). The machine force capacity was 135 kips (600 kN) both in tension and compression. Furthermore, the universal testing machine provides loads with an accuracy of 0.224 lb. (1.0 N) and head displacements with an accuracy of 3.9×10^{-6} in. (0.0001 mm).

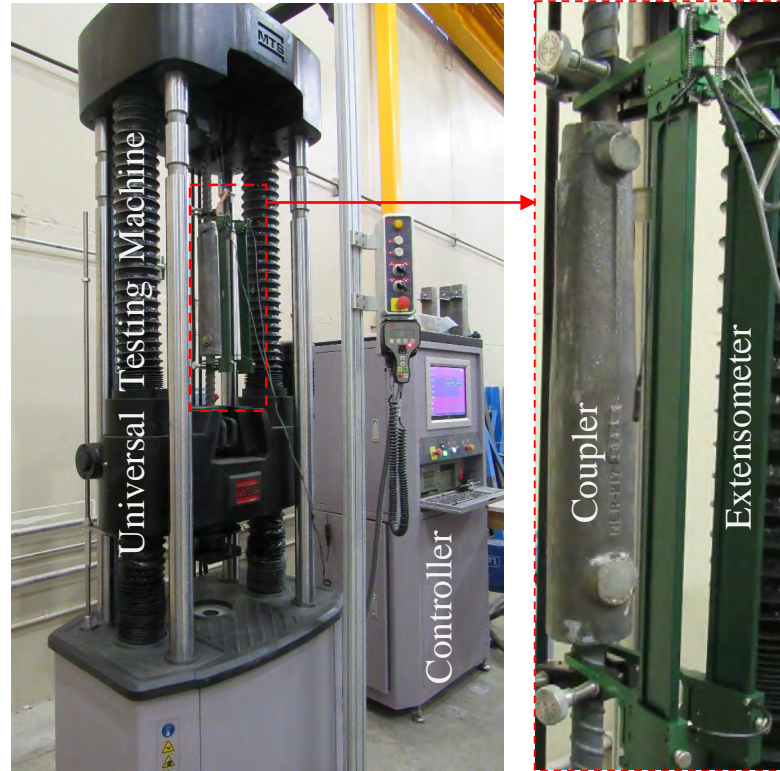


Figure 3.2 Test setup for mechanical bar splices

A unified geometry was needed for all test specimens to minimize variations in the results. Figure 3.3 shows the selected geometry for unspliced bars (according to ASTM E8, 2015) and spliced specimens, which was developed based on the requirements presented in ASTM A1034 (2016) and California Test 670 (2004). The total specimen length (L_{tot}) depends on the size of the bar and the length of the mechanical bar splice (L_{sp}). The coupler region length (L_{cr}) is defined as the coupler length plus α (Alpha) times the bar diameter ($\alpha \cdot d_b$) from each side of the coupler ends. Alpha was not more than twice the bar diameter in the present study according to ASTM A1034 (2016). The bar length outside the coupler region to the grip was at least six times the bar diameter to avoid localized failure. ASTM E8 (2015) requires at least $5d_b$ clear length for testing of a regular bar.

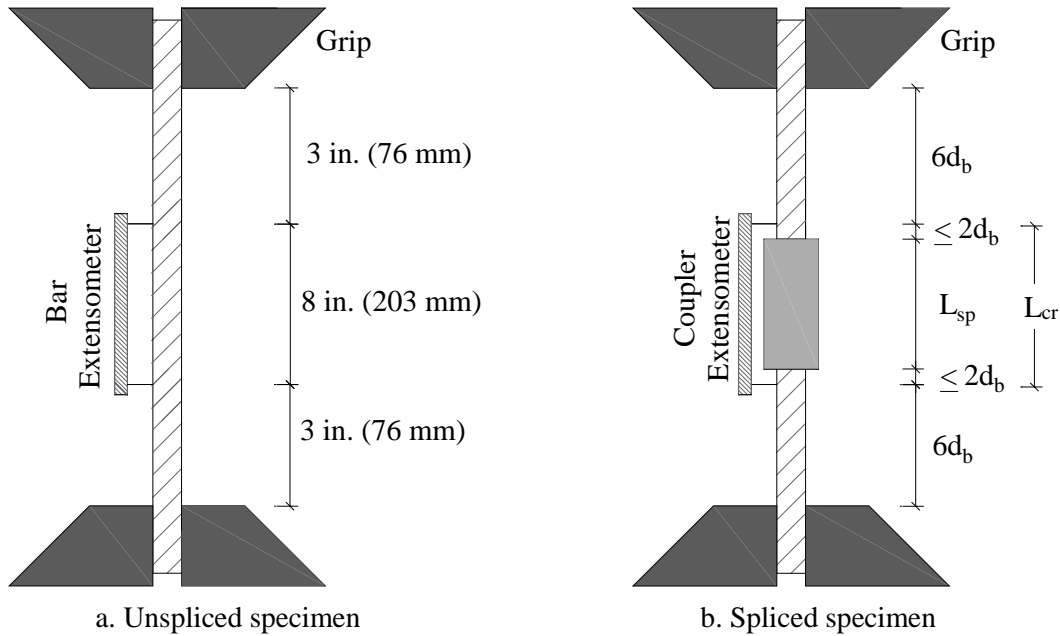


Figure 3.3 Geometry of unspliced and spliced test specimens

3.3.1 Instrumentation

Figure 3.4 shows two different types of extensometers that were used to measure the strains of unspliced and spliced specimens. The bar extensometer (Figure 3.4a) had a 4-in. (100-mm) stroke and could measure strains until the fracture of the bar. The accuracy of the bar extensometer was A-1 according to ASTM E83 (2010). The coupler extensometer (Figure 3.4b), which was a new product by Epsilon, was specifically made for mechanical bar splices, and its properties were modified based on the findings of the present study. The main modification was to increase the measuring length of the device from 0.5 in. (12 mm) to 1.5 in. (38 mm) to include long couplers. The accuracy of this extensometer meets the requirements of a B-1 device according to ASTM E83 (2010).



a. Bar extensometer



b. Coupler extensometer

Figure 3.4 Extensometers used for unspliced and spliced specimens

3.4 Mechanical Bar Splice Preparation

Figures 3.5 to 3.13 show the mechanical bar splice specimens used in the present study before and after the assembly. Bar end preparation and coupler assembly are different for each product, and the manufacturer's requirements should be followed. Depending on the type, the coupler preparation time may vary from a few minutes to a few days. For example, a threaded coupler, which may not need any field bar end preparation, can be assembled within a few minutes; a grouted sleeve coupler may need at least four days for the grout to cure and to gain a sufficient bond strength. Section 2 presents more discussion on the anchoring mechanism for each coupler type.



a. Unassembled



b. Assembled

Figure 3.5 Preparation of headed reinforcement couplers



a. Unassembled



b. Assembled

Figure 3.6 Preparation of Dayton grouted sleeve couplers



a. Unassembled



b. Assembled

Figure 3.7 Preparation of NMB grouted sleeve couplers



a. Unassembled



b. Assembled

Figure 3.8 Preparation of Dextra Type-A threaded couplers



a. Unassembled



b. Assembled

Figure 3.9 Preparation of Dextra Type-B threaded couplers



a. Unassembled



b. Assembled

Figure 3.10 Preparation of Erico threaded couplers



a. Unassembled



b. Assembled

Figure 3.11 Preparation of swaged couplers



a. Unassembled



b. Assembled

Figure 3.12 Preparation of hybrid couplers (swaged and threaded)



a. Unassembled



b. Assembled

Figure 3.13 Preparation of hybrid couplers (threaded and grouted)

3.5 Loading Protocols for Mechanical Bar Splices

Each type of the selected mechanical bar splices was tested under both uniaxial tensile monotonic and cyclic loading to failure.

3.5.1 Monotonic Loading

Monotonic testing of unspliced and spliced specimens was performed according to ASTM E8 (2012) by pulling the specimen to failure with a constant strain rate of 0.019 in./in./min., which was within the ASTM rate of 0.015 ± 0.006 in./in./min. This ASTM standard allows two speeds before and after the yielding of a bar to expedite the testing. Nevertheless, only the prior-to-yielding strain rate was used in the present study for all specimens during the entire test to minimize the test variables, since the anchoring mechanism of a coupler may change its yield strain. The data sampling rate was 10 Hz.

3.5.2 Cyclic Loading

Understanding the cyclic behavior of couplers under earthquake loading is essential to comment whether a coupler is suitable for use in plastic hinge regions of bridge columns. Strain-based loading protocols are usually preferred to stress-based protocols when the nonlinear behavior of a specimen is investigated. Except ISO/DIS 15835 (2017), other testing standards do not specify any requirements to explore the post-yield cyclic behavior of couplers. ISO/DIS 15835 (2017) specifies only two strain amplitudes after the yielding, which may not be sufficient in seismic regions where bars may undergo multiple and large strain cycles. Therefore, a new cyclic loading protocol is needed for mechanical bar splices to fully investigate their behavior under large strain demands.

The first challenge is how to determine the strain amplitudes especially when couplers alter the strain behavior compared with unspliced bars. To address this issue, it is proposed to use the coupler monotonic test data as the input for the cyclic testing. For example, a few target stresses can be selected (e.g., 10 points from zero stress to 100% of the peak stress with an interval of 10% of the peak stress (used in the present study), or a few points before the yielding and more closely spaced points beyond the yield point (as shown in Figure 3.14), then the strains corresponding to these stresses can be determined from the measured monotonic data (Figure 3.14). These strains are the target strains for the cyclic testing.

Another challenge for the cyclic testing of a coupler is to determine the number of load cycles. California Test 670 (2004) requires four cycles per amplitude, but these cycles are mainly in the elastic range. ISO/DIS 15835 (2017) specifies four cycles for each of the two post-yield strain amplitudes ($2\varepsilon_y$ and $5\varepsilon_y$). Even though four full cycles may be excessive, four tensile cycles (half cycles) per strain amplitude is recommended to conservatively investigate the coupler behavior under extreme loading. A minimum stress of 5,000 psi (34.5 MPa) is proposed as the lower tensile stress limit to avoid buckling of the bars in compression. The splice can be monotonically pulled to failure if the specimens do not fail after completion of all target cycles. The speed of the cyclic loading is recommended to be the same as that in the monotonic loading, which is 0.019 in./in./min., to avoid any variation.

One sample of cyclic loading history used in the present study is shown in Figure 3.15. Note the proposed cyclic loading regime is more rigorous than that in ISO/DIS 15835 (2017) since it includes more strain amplitudes, which are well beyond the yield point.

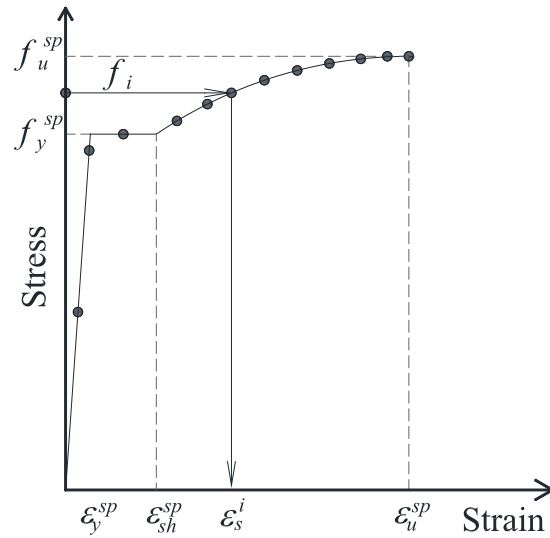


Figure 3.14 Target strains in cyclic testing of mechanical bar splices

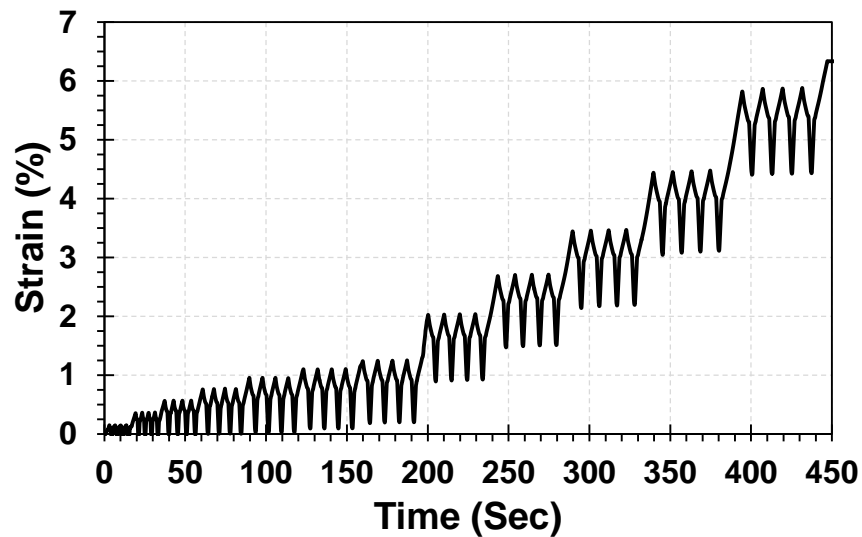


Figure 3.15 Sample of cyclic loading history for mechanical bar splices

3.6 References

- AASHTO SGS. (2011). "AASHTO Guide Specifications for LRFD Seismic Bridge Design," Washington, D.C., American Association of State Highway and Transportation Officials.
- ACI 439.3R-07. (2007). "Types of Mechanical Splices for Reinforcing Bars," Reported by American Concrete Institute Committee 439, 24 pp.
- ASTM A1034. (2016). "Standard Test Methods for Testing Mechanical Splices for Steel Reinforcing Bars," ASTM International, West Conshohocken, PA.

- ASTM A706. (2009). "Standard specification for Low-Alloy Steel Deformed and Plain Bars for Concrete Reinforcement," West Conshohocken, PA, 6 pp.
- ASTM E8. (2015). "Standard Test Methods for Tension Testing of Metallic Materials," ASTM International, West Conshohocken, PA, 29 pp.
- ASTM E83. (2010). "Standard Practice for Verification and Classification of Extensometer Systems," ASTM International, West Conshohocken, PA.
- California Test 670. (2004). "Method of Tests for Mechanical and Welded Reinforcing Steel Splices," Sacramento, CA, California Department of Transportation, 13 pp.
- Caltrans. (2015). "Authorized List of Couplers for Reinforcing Steel," Sacramento, CA, California Department of Transportation, September 21.
- Tazarv, M. and Saiidi, M.S. (2016). "Seismic Design of Bridge Columns Incorporating Mechanical Bar Splices in Plastic Hinge Regions," *Engineering Structures*, DOI: 10.1016/j.engstruct.2016.06.041, Vol 124, pp. 507-520.

4. RESULTS OF EXPERIMENTAL STUDIES ON MECHANICAL BAR SPLICES

4.1 Introduction

Using the loading protocols and test setup discussed in Section 3, 162 mechanical bar splices were tested to failure at the Lohr Structures Laboratory at South Dakota State University. Of which, 81 couplers were tested using the monotonic loading protocol, and 81 couplers were tested using the cyclic loading protocol. Furthermore, more than 170 unspliced bars were tested to failure to serve as the reference specimens. Acceptance criteria for mechanical bar splices proposed by Tazarv and Saiidi (2016) (Sec. 2.5.3.1) were adopted in the present study to identify “seismic couplers” for use in the plastic hinge region of bridge columns. Measured coupler stress-strain relationships, coupler failure modes, and a summary of test results are presented in this section.

4.2 Coupler Monotonic Test Results

Tables 3.2 to 3.6 present the test matrix for all mechanical bar splices used in the present study. A total of 81 mechanical bar splices consisting of No. 5 (16 mm), No. 8 (25 mm), and No. 10 (32 mm) splices were tested using the monotonic loading protocol detailed in Section 3.5. Five different types of couplers (headed, threaded, swaged, grouted, and hybrid) consisting of nine different products were included in this experimental program. Three spliced specimens were tested per product, and at least one unspliced bar was tested per product as the reference sample. This section presents the detailed findings of the monotonic testing for each coupler type and then concludes with a summary of the findings for all specimens.

4.2.1 Headed Reinforcement Couplers

Figures 4.1 to 4.3 show the measured stress-strain relationships for the No. 5 (16-mm), No. 8 (25-mm), and No. 10 (32-mm) headed reinforcement couplers, respectively. The unspliced reference bar data and the coupler failure mode are also included in these figures for completeness. All headed reinforcement couplers failed by the “bar fracture” outside the coupler region, thus they are seismic couplers.

The same-size headed couplers showed consistent stress-strain behavior. The average modulus of elasticity of the No. 5, No. 8, and No. 10 headed bar couplers was, respectively, 76%, 76%, and 63% lower than the conventional steel bar modulus of elasticity, which is 29000 ksi (200,000 MPa). Furthermore, it can be seen that the strain at peak stress, which was defined as the ultimate strain, was approximately the same for the couplers with the same bar sizes. Nevertheless, the average ultimate strain of the No. 5, No. 8, and No. 10 spliced specimens was, respectively, 44%, 41%, and 42% lower than that for the corresponding unspliced reference bars.

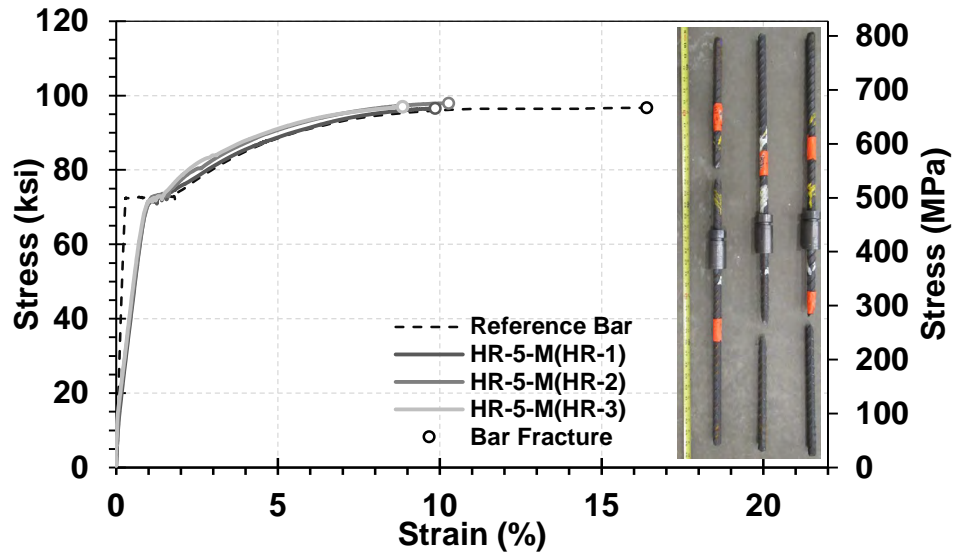


Figure 4.1 Monotonic test results for No. 5 (16-mm) headed reinforcement couplers

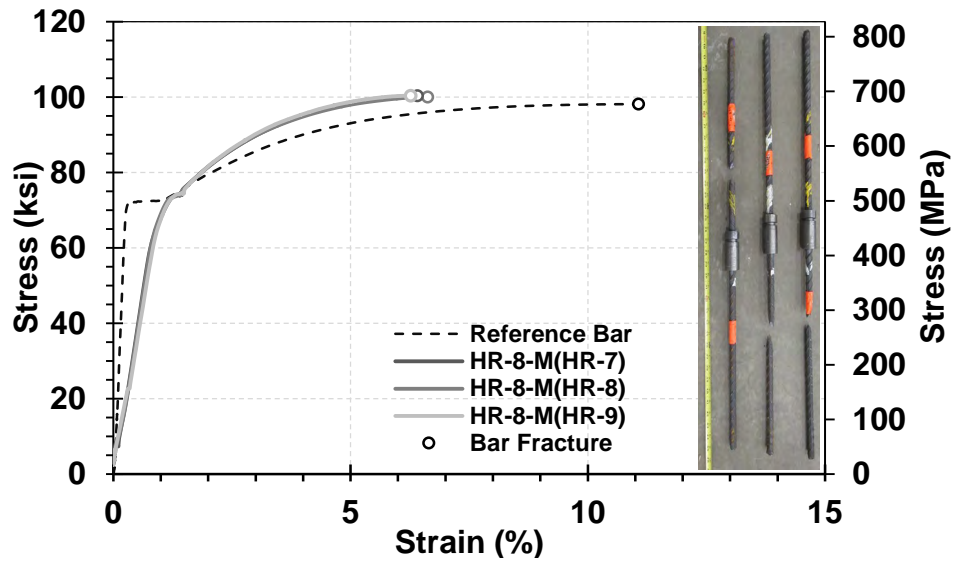


Figure 4.2 Monotonic test results for No. 8 (25-mm) headed reinforcement couplers

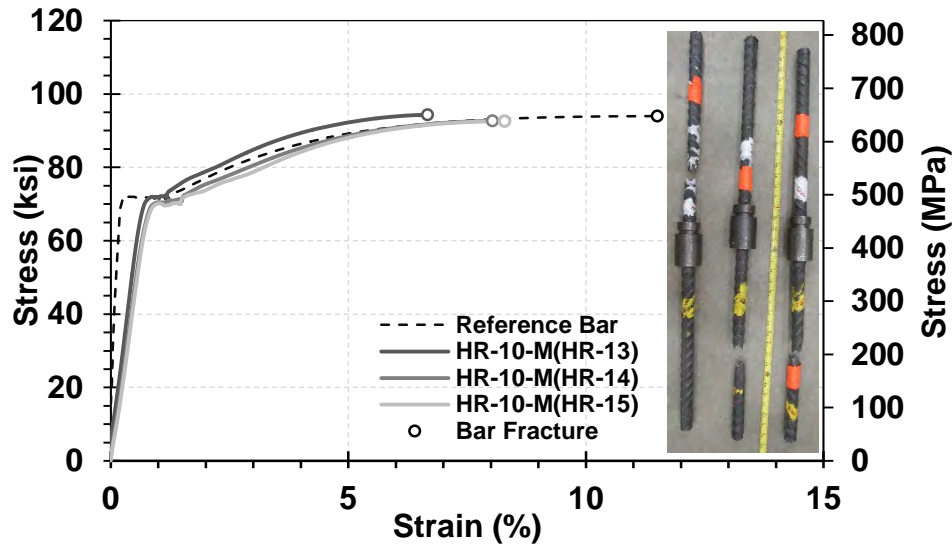


Figure 4.3 Monotonic test results for No. 10 (32-mm) headed reinforcement couplers

4.2.2 Threaded Couplers

Three different products were categorized as threaded couplers (Table 3.3) and three samples of each product per bar size were monotonically tested to failure.

4.2.2.1 Threaded Couplers (Type A by Dextra)

Figures 4.4 to 4.6 show the measured stress-strain relationships for the No. 5 (16-mm), No. 8 (25-mm), and No. 10 (32-mm) threaded couplers (Type A), respectively. Similar to what was done for headed couplers, the unspliced reference bar data and the coupler failure mode are also included in these figures for completeness. All threaded couplers failed by the bar fracture. However, the reinforcing steel bar of only one No. 10 (32-mm) splice fractured inside the coupler region with no change in the strain capacity. Overall, it can be concluded that this coupler type is a seismic coupler.

This threaded coupler type with the same bar sizes showed consistent stress-strain behavior. The average modulus of elasticity of the No. 5, No. 8, and No. 10 threaded couplers (Type A) was, respectively, 13%, 41%, and 35% lower than the conventional steel bar modulus of elasticity. Furthermore, it can be seen that the strain at the peak stress was approximately the same for the couplers with the same bar sizes. Nevertheless, the average ultimate strain of the No. 5, No. 8, and No. 10 spliced specimens was, respectively, 78%, 77%, and 87% lower than that for the corresponding unspliced reference bars, which are significant. Another observation was that this coupler did not show any strain plateau after yielding.

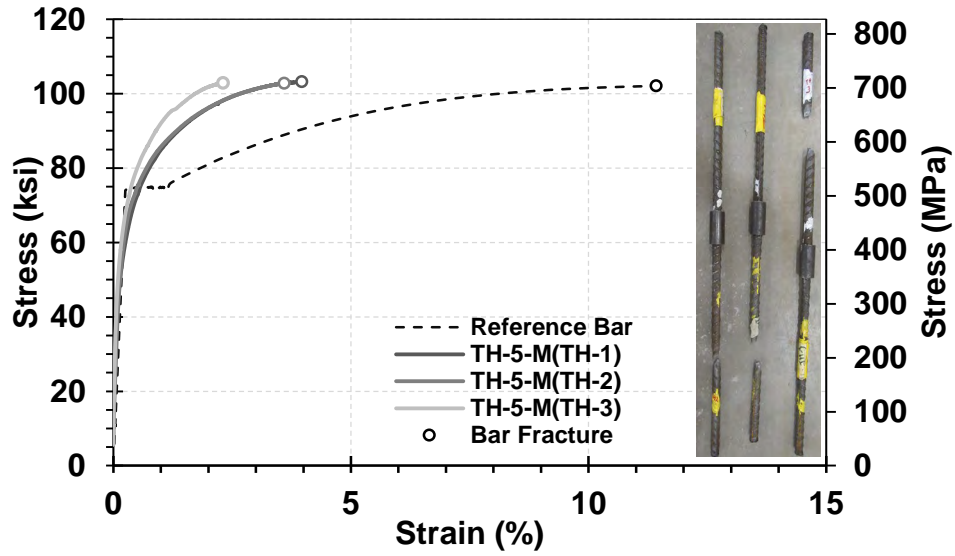


Figure 4.4 Monotonic test results for No. 5 (16-mm) threaded couplers (Type A)

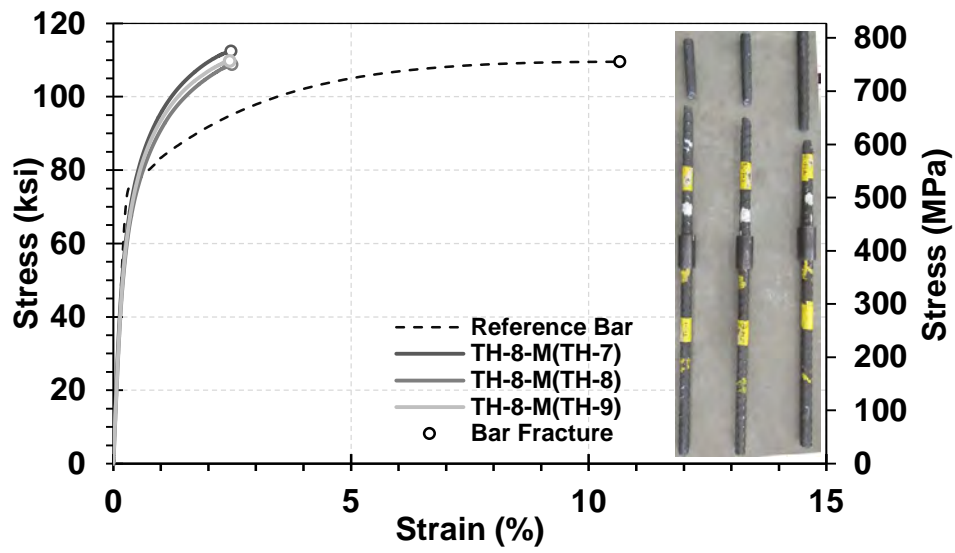


Figure 4.5 Monotonic test results for No. 8 (24-mm) threaded couplers (Type A)

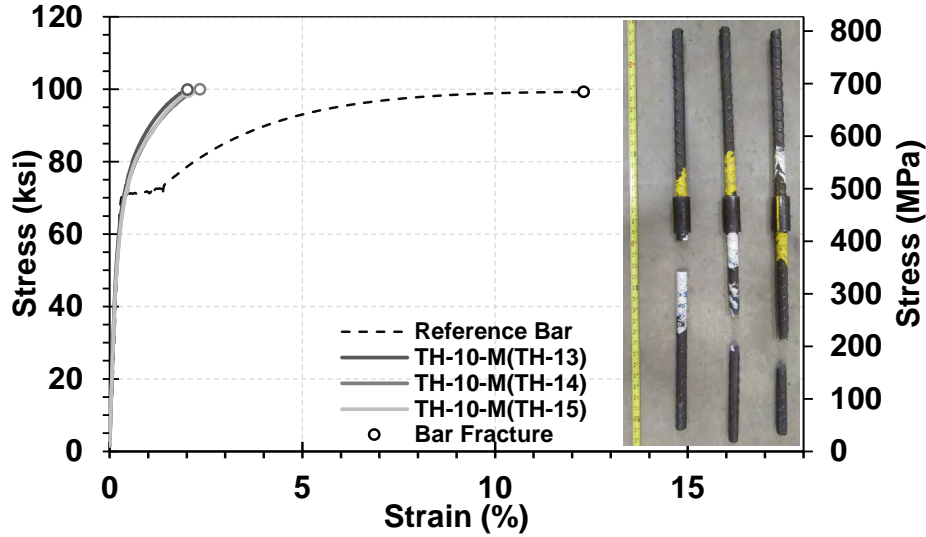


Figure 4.6 Monotonic test results for No. 10 (32-mm) threaded couplers (Type A)

4.2.2.2 Threaded Couplers (Type B by Dextra)

Figures 4.7 to 4.9 show the measured stress-strain relationships for the No. 5 (16-mm), No. 8 (25-mm), and No. 10 (32-mm) threaded couplers (Type B), respectively. All threaded couplers failed by the bar fracture outside the coupler region, thus they are seismic couplers.

The same-size splices showed consistent stress-strain behavior. The average modulus of elasticity of the No. 5, No. 8, and No. 10 threaded couplers (Type B) was, respectively, 42%, 30%, and 26% lower than the conventional steel bar modulus of elasticity. Furthermore, it can be seen that the ultimate strain was approximately the same for the couplers with the same bar sizes. Similar to the Type A threaded couplers, the average ultimate strain of the No. 5, No. 8, and No. 10 Type B threaded couplers was, respectively, 78%, 80%, and 78% lower than that for the corresponding unspliced reference bars. Further, this coupler did not exhibit any strain plateau after the yielding while the reference bar had strain plateau.

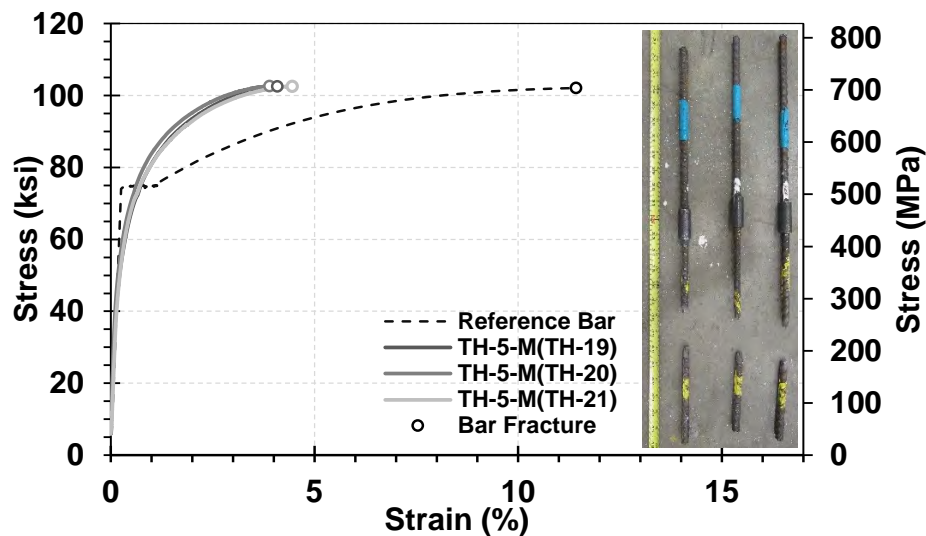


Figure 4.7 Monotonic test results for No. 5 (16-mm) threaded couplers (Type B)

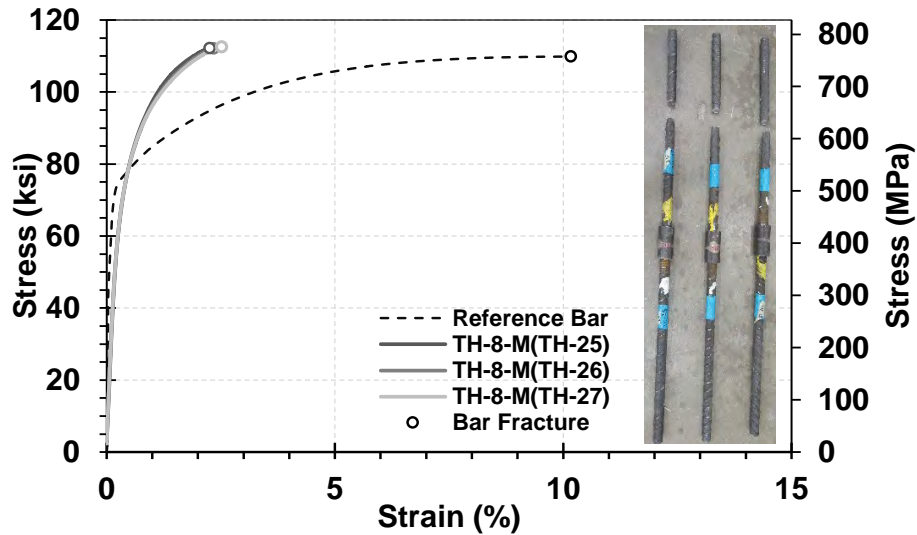


Figure 4.8 Monotonic test results for No. 8 (24-mm) threaded couplers (Type B)

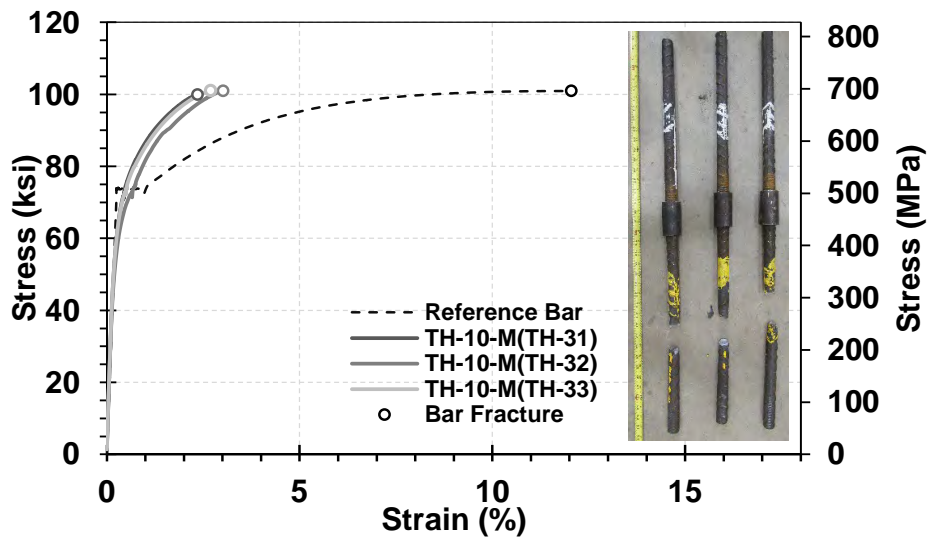


Figure 4.9 Monotonic test results for No. 10 (32-mm) threaded couplers (Type B)

4.2.2.3 Tapered Threaded Couplers (by Erico)

Figures 4.10 to 4.12 show the measured stress-strain relationships for the No. 5 (16-mm), No. 8 (25-mm), and No. 10 (32-mm) tapered threaded couplers, respectively. It can be seen that all tapered threaded couplers failed by the bar fracture outside the coupler region, thus they are seismic couplers.

The same size splices showed consistent stress-strain behavior. The average modulus of elasticity of the No. 5, No. 8, and No. 10 tapered threaded couplers was, respectively, 3%, 12%, and 37% lower than the conventional steel bar modulus of elasticity. Furthermore, the ultimate strain was approximately the same for the couplers with the same bar sizes. The average ultimate strain of the No. 5, No. 8, and No. 10 spliced specimens was, respectively, 47%, 68%, and 67% lower than that for the corresponding unspliced reference bars.

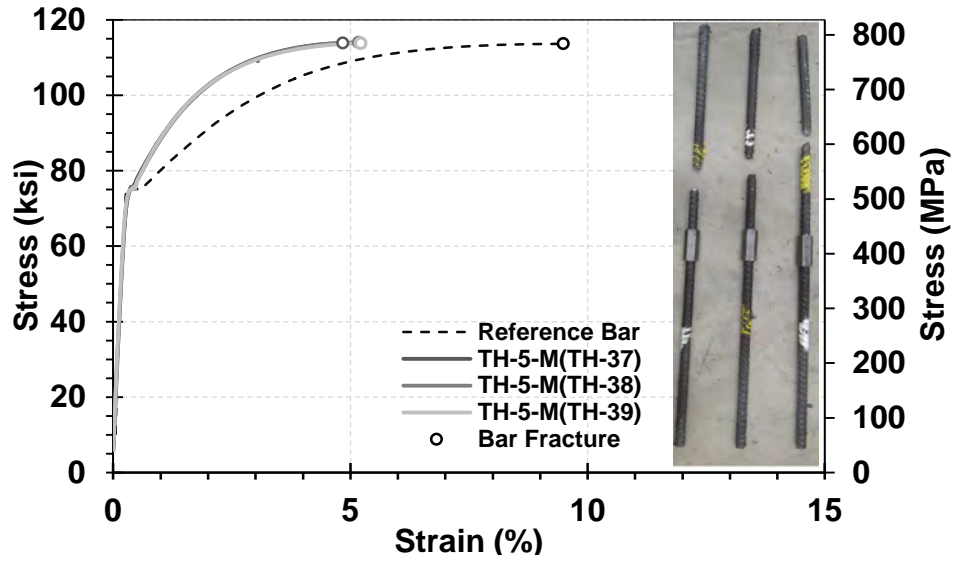


Figure 4.10 Monotonic test results for No. 5 (16-mm) tapered threaded couplers

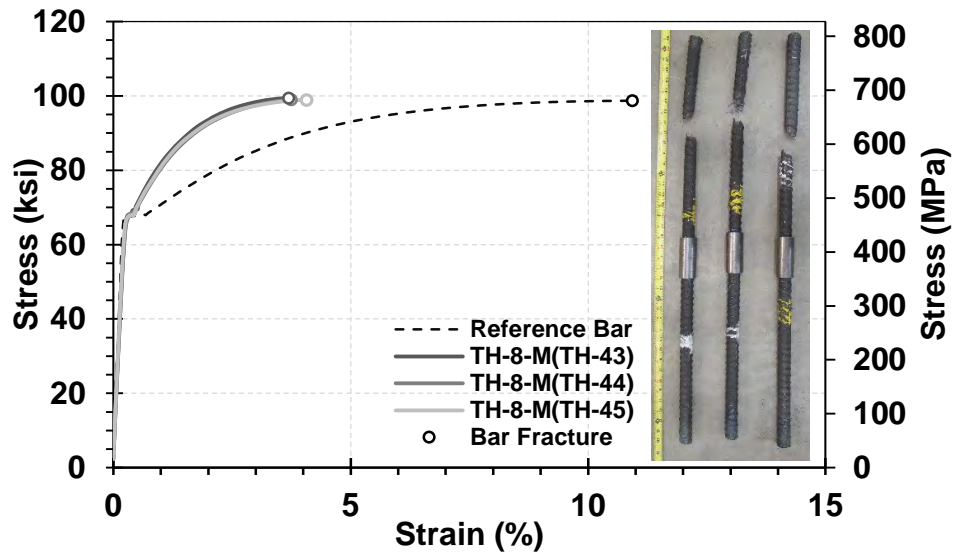


Figure 4.11 Monotonic test results for No. 8 (25-mm) tapered threaded couplers

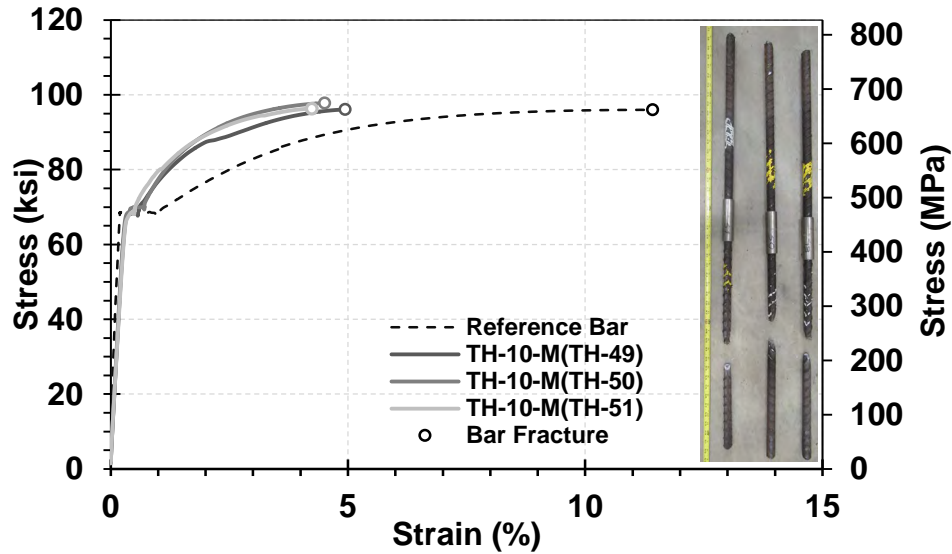


Figure 4.12 Monotonic test results for No. 10 (32-mm) tapered threaded couplers

4.2.3 Swaged Couplers

Figures 4.13 to 4.15 show the measured stress-strain relationships for the No. 5 (16-mm), No. 8 (25-mm), and No. 10 (32-mm) swaged couplers, respectively. One No. 5 (16-mm) swaged coupler (SW-2) failed by the coupler failure, and bar fractured in other eight specimens outside the coupler region. California Test 670 (2004) accepts couplers in which one out of four samples does not fail by the bar fracture. Note only three samples per bar size were tested in this project. Therefore, one may say that No. 5 swaged couplers are not seismic couplers since 33% of the test specimens did not fail by the bar fracture outside the coupler region. However, the measured data showed that the strain capacity of SW-2 is comparable to the other two in which bar fractured. Therefore, it was concluded that all swaged couplers tested in this study, including No. 5, are seismic couplers.

The splices with the same-size bars showed consistent stress-strain behavior. The average modulus of elasticity of the No. 5, No. 8, and No. 10 swaged couplers was, respectively, 11%, 31%, and 32% lower than the conventional steel bar modulus of elasticity. Furthermore, the ultimate strain was approximately the same for the couplers with the same bar sizes. The average ultimate strain of the No. 5, No. 8, and No. 10 spliced specimens was, respectively, 56%, 72%, and 67% lower than that for the corresponding unspliced reference bars.

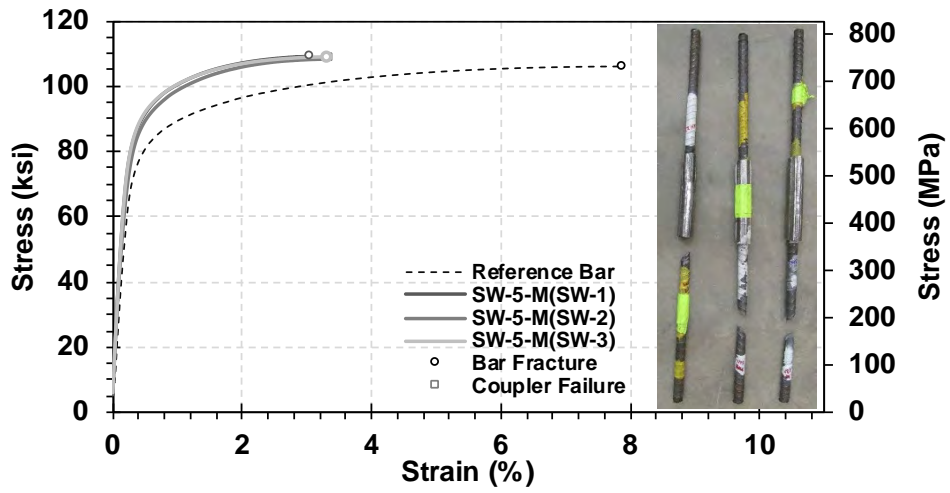


Figure 4.13 Monotonic test results for No. 5 (16-mm) swaged couplers

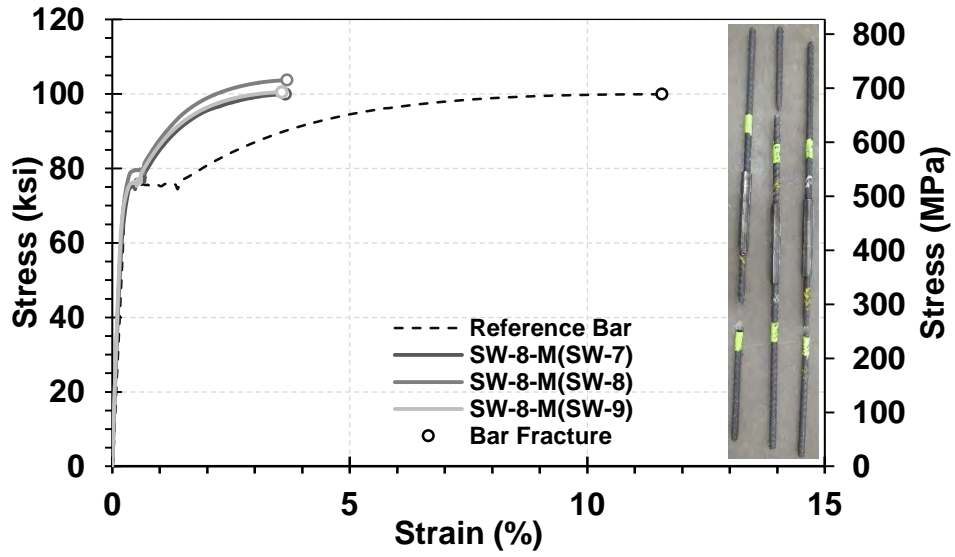


Figure 4.14 Monotonic test results for No. 8 (24-mm) swaged couplers

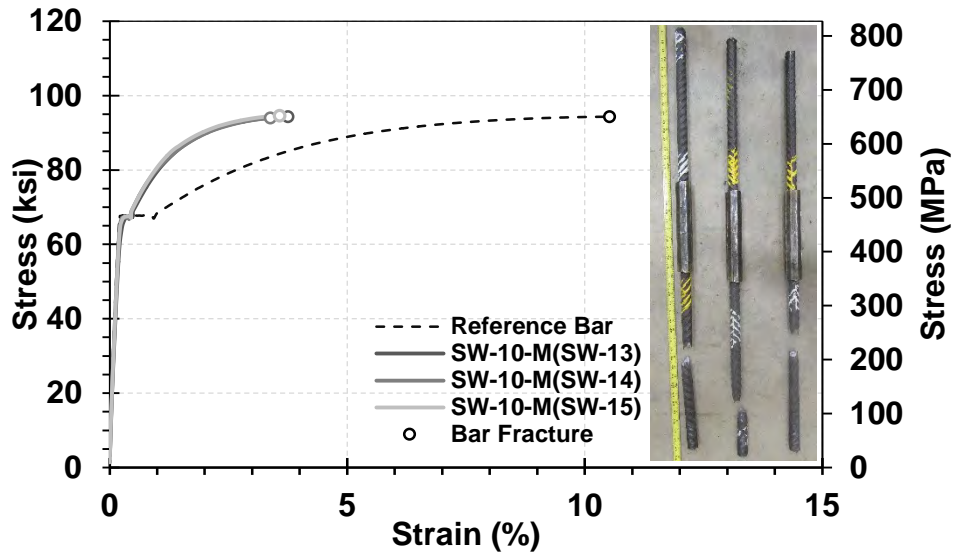


Figure 4.15 Monotonic test results for No. 10 (32-mm) swaged couplers

4.2.4 Grouted Sleeve Couplers

Two products were categorized as grouted sleeve couplers, and three samples of each product per bar size were monotonically tested to failure.

4.2.4.1 Grouted Sleeve Couplers (by Splice Sleeve North America, NMB)

Figures 4.16 to 4.18 show the measured stress-strain relationships for the No. 5 (16 mm), No. 8 (25 mm), and No. 10 (32 mm) grouted sleeve couplers (NMB), respectively. Table 4.1 presents the compressive strength of the grout used in these couplers, which was measured on different days in accordance to ASTM C109 (2012).

It can be seen that all No. 5 grouted sleeve couplers failed by the “bar pullout,” bar fractured in all No. 8 splices, and one No. 10 NMB coupler fractured (GC-13) at the middle of the sleeve. Bar fractured outside the coupler region in the other two No. 10 grouted sleeve splices (GC-14 and GC-15). Therefore, No. 5 (16-mm) NMB grouted sleeve couplers are not seismic couplers. No. 8 (25-mm) NMB grouted sleeve couplers are seismic couplers. Similar to the discussion provided for the swaged couplers, it can be concluded that the No. 10 (32-mm) NMB grouted sleeve couplers are also seismic couplers.

It is worth mentioning that bar deformation patterns may affect the bond strength in grouted couplers, especially for small size bars. Spiral bar deformations will result in a better bond (WJE, 2000). Steel bars used in all of the grouted couplers tested in this study had a spiral deformation.

The same size splices generally showed consistent stress-strain behavior. The average modulus of elasticity of the No. 5, No. 8, and No. 10 couplers was, respectively, 21%, 36%, and 31% lower than the conventional steel bar modulus of elasticity. Furthermore, the ultimate strain was approximately the same for the couplers with the same bar sizes. The average ultimate strain of the No. 5, No. 8, and No. 10 spliced specimens was, respectively, 56%, 72%, and 67% lower than that for the corresponding unspliced reference bars.

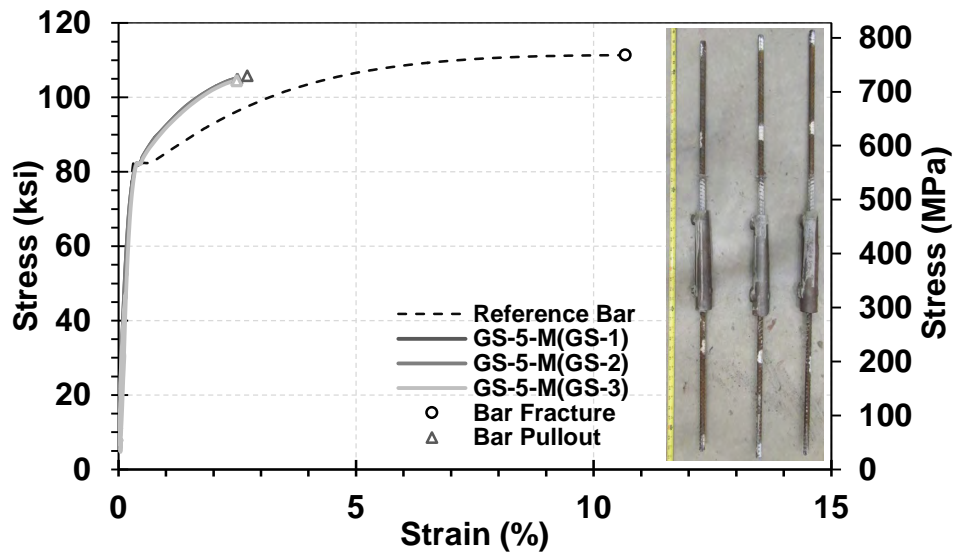


Figure 4.16 Monotonic test results for No. 5 (16-mm) grouted sleeve couplers (NMB)

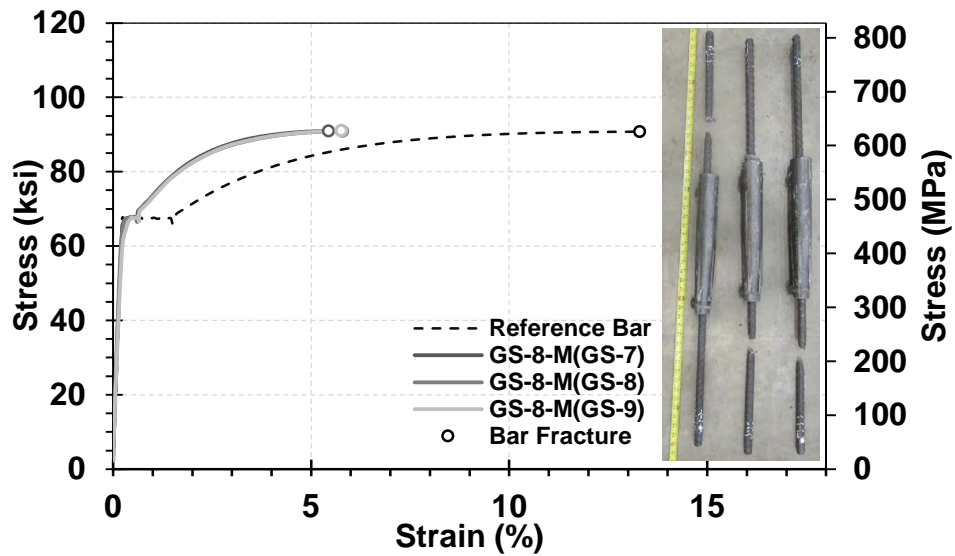


Figure 4.17 Monotonic test results for No. 8 (25-mm) grouted sleeve couplers (NMB)

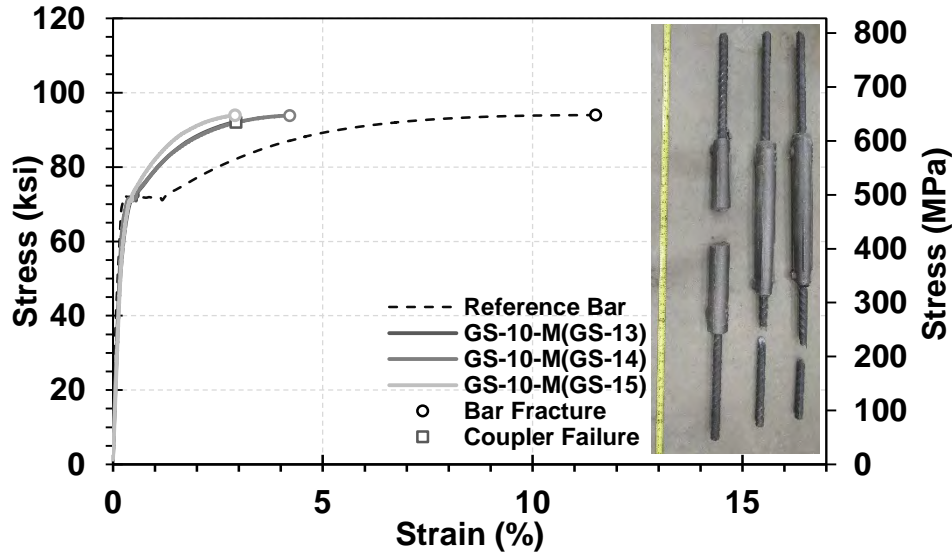


Figure 4.18 Monotonic test results for No. 10 (32-mm) grouted sleeve couplers (NMB)

Table 4.1 Measured compressive strength for grout used in grouted sleeve couplers (NMB)

Coupler Size	7 days, psi (MPa)	28 days, psi (MPa)	First Coupler Test Day, psi (MPa)	Last Coupler Test Day, psi (MPa)
No. 5 (16 mm)	6675 (46.0)	14145 (97.5)	15630 (107.8)	15545 (107.2)
No. 8 (25 mm)	6675 (46.0)	14145 (97.5)	15630 (107.8)	15545 (107.2)
No. 10 (32 mm)	8700 (60.0)	14350 (99.0)	14530 (100.2)	14605 (100.7)

4.2.4.2 Grouted Sleeve Couplers (by Dayton Superior)

Figures 4.19 to 4.21 show the measured stress-strain relationships for the No. 5 (16-mm), No. 8 (25-mm), and No. 10 (32-mm) grouted sleeve couplers (Dayton Superior), respectively. Table 4.2 presents the compressive strength of the grout used in this type of coupler, which was measured on different days in accordance to ASTM C109 (2012). Two No. 5 (16-mm) grouted sleeve couplers failed by the bar pullout and one with bar fracture outside the coupler region; thus, No. 5 (16-mm) grouted sleeve couplers (by Dayton Superior) are not seismic couplers. Bar fractured outside the coupler region for the No. 8 (25-mm) and No. 10 (32-mm) grouted sleeve couplers (by Dayton Superior); thus, they are seismic couplers.

The average modulus of elasticity of the No. 5, No. 8, and No. 10 grouted sleeve couplers (Dayton Superior) was, respectively, 33%, 9%, and 8% lower than the conventional steel bar modulus of elasticity. Furthermore, the ultimate strain of the same-size couplers with the mode of failure of bar fracture was approximately the same. The average ultimate strain of the No. 5, No. 8, and No. 10 spliced specimens was, respectively, 64%, 62%, and 56% lower than that for the corresponding unspliced reference bars.

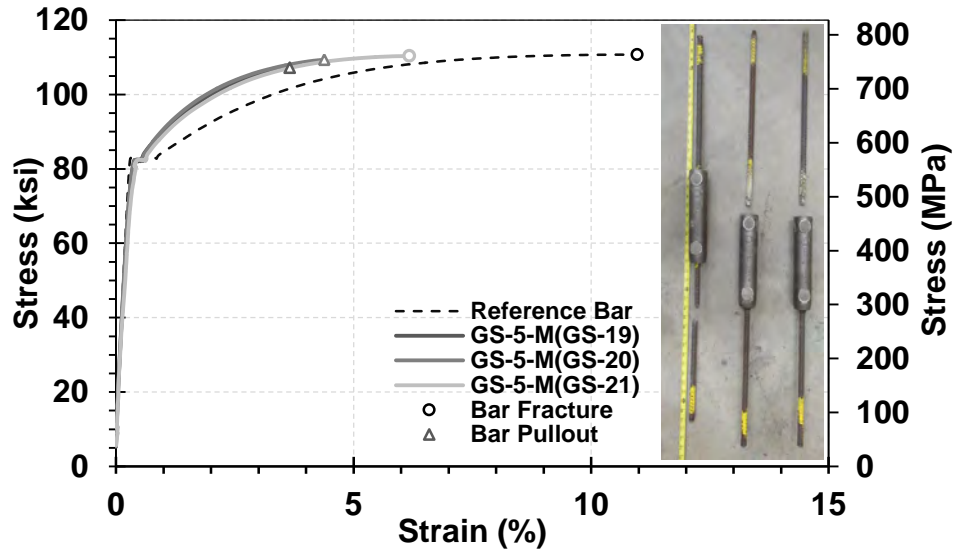


Figure 4.19 Monotonic test results for No. 5 (16-mm) grouted sleeve couplers (Dayton Superior)

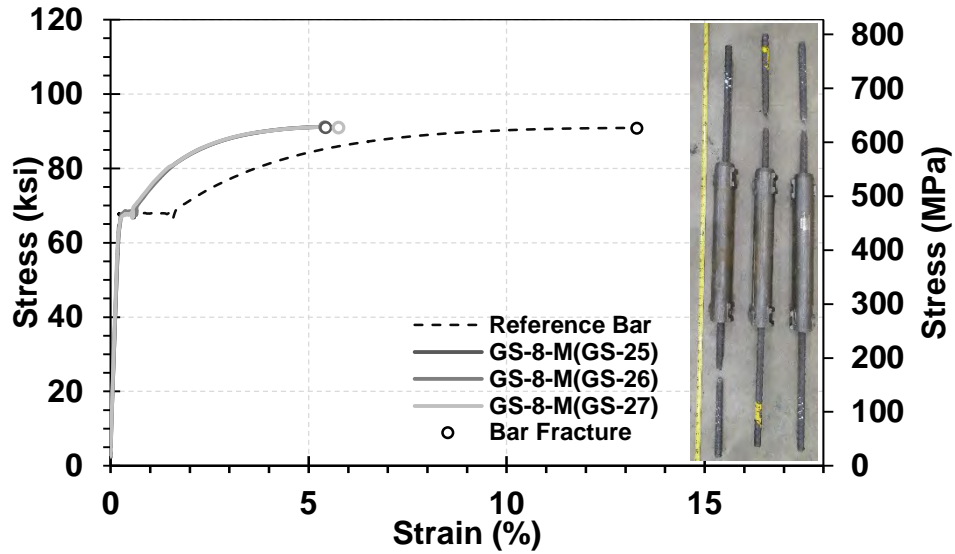


Figure 4.20 Monotonic test results for No. 8 (24-mm) grouted sleeve couplers (Dayton Superior)

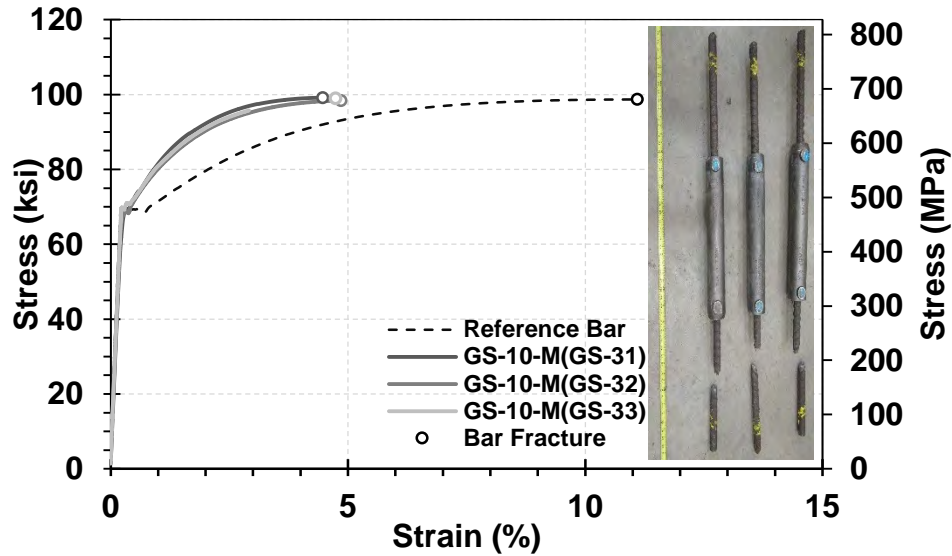


Figure 4.21 Monotonic test results for No. 10 (32-mm) grouted sleeve couplers (Dayton Superior)

Table 4.2 Measured compressive strength for grout used in grouted sleeve coupler (by Dayton)

Coupler Size	7 days, psi (MPa)	28 days, psi (MPa)	First Coupler Test Day, psi (MPa)	Last Coupler Test Day, psi (MPa)
No. 5 (16 mm)	10630 (73.3)	11220 (77.4)	12430 (85.7)	14275 (98.4)
No.8 (25 mm)	10630 (73.3)	11220 (77.4)	12430 (85.7)	14275 (98.4)
No. 10 (32 mm)	12860 (88.7)	13300 (91.7)	13380 (92.2)	13915 (95.9)

4.2.5 Hybrid Couplers

Two products were categorized as hybrid couplers, and three samples of each product per bar size were monotonically tested to failure. In one of the products, bars were spliced through grouted and threaded mechanisms at the ends of the coupler. In the other hybrid coupler, bars were spliced using threaded mechanism at the middle and swaged mechanism at the ends.

4.2.5. Hybrid Couplers (Threaded & Swaged)

Figures 4.22 to 4.24 show the measured stress-strain relationships for the No. 5 (16-mm), No. 8 (25-mm), and No. 10 (32-mm) hybrid couplers (threaded and swaged), respectively. All threaded-swaged hybrid couplers failed by the bar fracture outside the coupler region; thus, they are seismic couplers.

The same size splices generally showed consistent stress-strain behavior. The average modulus of elasticity of the No. 5, No. 8, and No. 10 threaded-swaged hybrid couplers was, respectively, 5%, 3%, and 25% lower than the conventional steel bar modulus of elasticity. Furthermore, the ultimate strain was almost the same for the couplers with the same bar sizes. The average ultimate strain of the No. 5, No. 8, and No. 10 spliced specimens was, respectively, 60%, 74%, and 64% lower than that for the corresponding unspliced reference bars.

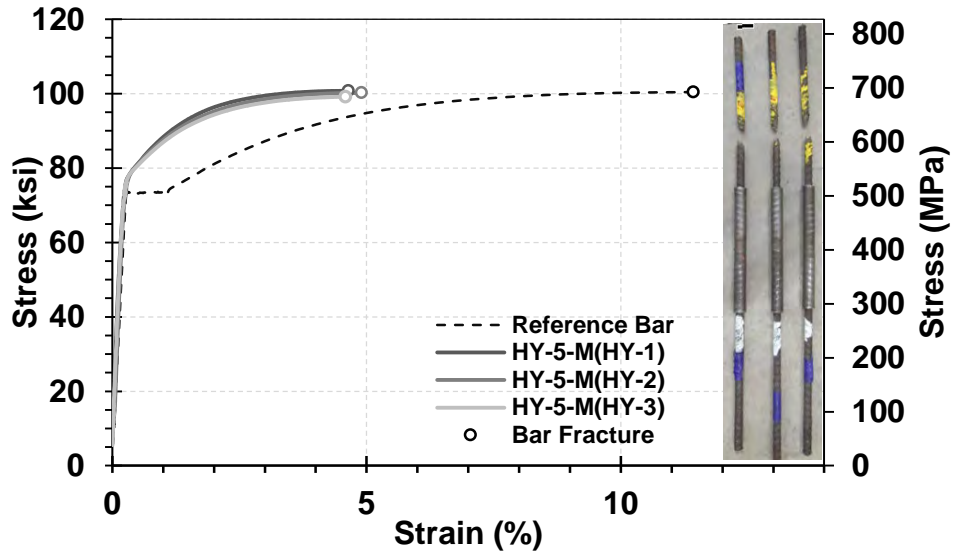


Figure 4.22 Monotonic test results for No. 5 (16-mm) threaded-swaged hybrid couplers

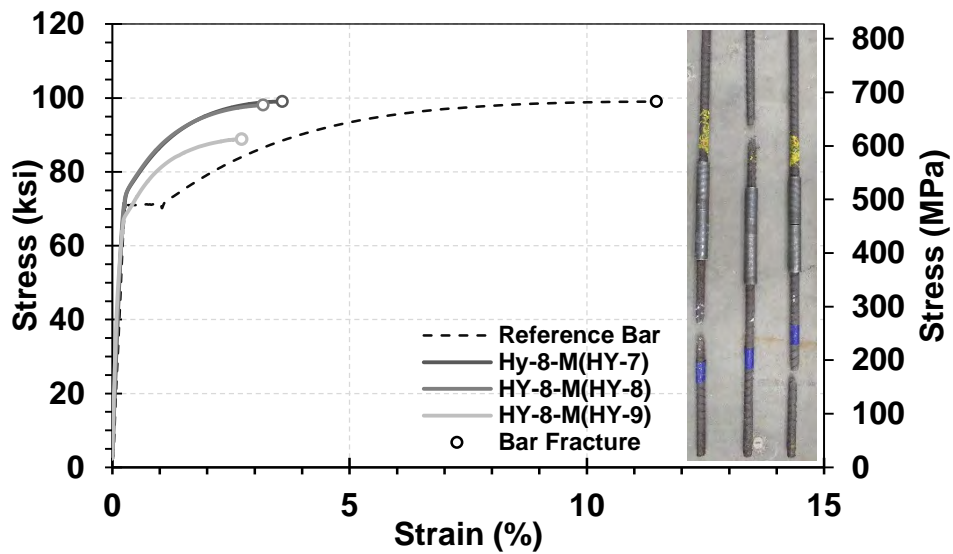


Figure 4.23 Monotonic test results for No. 8 (24-mm) threaded-swaged hybrid couplers

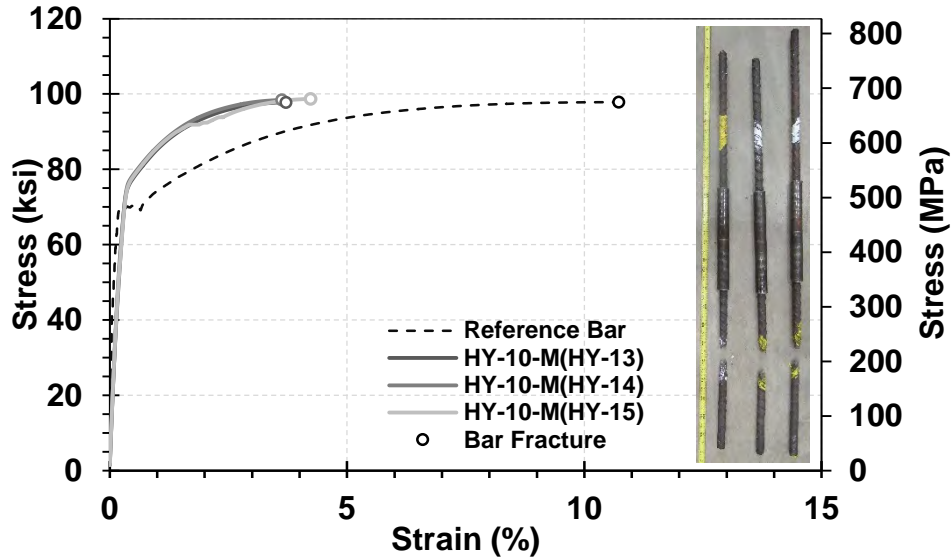


Figure 4.24 Monotonic test results for No. 10 (32-mm) threaded-swaged hybrid couplers

4.2.5.2 Hybrid Couplers (Grouted & Threaded)

Figures 4.25 to 4.27 show the measured stress-strain relationships for the No. 5 (16-mm), No. 8 (25-mm), and No. 10 (32-mm) hybrid couplers (grouted and threaded), respectively. Table 4.3 presents the compressive strength of the grout used in this type of coupler, which was measured on different days in accordance to ASTM C109 (2012). Except for one No. 10 splice (HY-33), all grouted-threaded hybrid couplers failed by the bar fracture outside the coupler region. The tapered threaded bar in HY-33 fractured at the thread, but with the same strength and strain capacity as those for the other two No. 10 couplers. Overall, all grouted-threaded couplers tested in this study are seismic couplers.

The same size splices generally showed consistent stress-strain behavior. The average modulus of elasticity of the No. 5, No. 8, and No. 10 hybrid couplers (grouted-threaded) was, respectively, 14%, 67%, and 33% lower than the conventional steel bar modulus of elasticity. Furthermore, the ultimate strain was approximately the same for the couplers with the same bar sizes. The average ultimate strain of the No. 5, No. 8, and No. 10 spliced specimens was, respectively, 67%, 74%, and 68% lower than that for the corresponding unspliced reference bars.

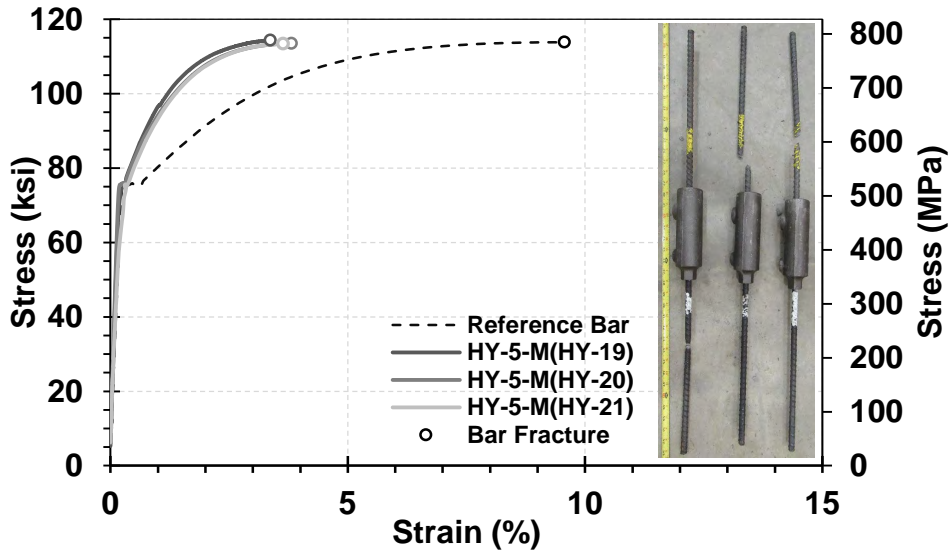


Figure 4.25 Monotonic test results

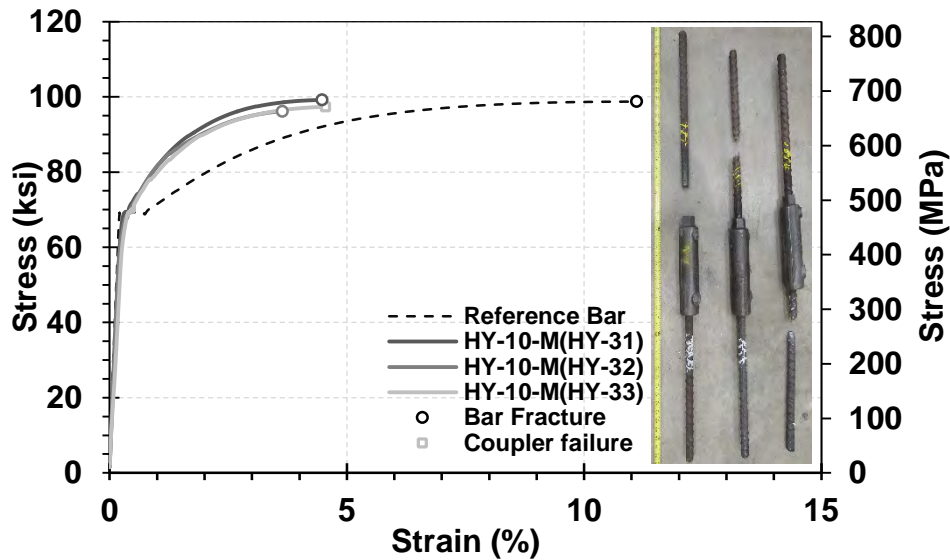


Figure 4.27 Monotonic test results for No. 10 (32-mm) grouted-threaded hybrid couplers

Table 4.3 Measured compressive strength for grout used in grouted-threaded hybrid couplers

Coupler Size	7 days, psi (MPa)	28 days, psi (MPa)	First Coupler Test Day, psi (MPa)	Last Coupler Test Day, psi (MPa)
No. 5 (16 mm)	13805 (95.2)	19920 (137.4)	23760 (163.8)	24105 (166.2)
No.8 (25 mm)	13805(95.2)	19920 (137.4)	23760 (163.8)	24105 (166.2)
No. 10 (32 mm)	14720(101.5)	21080 (145.3)	16280 (112.2)	22480 (155)

4.3 Summary of Coupler Monotonic Test Results

The experimental findings presented in the previous sections indicate that different couplers exhibit different stress-strain behavior depending on their size, type, and product. Tazarv and Saiidi (2016) proposed a generic stress-strain material model for couplers, as discussed in Section 2.5.3.1. The key input of this model is the “coupler rigid length factor, β ” and the mechanical properties of the splicing bars. The coupler rigid length factor should be determined from test data (Eq. 2.1). It was recommended to use the ultimate strains of the spliced and unspliced specimens in the calculation of β . However, one may obtain this factor using multiple points and report the average as the design value.

In an attempt to explore the best procedure of obtaining the coupler rigid length factor, three methods were followed. In the first method, the beta factor (β_u) was calculated using the ultimate strain of the spliced and unspliced specimens as recommended by Tazarv and Saiidi (2016). In the second and third methods, the stress range from the yield to the peak stress was divided into 10 equally spaced stress levels (Figure 4.28), then the spliced and unspliced specimens’ strains corresponding to these stresses were used in the β calculation. β_{3p} was the average of these factors using the last three points, and β_{10p} was the average of these factors using all 10 points.

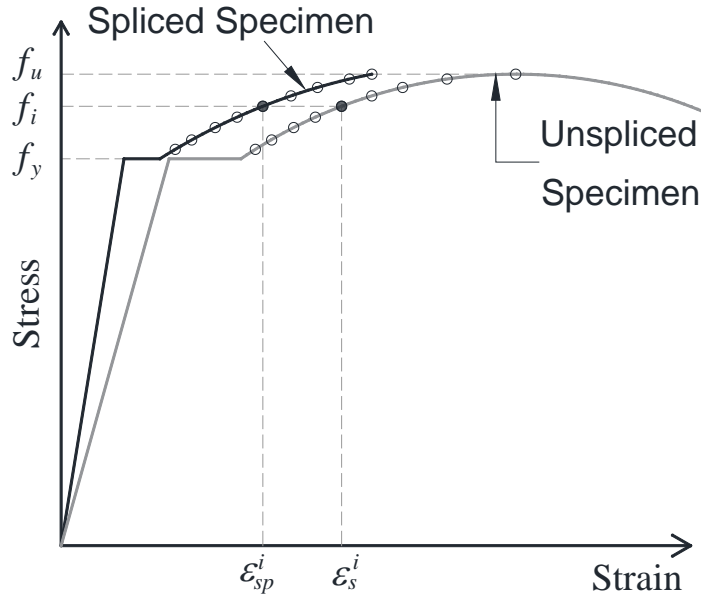


Figure 4.28 Calculation of coupler rigid length factor using measured strain data

4.3.1 Measured Coupler Rigid Length Factors

Table 4.4 presents the coupler rigid length factor obtained for each of 81 couplers tested under the monotonic loading. The three different rigid length factors discussed above, the error between the measured and calculated ultimate strains per method of the calculation of beta, and the coefficient of determination were included in the table. The R^2 shows the correlation between the measured and calculated stress-strain relationships using each beta. An R^2 of 1.0 (or 100 in the table) indicates a perfect match between the measured and calculated stress-strain relationships, and a smaller R^2 indicates an inferior match. Figure 4.29 shows the measured and calculated stress-strain relationships for different coupler types using three values of beta. It can be inferred that all of the three proposed methods of calculation of beta are viable. Nevertheless, the beta using the ultimate point (β_u) resulted in minimal errors between the measured and calculated ultimate strains for all splices, and could reproduce the measured stress-strain behavior with a reasonable accuracy. β_u might be used as the design value for bar couplers.

It should be noted that the main use of this coupler model will be to quantify the coupler effect on the seismic performance of mechanically spliced bridge columns. As discussed in Section 2, previous studies found that couplers usually reduce the displacement capacity of bridge columns. Thus, in a displacement-based design, the ultimate strains of couplers would be more important than the initial behavior to accurately calculate the bridge ultimate displacements. The error in the prior-to-yielding branch of the coupler-calculated stress-strain relationship will have minimal effects on the column seismic behavior since the coupler length is insignificant relative to the column length.

Table 4.4 Measured coupler rigid length factors

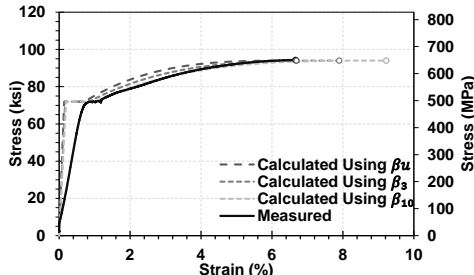
Specimen	L_{sp}	α	L_{cr}	ϵ_u in %	β_u	β_{3p}	β_{10p}	Error in Ultimate Strain, (R^2), All in %		
								β_u	β_{3p}	β_{10p}
Headed Reinforcement Couplers										
HR-5-M(HR-1)	2.40	2.00	4.90	9.8	0.81	0.26	0.15	0.06, (86.59)	45.39, (93.31)	54.11, (92.86)
HR-5-M(HR-2)	2.40	2.00	4.90	10.3	0.90	0.55	0.27	0.07, (88.07)	30.80, (92.78)	55.25, (94.12)
HR-5-M(HR-3)	2.40	2.00	4.90	8.8	0.68	0.58	0.42	0.07, (91.11)	7.40, (91.68)	19.09, (92.22)
HR-8-M(HR-7)	3.25	1.25	5.75	6.4	0.74	0.70	0.37	0.07, (75.43)	3.88, (76.58)	36.46, (81.53)
HR-8-M(HR-8)	3.25	1.25	5.75	6.6	0.72	0.67	0.35	0.07, (73.07)	4.63, (74.42)	35.58, (74.30)
HR-8-M(HR-9)	3.25	1.25	5.75	6.3	0.78	0.73	0.39	0.07, (72.69)	4.91, (74.49)	38.96, (79.63)
HR-10-M(HR-13)	3.88	1.25	7.00	6.7	0.76	0.57	0.36	0.45, (73.17)	18.68, (78.36)	38.64, (82.21)
HR-10-M(HR-14)	3.88	1.25	7.00	8.0	0.48	0.00	0.00	0.20, (68.01)	44.46, (81.05)	53.88, (82.61)
HR-10-M(HR-15)	3.88	1.25	7.00	8.3	0.44	0.00	0.00	0.17, (68.36)	45.26, (77.44)	60.75, (80.30)
Threaded Couplers (Type A)										
TH-5-M(TH-1)	1.75	2.00	4.25	3.9	1.57	1.83	1.71	0.07, (91.33)	31.04, (88.83)	16.20, (90.74)
TH-5-M(TH-2)	1.75	2.00	4.25	3.5	1.68	1.92	1.85	0.07, (94.67)	35.58, (86.86)	32.20, (90.94)
TH-5-M(TH-3)	1.75	2.00	4.25	2.3	1.93	2.09	2.01	0.07, (95.38)	31.75, (88.68)	15.41, (93.63)
TH-8-M(TH-7)	2.63	1.25	5.13	2.5	1.49	1.41	1.07	0.08, (74.43)	18.22, (78.70)	93.92, (73.63)
TH-8-M(TH-8)	2.63	1.25	5.13	2.5	1.49	1.20	0.85	0.08, (75.21)	63.11, (77.80)	139.44, (72.89)
TH-8-M(TH-9)	2.63	1.25	5.13	2.4	1.47	1.21	0.94	0.08, (71.17)	39.11, (78.24)	110.17, (72.95)
TH-10-M(TH-13)	3.06	1.25	6.25	2.0	1.64	1.40	1.31	1.09, (76.89)	28.59, (88.14)	57.97, (93.14)
TH-10-M(TH-14)	3.06	1.25	6.25	2.3	1.52	1.33	1.11	0.89, (77.96)	57.32, (88.14)	80.69, (93.14)
TH-10-M(TH-15)	3.06	1.25	6.25	2.0	1.58	1.43	1.28	1.07, (75.26)	75.62, (82.49)	107.15, (88.39)
Threaded Couplers (Type B)										
TH-5-M(TH-19)	1.75	2.00	4.25	4.1	1.58	1.80	1.53	0.07, (95.38)	25.72, (88.68)	5.72, (93.63)
TH-5-M(TH-20)	1.75	2.00	4.25	3.9	1.63	1.85	1.64	0.07, (93.72)	28.07, (85.90)	1.67, (93.52)
TH-5-M(TH-21)	1.75	2.00	4.25	4.4	1.52	1.70	1.51	0.07, (87.16)	19.46, (77.97)	1.37, (88.07)
TH-8-M(TH-25)	2.63	1.25	5.13	2.3	1.51	1.43	1.01	0.08, (70.81)	19.40, (76.16)	115.70, (74.93)
TH-8-M(TH-26)	2.63	1.25	5.13	2.3	1.46	1.34	0.72	0.08, (76.194)	25.34, (78.76)	151.94, (74.93)
TH-8-M(TH-27)	2.63	1.25	5.13	2.5	1.48	1.39	1.06	0.08, (75.91)	19.44, (79.33)	89.50, (70.94)
TH-10-M(TH-31)	3.06	1.25	6.25	2.4	1.70	1.60	1.50	0.89, (65.17)	59.29, (77.32)	81.91, (83.13)
TH-10-M(TH-32)	3.06	1.25	6.25	3.0	1.64	1.40	1.32	0.67, (62.78)	37.81, (83.05)	81.34, (86.45)
TH-10-M(TH-33)	3.06	1.25	6.25	2.7	1.69	1.43	1.32	0.75, (65.36)	32.46, (79.54)	64.65, (83.92)

Table 4.4 continued

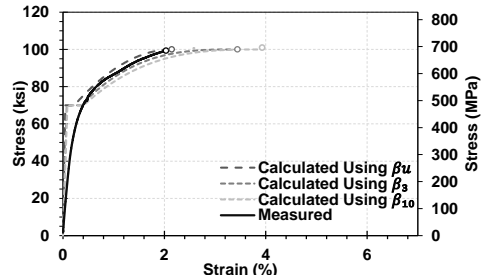
Specimen	L_{sp}	α	L_{cr}	ϵ_u in %	β_u	β_{3p}	β_{10p}	Error in Ultimate Strain, (R^2), All in %		
								β_u	β_{3p}	β_{10p}
Threaded Couplers (Erico)										
TH-5-M(TH-37)	2.38	2.00	4.88	4.8	1.00	0.94	0.89	0.11, (95.94)	5.87, (95.93)	10.71, (95.73)
TH-5-M(TH-38)	2.38	2.00	4.88	5.2	0.89	0.83	0.80	0.08, (96.58)	5.63, (95.84)	8.30, (96.13)
TH-5-M(TH-39)	2.38	2.00	4.88	5.2	0.96	0.85	0.83	0.08, (96.68)	10.13, (96.01)	11.80, (95.91)
TH-8-M(TH-43)	3.75	1.25	6.25	3.7	1.10	1.09	0.99	0.08, (91.56)	2.75, (92.18)	19.12, (94.64)
TH-8-M(TH-44)	3.75	1.25	6.25	3.7	1.13	0.98	0.92	0.08, (88.10)	28.00, (93.99)	38.60, (95.05)
TH-8-M(TH-45)	3.75	1.25	6.25	4.1	1.06	0.98	0.89	0.07, (93.86)	13.37, (95.58)	27.81, (96.45)
TH-10-M(TH-49)	4.20	1.25	7.38	4.9	0.99	0.84	0.87	0.07, (80.90)	16.90, (84.21)	19.36, (83.95)
TH-10-M(TH-50)	4.20	1.25	7.38	4.5	1.04	0.79	0.75	0.06, (75.09)	41.14, (81.13)	34.31, (81.58)
TH-10-M(TH-51)	4.20	1.25	7.38	4.2	1.10	1.03	1.00	0.07, (70.08)	13.13, (73.68)	10.83, (73.15)
Swaged Couplers										
SW-5-M(SW1-1)	5.25	2.00	7.75	3.1	0.91	1.06	0.91	0.08, (84.91)	27.29, (77.75)	1.6, (84.27)
SW-5-M(SW2-1)	5.25	2.00	7.75	3.3	0.92	0.78	0.69	0.09, (84.68)	26.59, (91.76)	42.23, (94.20)
SW-5-M(SW-3)	5.25	2.00	7.75	3.3	0.95	0.87	0.78	0.09, (82.69)	15.70, (92.28)	32.16, (88.33)
SW-8-M(SW-7)	7.90	1.25	10.40	3.6	0.90	0.86	0.83	0.09, (92.26)	10.40, (93.75)	18.20, (94.5)
SW-8-M(SW-8)	7.90	1.25	10.40	3.7	0.89	0.93	0.87	0.08, (92.99)	9.01, (93.75)	6.41, (94.50)
SW-8-M(SW-9)	7.90	1.25	10.40	3.6	0.90	0.95	0.91	0.08, (94.14)	12.53, (92.06)	2.73, (93.77)
SW-10-M(SW-13)	9.50	1.25	12.68	3.8	0.86	0.85	0.81	0.07, (93.22)	1.25, (93.43)	9.60, (94.48)
SW-10-M(SW-14)	9.50	1.25	12.68	3.4	0.97	0.83	0.82	0.07, (89.15)	37.45, (94.92)	39.50, (95.05)
SW-10-M(SW-15)	9.50	1.25	12.68	3.6	0.96	0.86	0.83	0.06, (89.18)	25.68, (93.64)	35.67, (94.51)
Grouted Sleeve Couplers (NMB)										
GS-5-M(GS-1)	9.63	2.00	12.13	2.5	0.94	0.56	0.57			
GS-5-M(GS-2)	9.63	2.00	12.13	2.5	0.96	0.58	0.58	Not Seismic Coupler		
GS-5-M(GS-3)	9.63	2.00	12.13	2.5	0.97	0.56	0.55			
GS-8-M(GS-7)	14.50	1.25	17.00	5.4	0.69	0.68	0.67	0.07, (95.55)	2.05, (95.78)	5.27, (96.08)
GS-8-M(GS-8)	14.50	1.25	17.00	5.8	0.66	0.65	0.65	0.07, (96.45)	1.90, (96.58)	1.92, (96.58)
GS-8-M(GS-9)	14.50	1.25	17.00	5.8	0.66	0.66	0.65	0.07, (95.48)	1.05, (95.86)	3.49, (95.61)
GS-10-M(GS-13)	18.00	1.25	21.20	2.9	0.88	0.67	0.67	0.43, (77.62)	71.56, (92.39)	71.12, (92.35)
GS-10-M(GS-14)	18.00	1.25	21.20	4.2	0.75	0.67	0.67	0.26, (89.00)	18.28, (93.34)	17.19, (93.17)
GS-10-M(GS-15)	18.00	1.25	21.20	2.9	0.88	0.81	0.78	0.41, (77.49)	24.58, (77.31)	32.26, (79.55)

Table 4.4 continued

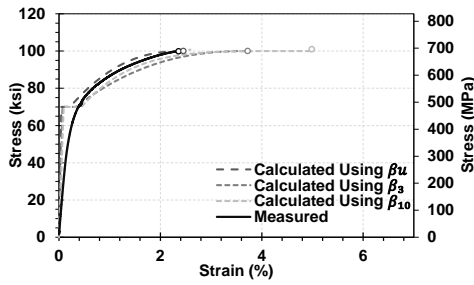
Specimen	L_{sp}	α	L_{cr}	ϵ_u in %	β_u	β_{3p}	β_{10p}	Error in Ultimate Strain, (R^2), All in %		
								β_u	β_{3p}	β_{10p}
Grouted Sleeve Couplers (Dayton)										
GS-5-M(GS-19)	9.50	2.00	12.00	3.6	0.84	0.47	0.49			
GS-5-M(GS-20)	9.50	2.00	12.00	4.4	0.76	0.51	0.52	Not Seismic Coupler		
GS-5-M(GS-21)	9.50	2.00	12.00	6.2	0.55	0.42	0.42			
GS-8-M(GS-25)	16.50	1.25	19.00	5.6	0.67	0.69	0.69	0.07, (95.95)	3.82, (95.63)	3.97, (95.61)
GS-8-M(GS-26)	16.50	1.25	19.00	5.4	0.70	0.70	0.69	0.07, (95.29)	0.05, (95.42)	1.21, (95.31)
GS-8-M(GS-27)	16.50	1.25	19.00	5.5	0.67	0.69	0.70	0.08, (95.45)	3.61, (96.19)	5.17, (96.05)
GS-10-M(GS-31)	18.00	1.25	21.20	4.5	0.70	0.70	0.67	0.24, (92.57)	0.48, (92.54)	7.09, (93.63)
GS-10-M(GS-32)	18.00	1.25	21.20	4.8	0.66	0.57	0.59	0.20, (94.26)	17.97, (96.29)	13.22, (95.92)
GS-10-M(GS-33)	18.00	1.25	21.20	4.7	0.66	0.57	0.59	0.20, (94.83)	17.97, (95.49)	13.22, (95.83)
Hybrid Couplers (Dextra Company)										
HY-5-M(HY-1)	8.13	2.00	10.63	4.6	0.78	0.86	0.92	0.08, (94.63)	15.04, (92.76)	26.15, (90.24)
HY-5-M(HY-2)	8.13	2.00	10.63	4.9	0.74	0.82	0.89	0.08, (88.54)	13.04, (83.75)	25.81, (75.81)
HY-5-M(HY-3)	8.13	2.00	10.63	4.6	0.80	0.84	0.90	0.08, (93.44)	7.28, (87.12)	19.69, (91.84)
HY-8-M(HY-7)	9.31	1.25	11.81	3.6	0.87	0.85	0.88	0.03, (86.79)	5.15, (88.36)	0.98, (86.48)
HY-8-M(HY-8)	9.31	1.25	11.81	3.2	0.93	0.91	0.92	0.02, (83.59)	7.12, (85.98)	2.37, (84.44)
HY-8-M(HY-9)	9.31	1.25	11.81	2.7	0.95	0.89	0.93	0.02, (91.95)	18.86, (95.15)	5.04, (93.02)
HY-10-M(HY-13)	10.63	1.25	13.80	3.7	0.85	0.79	0.80	0.08, (70.07)	13.63, (76.10)	10.25, (74.78)
HY-10-M(HY-14)	10.63	1.25	13.80	3.6	0.90	0.88	0.91	0.08, (75.29)	4.42, (77.74)	1.86, (74.25)
HY-10-M(HY-15)	10.63	1.25	13.80	4.2	0.79	0.72	0.79	0.07, (77.95)	12.78, (82.62)	0.63, (77.71)
Hybrid Couplers (Erico International)										
HY-5-M(HY-19)	7.88	2.00	10.38	3.4	0.80	0.79	0.73	0.10, (92.30)	4.03, (93.08)	11.66, (94.00)
HY-5-M(HY-20)	7.88	2.00	10.38	3.8	0.85	0.83	0.80	0.11, (95.32)	2.91, (96.31)	13.37, (96.92)
HY-5-M(HY-21)	7.88	2.00	10.38	3.6	0.79	0.72	0.70	0.10, (93.27)	12.26, (94.26)	16.92, (94.33)
HY-8-M(HY-25)	8.75	1.25	11.25	4.5	0.78	0.75	0.73	0.08, (94.37)	6.81, (95.58)	10.38, (96.10)
HY-8-M(HY-26)	8.75	1.25	11.25	2.8	0.77	0.78	0.76	0.08, (95.05)	1.08, (94.86)	1.25, (95.29)
HY-8-M(HY-27)	8.75	1.25	11.25	3.8	0.86	0.84	0.93	0.08, (98.02)	4.83, (97.87)	16.59, (97.49)
HY-10-M(HY-31)	10.75	1.25	13.93	4.5	0.77	0.77	0.73	0.07, (91.65)	0.31, (91.60)	7.25, (92.91)
HY-10-M(HY-32)	10.75	1.25	13.93	3.6	0.88	0.82	0.81	0.07, (84.77)	16.07, (89.02)	16.52, (89.12)
HY-10-M(HY-33)	10.75	1.25	13.93	4.6	0.78	0.81	0.79	0.06, (84.89)	6.69, (83.13)	1.75, (84.47)



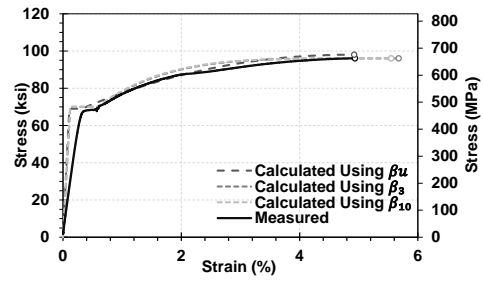
a. Headed Reinforcement



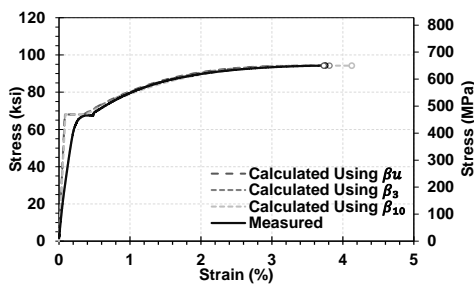
b. Threaded Type A by Dextra



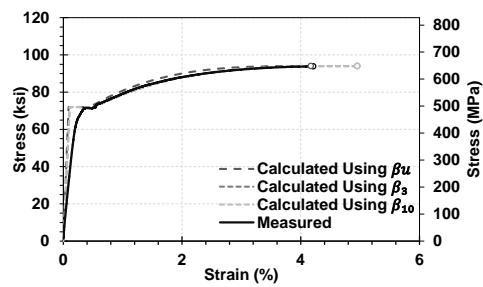
c. Threaded Type B by Dextra



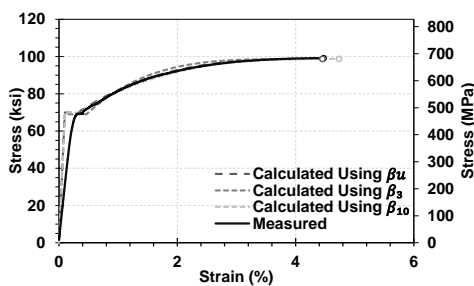
d. Taper Threaded Erico



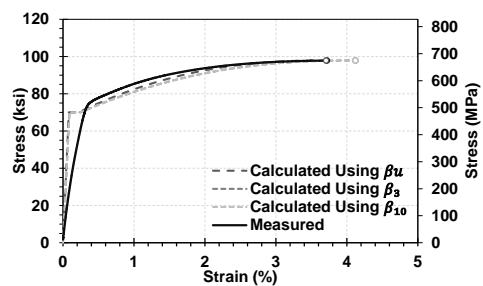
e. Swaged



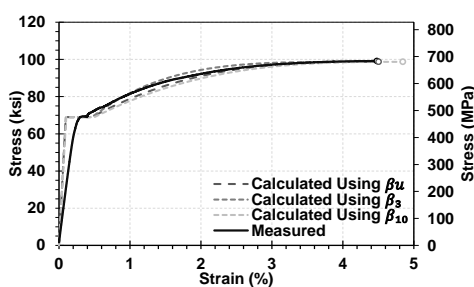
f. Grouted Sleeve by NMB



g. Grouted Sleeve by Dayton



h. Hybrid by Dextra



i. Hybrid by Erico

Figure 4.29 Calculated and measured stress-strain relationships for No.10 (32-mm) couplers using different Beta

Table 4.5 presents the failure mode for all 81 couplers tested under the monotonic loading. It can be concluded that bar fractured in most of these splices, except No. 5 (16-mm) grouted sleeve couplers. Small size bars are not usually used as the longitudinal reinforcement of bridge columns. Therefore, the selected No. 8 (25-mm) and No. 10 (32-mm) couplers in the present study are seismic couplers and may be used in the plastic hinge region of bridge columns following a verified design method, such as those proposed by Tazarv and Saiidi (2016).

Table 4.5 Coupler failure modes under monotonic loading

Coupler Type	Size	Failure Mode			Remarks
		Bar Fracture	Bar Pullout	Coupler Failure	
Headed Bar Coupler	No. 5 (16 mm)	XXX			Seismic Coupler
	No. 8 (24 mm)	XXX			Seismic Coupler
	No. 10 (32 mm)	XXX			Seismic Coupler
Swaged Coupler	No. 5 (16 mm)	XXX			Seismic Coupler
	No. 8 (24 mm)	XX		X	Seismic Coupler
	No. 10 (32 mm)	XXX			Seismic Coupler
Threaded Coupler (Type A)	No. 5 (16 mm)	XXX			Seismic Coupler
	No. 8 (24 mm)	XXX			Seismic Coupler
	No. 10 (32 mm)	XXX			Seismic Coupler
Threaded Coupler (Type B)	No. 5 (16 mm)	XXX			Seismic Coupler
	No. 8 (24 mm)	XXX			Seismic Coupler
	No. 10 (32 mm)	XXX			Seismic Coupler
Threaded Coupler (Taper)	No. 5 (16 mm)	XXX			Seismic Coupler
	No. 8 (24 mm)	XXX			Seismic Coupler
	No. 10 (32 mm)	XXX			Seismic Coupler
Grouted Coupler (NMB)	No. 5 (16 mm)		XXX		
	No. 8 (24 mm)	XXX			Seismic Coupler
	No. 10 (32 mm)	XXX			Seismic Coupler
Grouted Coupler (Dayton)	No. 5 (16 mm)	X	XX		
	No. 8 (24 mm)	XXX			Seismic Coupler
	No. 10 (32 mm)	XXX			Seismic Coupler
Hybrid Coupler (Threaded and Swaged)	No. 5 (16 mm)	XXX			Seismic Coupler
	No. 8 (24 mm)	XXX			Seismic Coupler
	No. 10 (32 mm)	XXX			Seismic Coupler
Hybrid Coupler (Grouted and Threaded)	No. 5 (16 mm)	XXX			Seismic Coupler
	No. 8 (24 mm)	XXX			Seismic Coupler
	No. 10 (32 mm)	XX		X	Seismic Coupler

X = one sample

4.3.2 Recommended Coupler Rigid Length Factors (β)

Table 4.6 presents the proposed rigid length factor for different coupler types and sizes. These values are based on the average of three measured β_u rounded up to the nearest 0.05.

Table 4.6 Recommended coupler rigid length factors (β)

Coupler Type	No. 5 (16 mm)	No. 8 (24 mm)	No. 10 (32 mm)
Headed Reinforcement	0.80	0.75	0.55
Threaded (Dextra-Type A)	1.70	1.5	1.60
Threaded (Dextra-Type B)	1.60	1.5	1.65
Threaded (Erico)	0.95	1.10	1.05
Swaged	0.90	0.90	0.95
Grouted Sleeve (NMB)	0.95	0.65	0.85
Grouted Sleeve (Dayton)	0.70	0.70	0.65
Hybrid (Dextra)	0.80	0.90	0.85
Hybrid (Erico)	0.80	0.80	0.80

Figure 4.30 shows the stress-strain relationships for the spliced and unspliced No. 10 ASTM A706 Grade 60 (2009) reinforcing steel bars using the AASHTO SGS (2011) expected properties. The spliced specimen behavior was based on the recommended β presented in Table 4.6. It can be seen that the headed coupler exhibits the highest strain capacity (66.7% of the unspliced bar) and the threaded coupler shows the lowest strain capacity (10% of the unspliced bar) compared with other coupler types. Furthermore, the strain capacity of swaged, grouted, and hybrid couplers are in the range of 25% to 40% of the unspliced reinforcing steel bar ultimate strain.

It should be noted that the coupler length, coupler location, and coupler rigid length factor are needed to successfully quantify the coupler effect on the seismic performance of bridge columns based on the methods proposed in Tazarv and Saiidi (2016). Therefore, an extreme rigid length factor for a coupler does not necessarily mean that the displacement capacity of a bridge column incorporating that coupler is significantly affected. All three parameters should be included when investigating the coupler effects on ductile member performance.

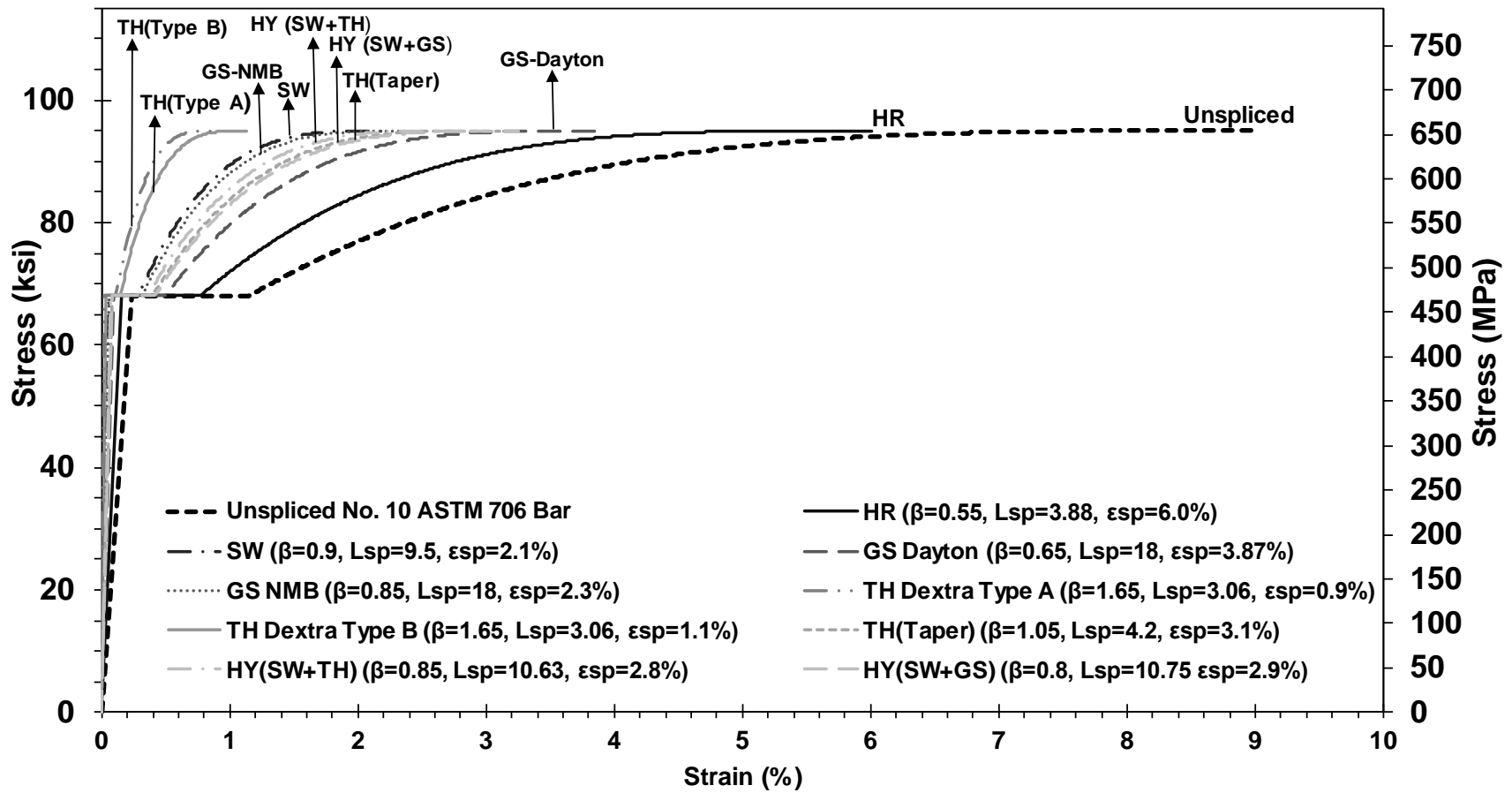
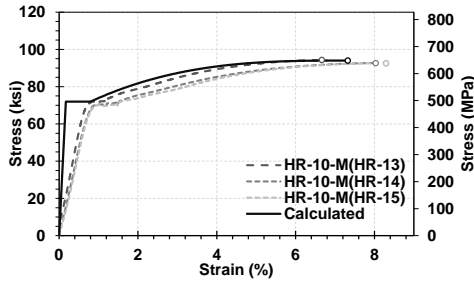


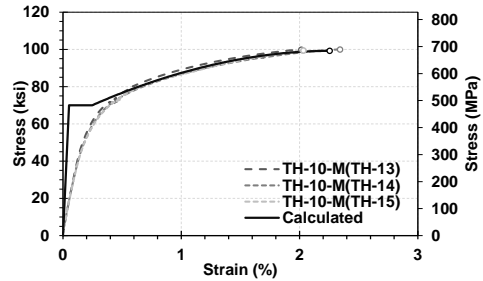
Figure 4.30 Calculated stress-strain relationships for spliced and unspliced No.10 (32-mm) ASTM A706 reinforcing steel bars

4.3.3 Coupler Material Model Verification

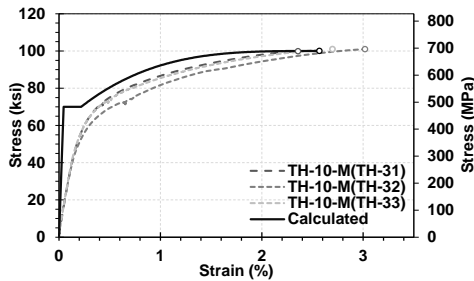
Figure 4.31 shows the calculated and measured stress-strain relationships for different mechanical bar splices using the recommended coupler rigid length factors (Table 4.6). The measured data for all three specimens tested per coupler product were included in the figure for comparison. It can be seen that the coupler model using the recommended rigid length factors could reproduce the measured behavior with good accuracy. The calculated ultimate strains were no more than 15% different than the average measured ultimate strains per product (shown in subfigures). The splice prior-to-yielding behavior could not be well predicted, and mainly overestimated, since the model proposed by Tazarv and Saiidi (2016) is calibrated for the ultimate strains, which are important in the displacement-based design of bridge columns. As discussed before, the higher initial stiffness seen in this coupler model is expected to have minimal effects on the seismic performance of bridge columns due to the relatively small length of couplers compared with the column length.



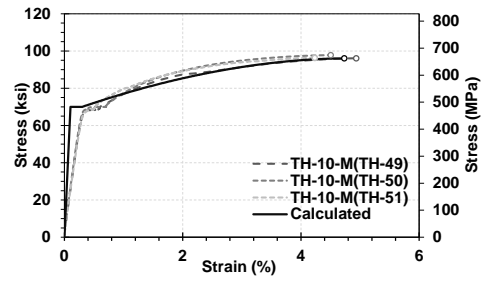
a. Headed Reinforcement



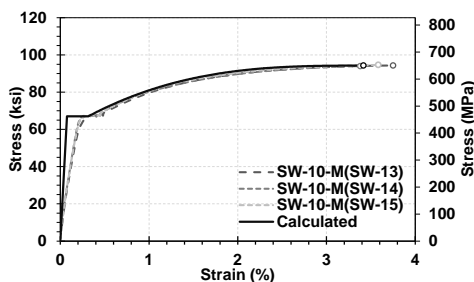
b. Threaded Type A by Dextra



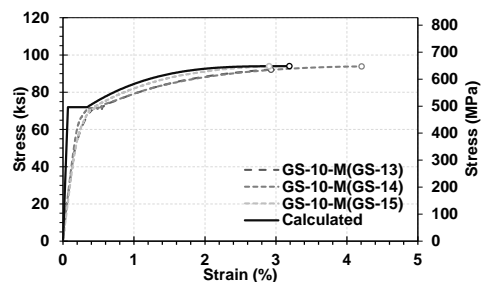
c. Threaded Type B by Dextra



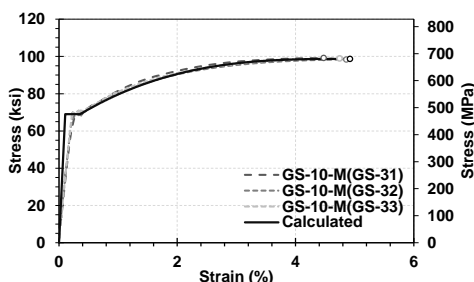
d. Taper Threaded Erico



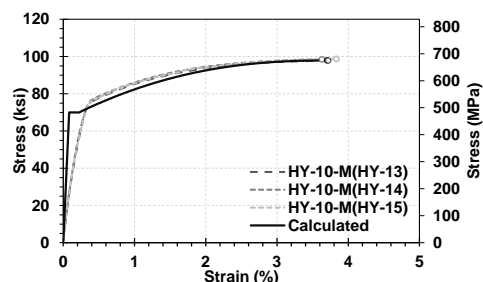
e. Swaged



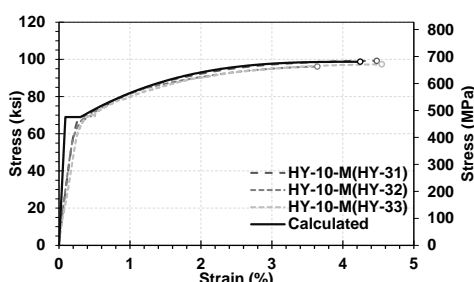
f. Grouted Sleeve by NMB



g. Grouted Sleeve by Dayton



h. Hybrid by Dextra



i. Hybrid by Erico

Figure 4.31 Calculated and measured stress-strain relationships for No.10 (32-mm) couplers using recommended Beta

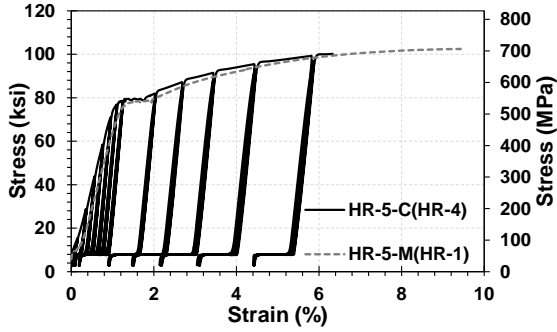
4.4 Coupler Cyclic Test Results

Cyclic testing of 81 mechanical bar splices was performed using the loading protocol described in Section 3.5.2. The measured stress-strain relationship from the monotonic testing of the same coupler type and size was utilized as reference data for the cyclic testing. In some of the cyclic tests, coupler extensometer strains (Figure 3.2) were not reliable. Furthermore, the coupler extensometer was removed before the splice failure to avoid damaging the device. Due to these issues, strains from both the extensometer and the machine head displacements were included in the following sections for completeness and for better understanding the coupler cyclic performance.

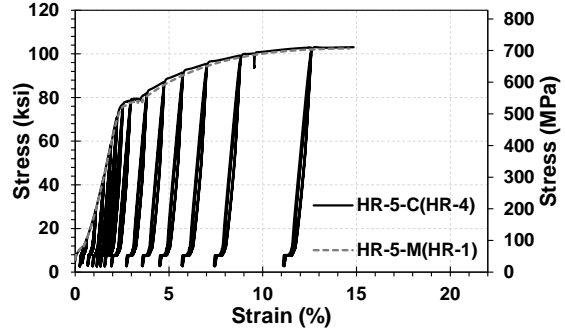
4.4.1 Headed Reinforcement Couplers

Nine headed reinforcement couplers were tested under the cyclic loading, three samples per bar size. Figures 4.32 to 4.34 show the measured cyclic stress-strain hysteresis for the No. 5 (16-mm), No. 8 (25-mm), and No. 10 (32-mm) headed reinforcement couplers, respectively. In all cases, the envelope of the splice cyclic behavior was the same as the monotonic behavior. The hysteretic loop was close to what is expected for a steel bar, but sometimes with a minor pinching at the reloading stresses (e.g., Figure 4.32), which could be because of a small gap between the headed bars inside the couplers.

Figure 4.35 shows the mode of failure for these samples after completion of the cyclic testing. Bar fractured in all of the headed reinforcement couplers outside the coupler region; thus, they are seismic couplers under cyclic loads.

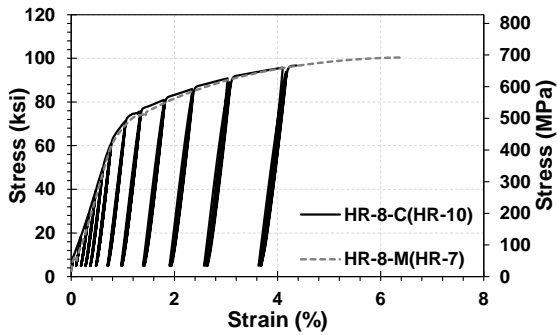


a. Coupler region strains using extensometer displacements

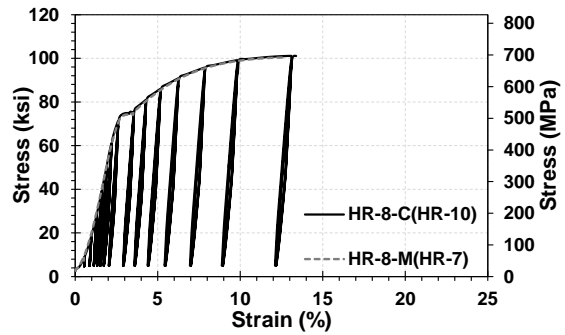


b. Specimen total strains using actuator displacements

Figure 4.32 Cyclic test results for No. 5 (16-mm) headed reinforcement couplers

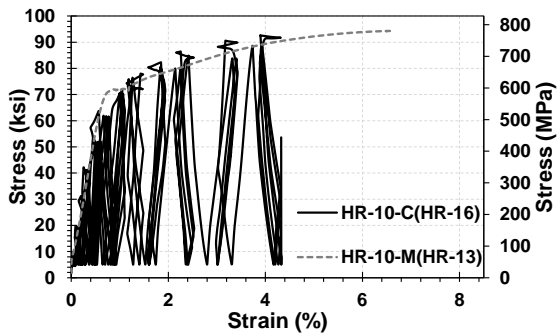


a. Coupler region strains using extensometer displacements

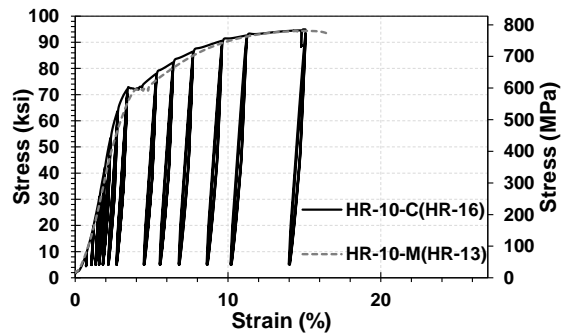


b. Specimen total strains using actuator displacements

Figure 4.33 Cyclic test results for No. 8 (24-mm) headed reinforcement couplers



a. Coupler region strains using extensometer displacements



b. Specimen total strains using actuator displacements

Figure 4.34 Cyclic test results for No. 10 (32-mm) headed reinforcement couplers

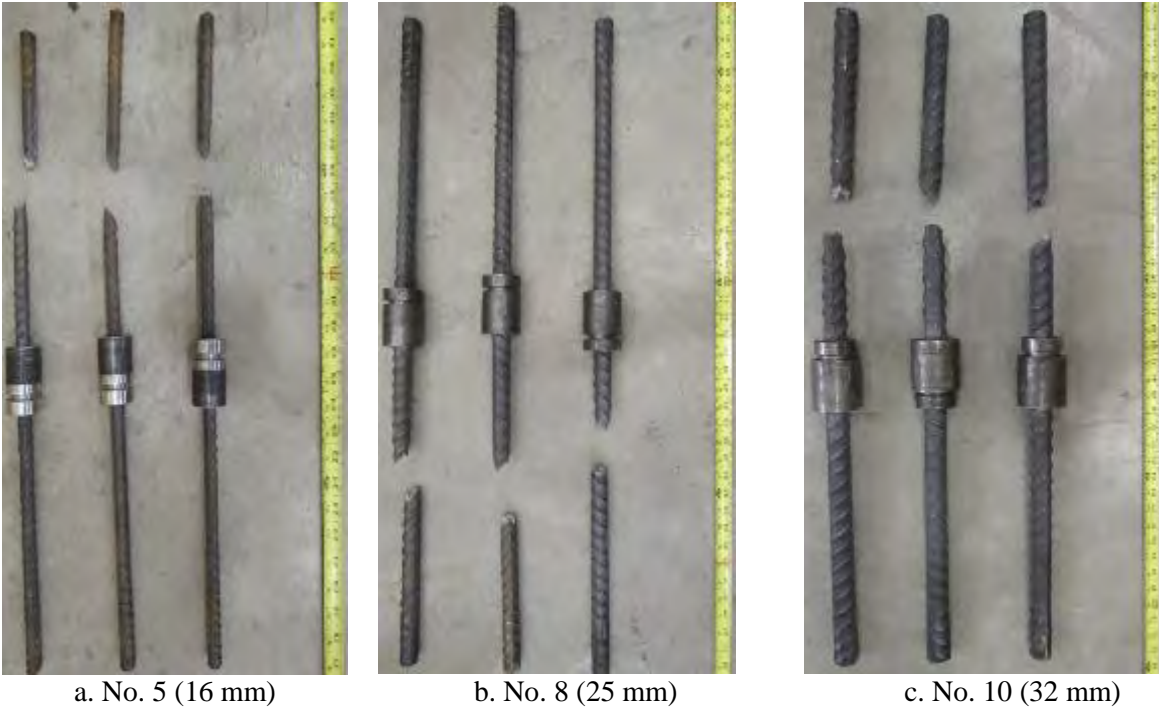


Figure 4.35 Failure of headed reinforcement couplers under cyclic loading

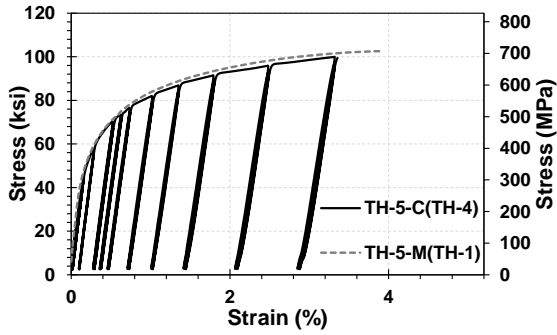
4.4.2 Threaded Couplers

Three products were categorized as the threaded coupler, and three samples of each product per bar size were cyclically tested to failure.

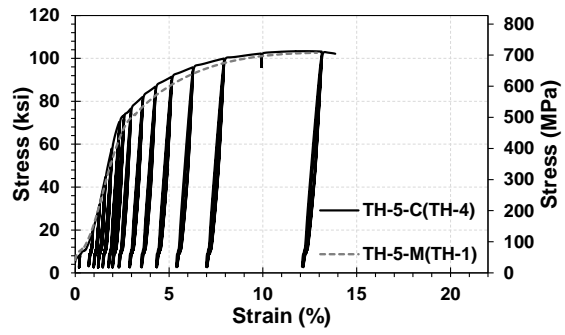
4.4.2.1 Threaded Couplers (Type A by Dextra)

Nine threaded couplers (Type A) were tested under the cyclic loading, three samples per bar size. Figures 4.36 to 4.38 show the measured cyclic stress-strain hysteresis for the No. 5 (16-mm), No. 8 (25-mm), and No. 10 (32-mm) threaded (Type A) couplers, respectively. In all cases, the envelope of the splice cyclic behavior was approximately the same as the monotonic behavior. The hysteretic loop was close to what is expected for a steel bar.

Figure 4.39 shows the mode of failure for these samples after completion of the cyclic testing. Bar fractured in all threaded couplers (Type A) outside the coupler region; thus, they are seismic couplers under cyclic loads.

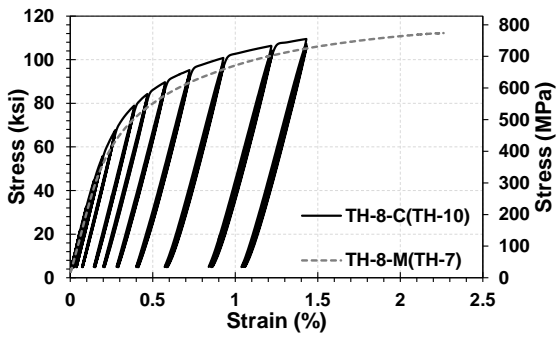


a. Coupler region strains using extensometer displacements

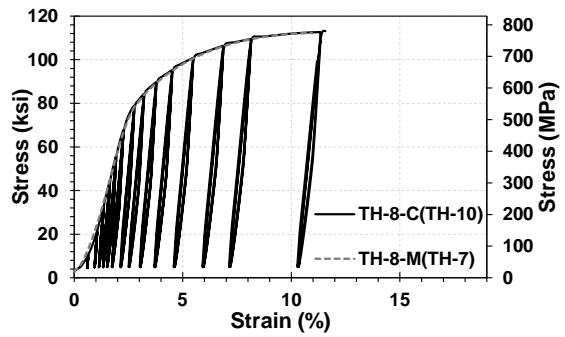


b. Specimen total strains using actuator displacements

Figure 4.36 Cyclic test results for No. 5 (16-mm) threaded couplers (Type A)

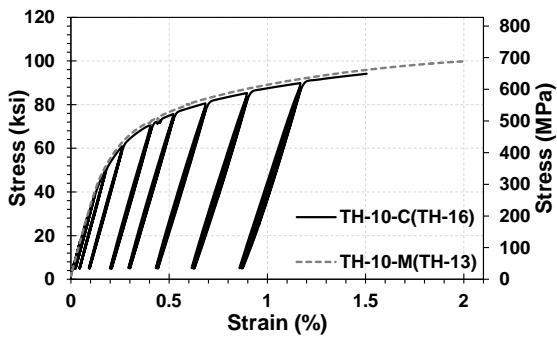


a. Coupler region strains using extensometer displacements

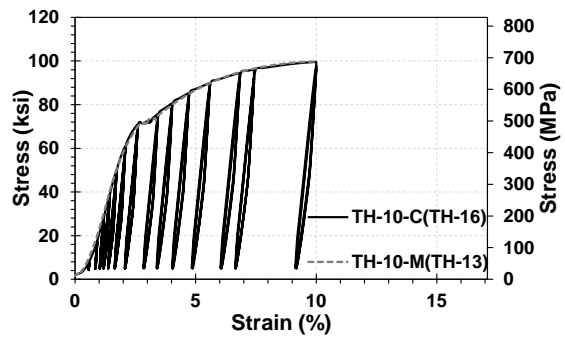


b. Specimen total strains using actuator displacements

Figure 4.37 Cyclic test results for No. 8 (24-mm) threaded couplers (Type A)



a. Coupler region strains using extensometer displacements



b. Specimen total strains using actuator displacements

Figure 4.38 Cyclic test results for No. 10 (32-mm) threaded couplers (Type A)

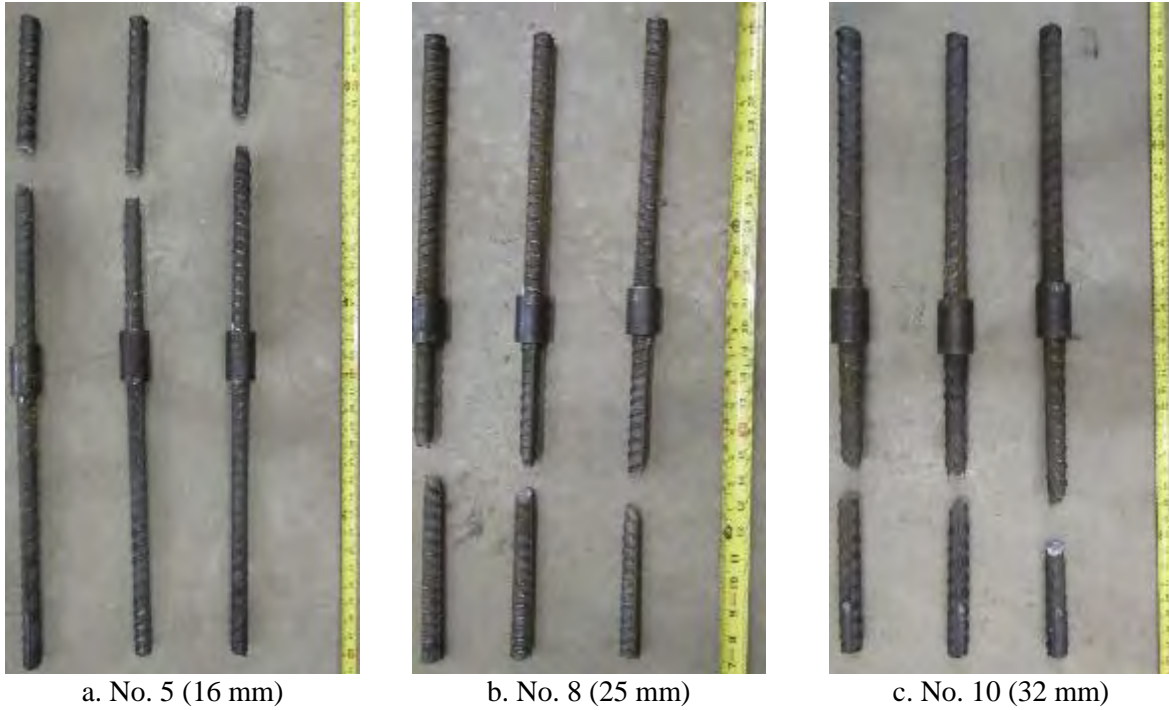
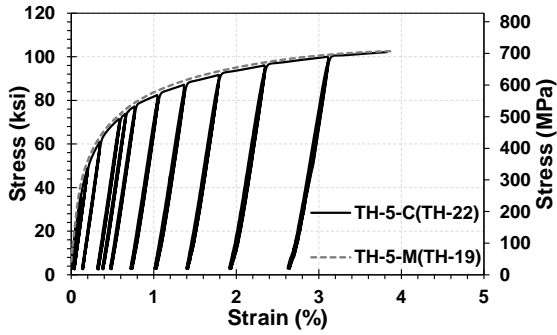


Figure 4.39 Failure of threaded couplers (Type A) under cyclic loading

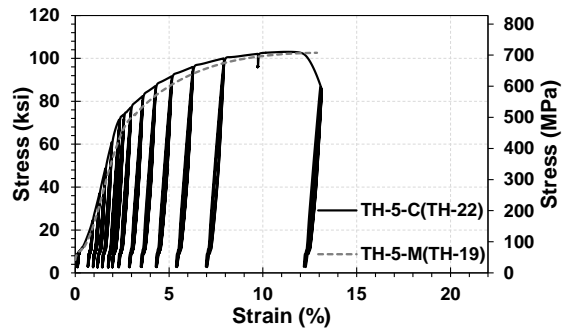
4.4.2.2 Threaded Couplers (Type B by Dextra)

Nine threaded couplers (Type B) were tested under the cyclic loading, three samples per bar size. Figures 4.40 to 4.42 show the measured cyclic stress-strain hysteresis for the No. 5 (16-mm), No. 8 (25-mm), and No. 10 (32-mm) threaded couplers (Type B), respectively. In all cases, the envelope of the splice cyclic behavior was the same as the monotonic behavior. The hysteretic loop was close to what is expected for a steel bar.

Figure 4.43 shows the mode of failure for these samples after completion of the cyclic testing. Bar fractured in all the threaded couplers (Type B) outside the coupler region; thus, they are seismic couplers under cyclic loads.

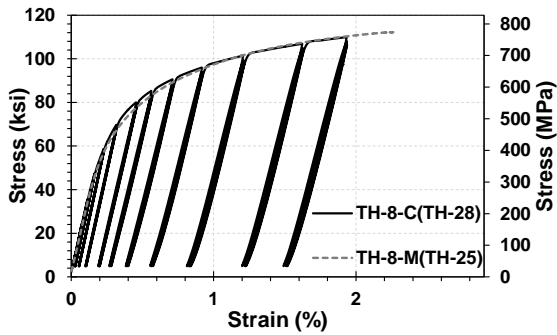


a. Coupler region strains using extensometer displacements

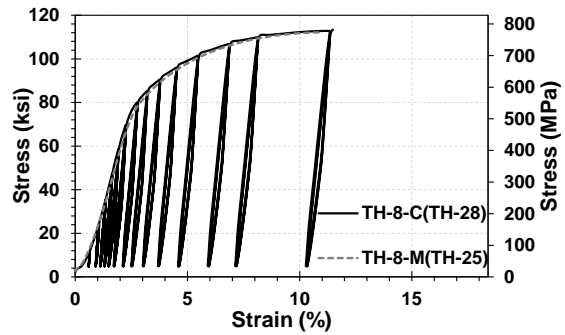


b. Specimen total strains using actuator displacements

Figure 4.40 Cyclic test results for No. 5 (16-mm) threaded couplers (Type B)

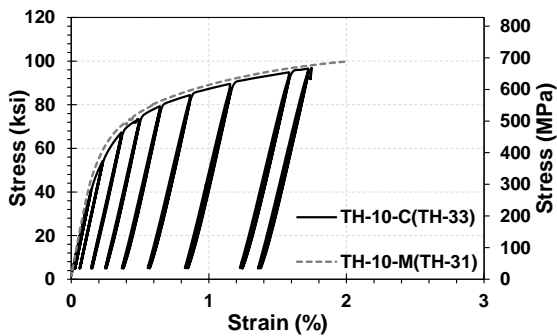


a. Coupler region strains using extensometer displacements

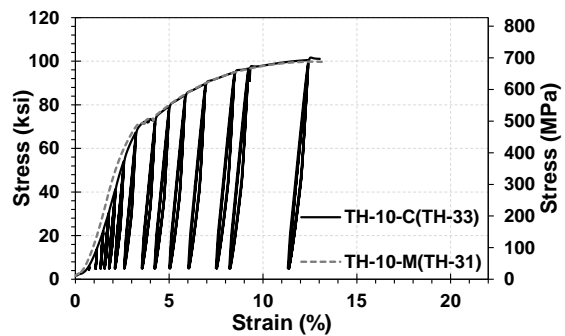


b. Specimen total strains using actuator displacements

Figure 4.41 Cyclic test results for No. 8 (24-mm) threaded couplers (Type B)



a. Coupler region strains using extensometer displacements



b. Specimen total strains using actuator displacements

Figure 4.42 Cyclic test results for No. 10 (32-mm) threaded couplers (Type B)

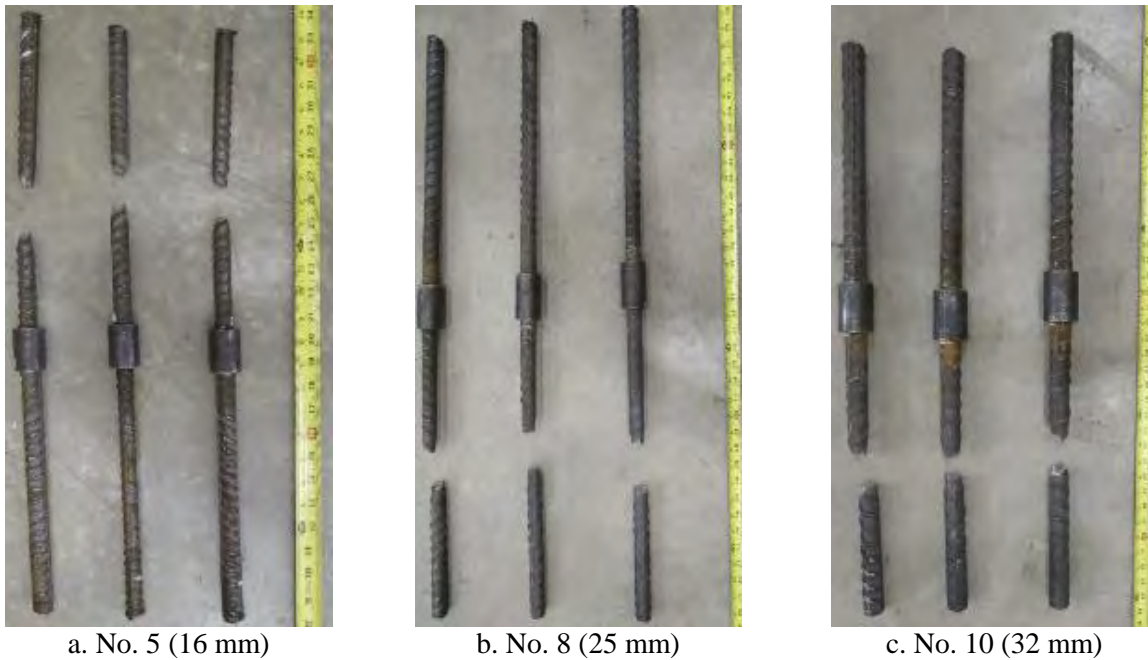
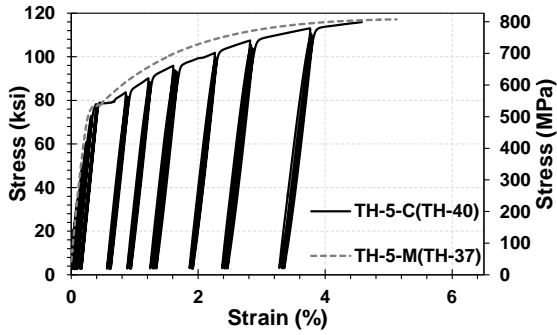


Figure 4.43 Failure of threaded couplers (Type B) under cyclic loading

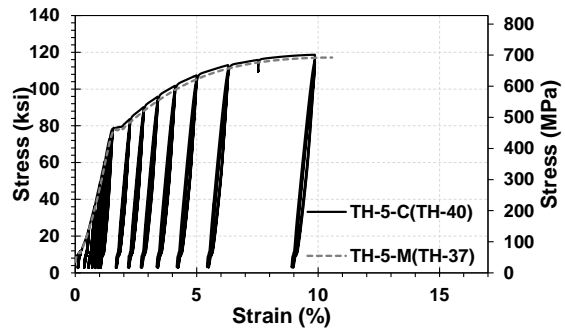
4.4.2.3 Tapered Threaded Couplers (by Erico)

Nine tapered threaded couplers were tested under the cyclic loading, three samples per bar size. Figures 4.44 to 4.46 show the measured cyclic stress-strain hysteresis for the No. 5 (16-mm), No. 8 (25-mm), and No. 10 (32-mm) tapered threaded couplers, respectively. In all cases, the envelope of the splice cyclic behavior was approximately the same as the monotonic behavior. The hysteretic loop was close to what is expected for a steel bar.

Figure 4.47 shows the mode of failure for these samples after completion of the cyclic testing. Bar fractured in all the tapered threaded couplers outside the coupler region; thus, they are seismic couplers under cyclic loads.

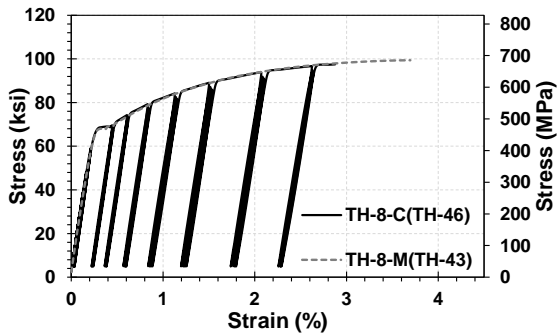


a. Coupler region strains using extensometer displacements

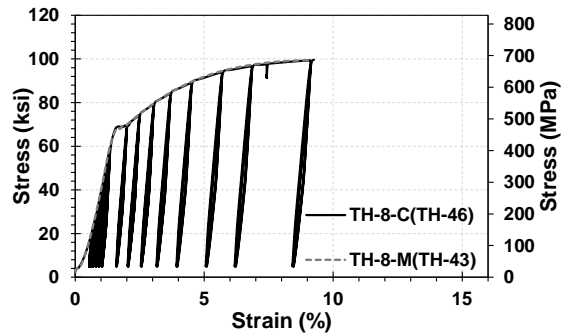


b. Specimen total strains using actuator displacements

Figure 4.44 Cyclic test results for No. 5 (16-mm) tapered threaded couplers

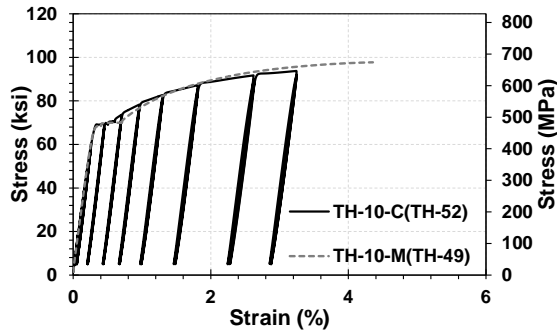


a. Coupler region strains using extensometer displacements

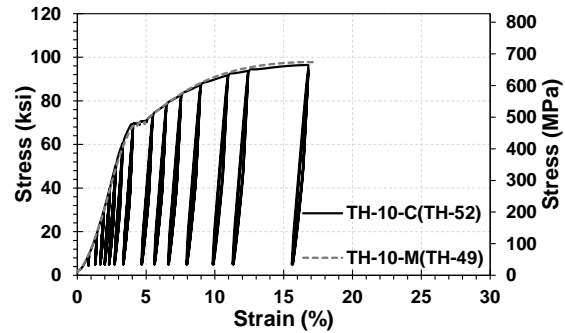


b. Specimen total strains using actuator displacements

Figure 4.45 Cyclic test results for No. 8 (24-mm) tapered threaded couplers



a. Coupler region strains using extensometer displacements



b. Specimen total strains using actuator displacements

Figure 4.46 Cyclic test results for No. 10 (32-mm) tapered threaded couplers

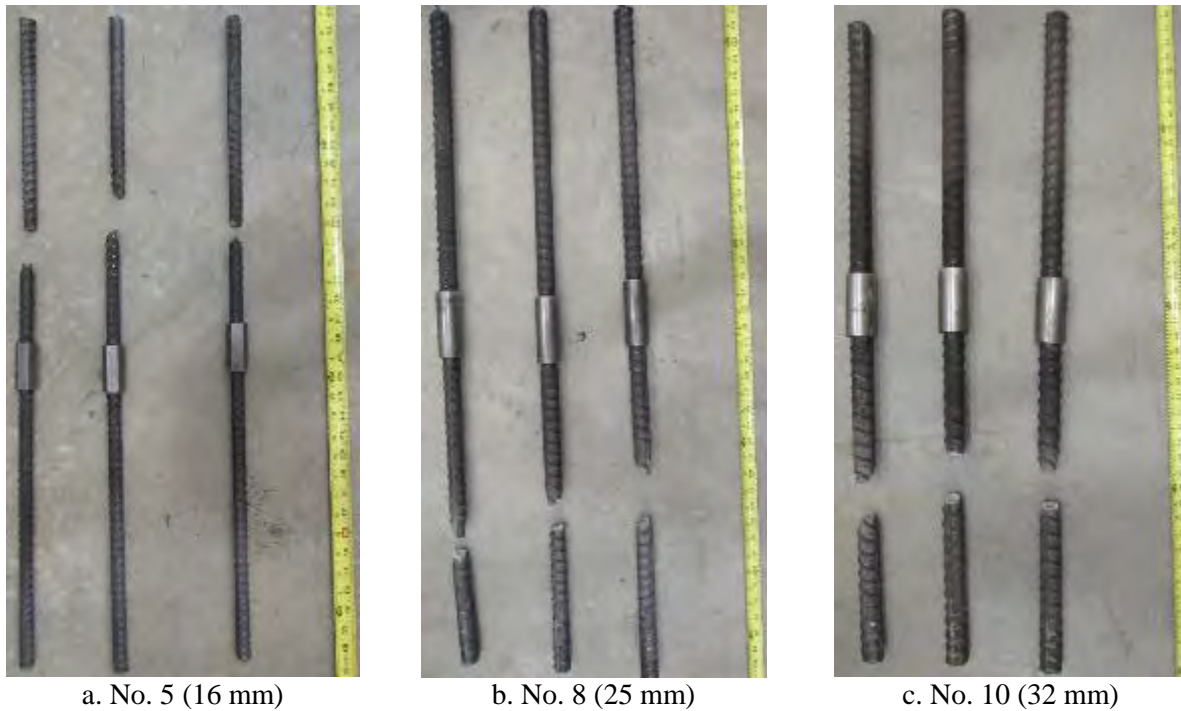
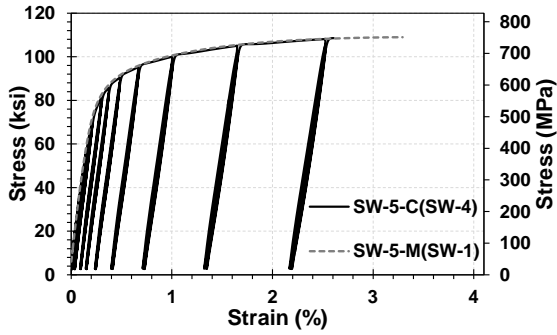


Figure 4.47 Failure of tapered threaded couplers under cyclic loading

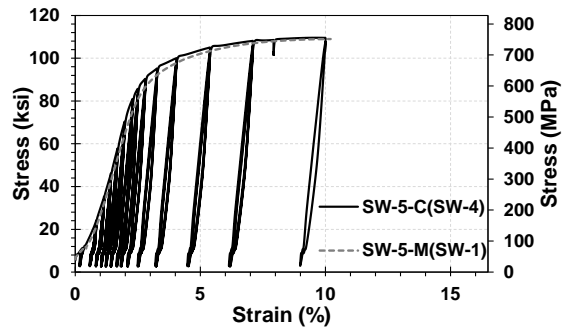
4.4.3 Swaged Couplers

Nine swaged couplers were tested under the cyclic loading, three samples per bar size. Figures 4.48 to 4.50 show the measured cyclic stress-strain hysteresis for the No. 5 (16-mm), No. 8 (25-mm), and No. 10 (32-mm) swaged couplers, respectively. In all cases, the envelope of the splice cyclic behavior was approximately the same as the monotonic behavior. The hysteretic loop was close to what is expected for a steel bar.

Figure 4.51 shows the mode of failure for these samples after completion of the cyclic testing. Bar fractured in all of the swaged couplers outside the coupler region; thus, they are seismic couplers under cyclic loads.

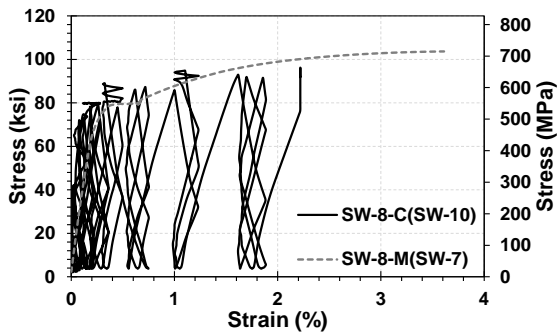


a. Coupler region strains using extensometer displacements

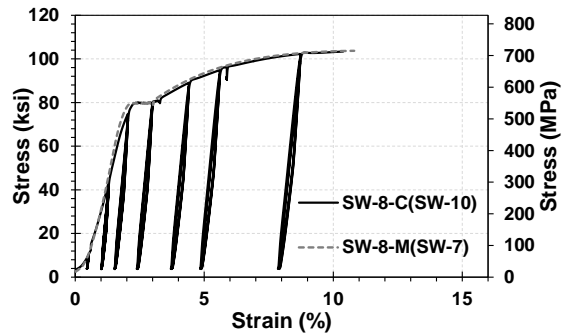


b. Specimen total strains using actuator displacements

Figure 4.48 Cyclic test results for No. 5 (16-mm) swaged couplers

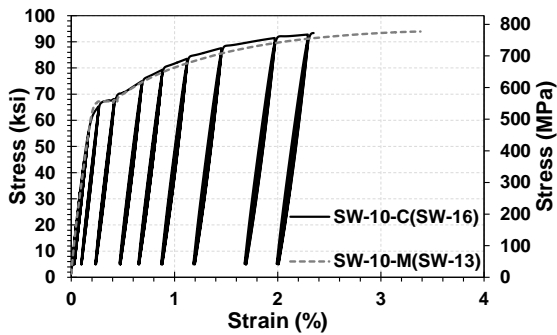


a. Coupler region strains using extensometer displacements

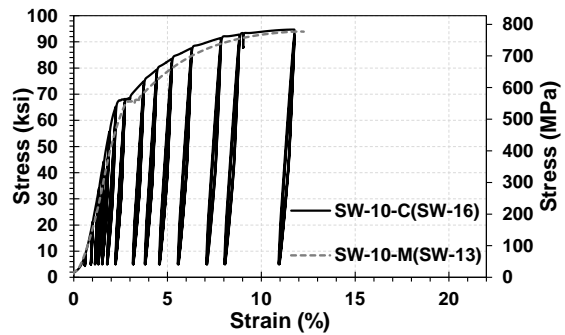


b. Specimen total strains using actuator displacements

Figure 4.49 Cyclic test results for No. 8 (24-mm) swaged couplers



a. Coupler region strains using extensometer displacements



b. Specimen total strains using actuator displacements

Figure 4.50 Cyclic test results for No. 10 (32-mm) swaged couplers



Figure 4.51 Failure of swaged couplers under cyclic loading

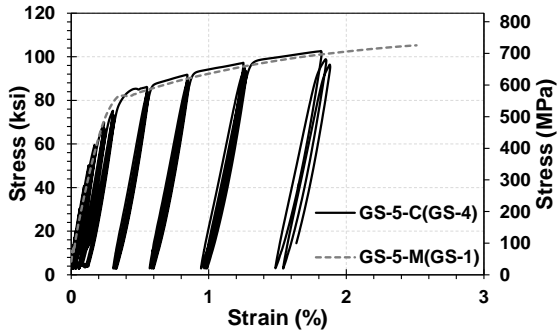
4.4.4 Grouted Sleeve Couplers

Two products were categorized as grouted sleeve couplers, and three samples of each product per bar size were cyclically tested to failure.

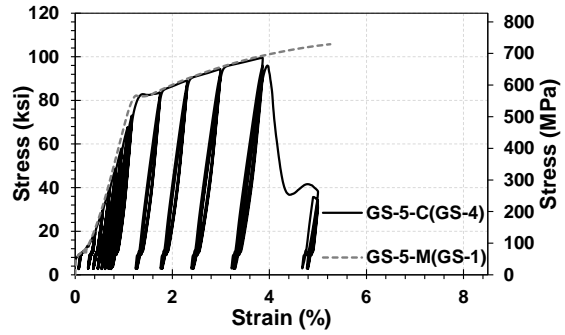
4.4.4.1 Grouted Sleeve Couplers (by Splice Sleeve North America, NMB)

Nine grouted couplers were tested under the cyclic loading, three samples per bar size. Figures 4.52 to 4.54 show the measured cyclic stress-strain hysteresis for the No. 5 (16-mm), No. 8 (25-mm), and No. 10 (32-mm) NMB grouted sleeve couplers, respectively. In all cases, the envelope of the splice cyclic behavior was approximately the same as the monotonic behavior. The hysteretic loop was close to what is expected for a steel bar.

Figure 4.55 shows the mode of failure for these samples after completion of the cyclic tests. Bar fractured in all the No. 8 (25-mm) and No. 10 (32-mm) NMB grouted sleeve couplers outside the coupler region; thus, they are seismic couplers under cyclic loads. Bar pulled out from the sleeve in two of the No. 5 (16-mm) NMB couplers and bar fractured in the third specimen. Therefore, No. 5 (16-mm) NMB couplers are not seismic couplers.

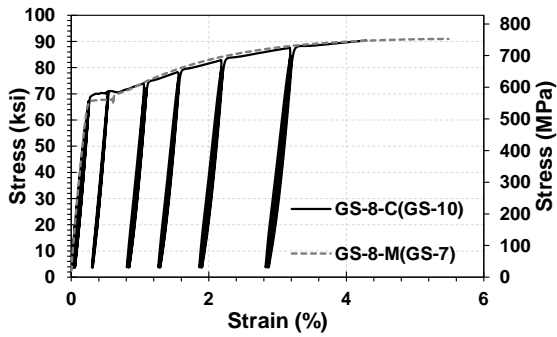


a. Coupler region strains using extensometer displacements

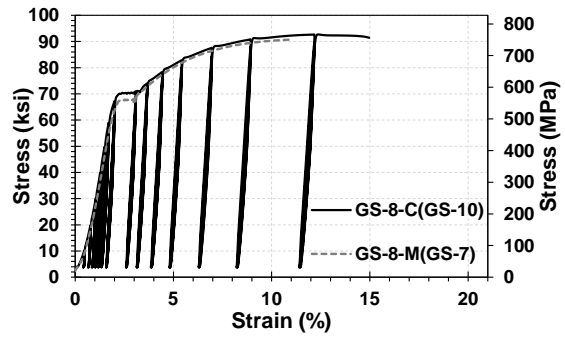


b. Specimen total strains using actuator displacements

Figure 4.52 Cyclic test results for No. 5 (16-mm) grouted sleeve couplers (NMB)

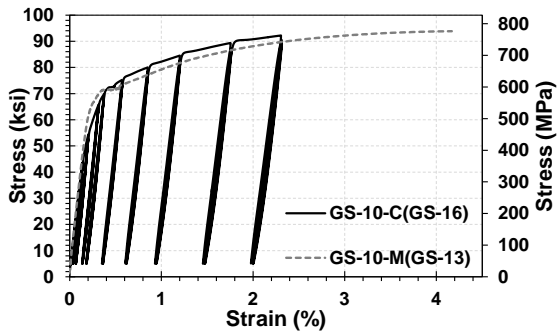


a. Coupler region strains using extensometer displacements

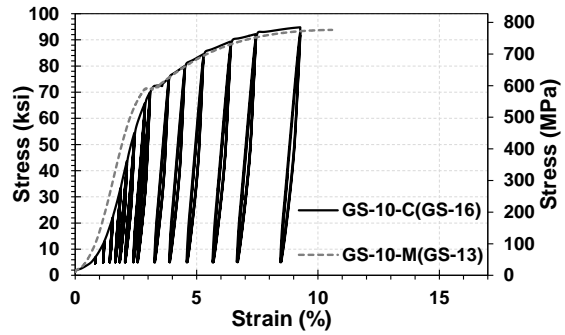


b. Specimen total strains using actuator displacements

Figure 4.53 Cyclic test results for No. 8 (24-mm) grouted sleeve couplers (NMB)



a. Coupler region strains using extensometer displacements



b. Specimen total strains using actuator displacements

Figure 4.54 Cyclic test results for No. 10 (32-mm) grouted sleeve couplers (NMB)

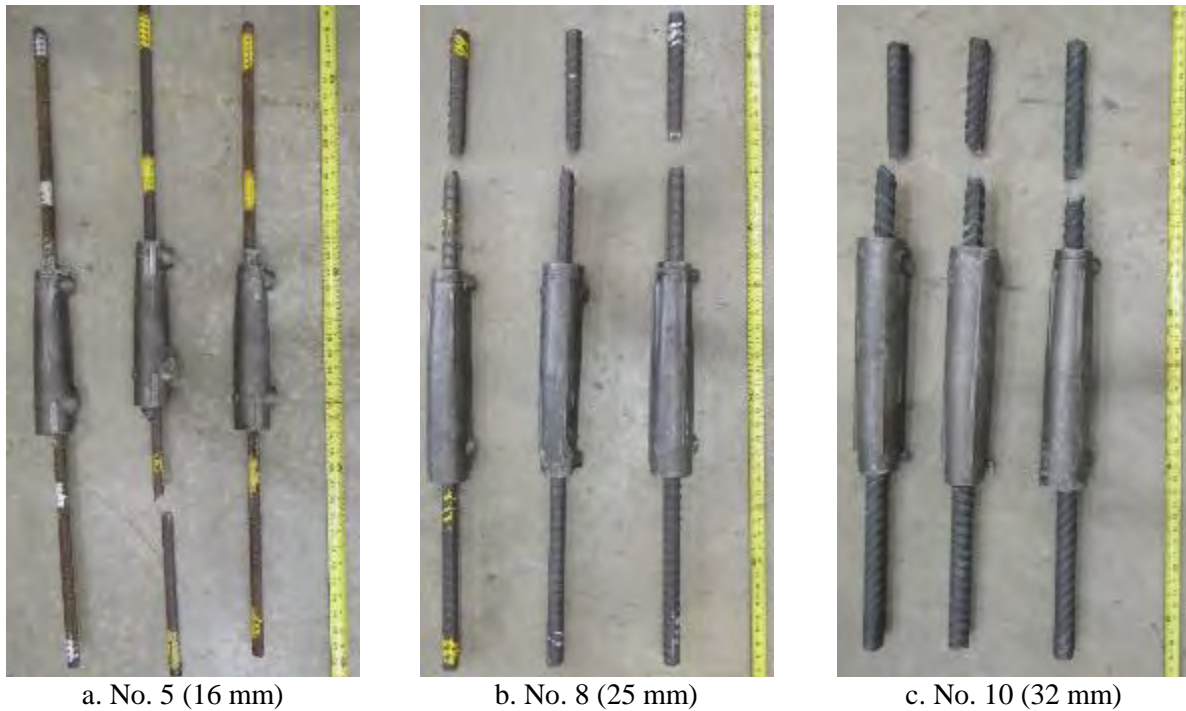
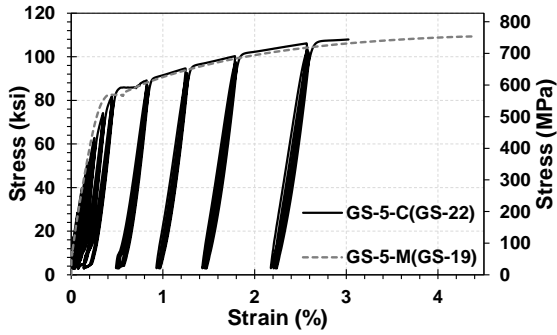


Figure 4.55 Failure of NMB grouted sleeve couplers under cyclic loading

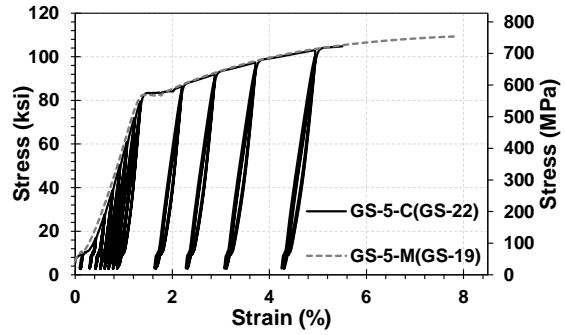
4.4.4.2 Grouted Sleeve Couplers (by Dayton Superior)

Nine grouted sleeve couplers (by Dayton Superior) were tested under the cyclic loading, three samples per bar size. Figures 4.56 to 4.58 show the measured cyclic stress-strain hysteresis for the No. 5 (16-mm), No. 8 (25-mm), and No. 10 (32-mm) grouted sleeve couplers (Dayton Superior), respectively. In all cases, the envelope of the splice cyclic behavior was the same as the monotonic behavior. The hysteretic loop was close to what is expected for a steel bar.

Figure 4.59 shows the mode of failure for these samples after completion of the cyclic tests. Bar fractured in all of No. 8 (25-mm) and No. 10 (32-mm) grouted sleeve couplers (Dayton Superior) outside the coupler region; thus, they are seismic couplers under cyclic loads. Bar pulled out from the sleeve in all of the No. 5 (16-mm) couplers. Therefore, No. 5 (16-mm) grouted sleeve couplers (Dayton Superior) are not seismic couplers.

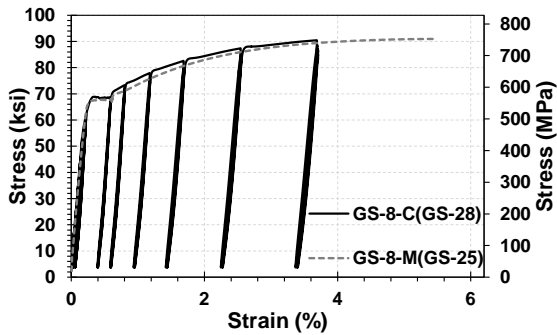


a. Coupler region strains using extensometer displacements

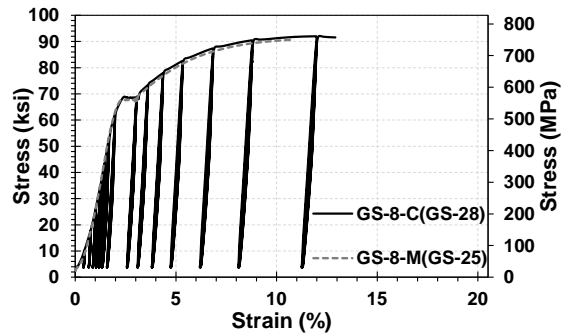


b. Specimen total strains using actuator displacements

Figure 4.56 Cyclic test results for No. 5 (16-mm) grouted sleeve couplers (Dayton Superior)

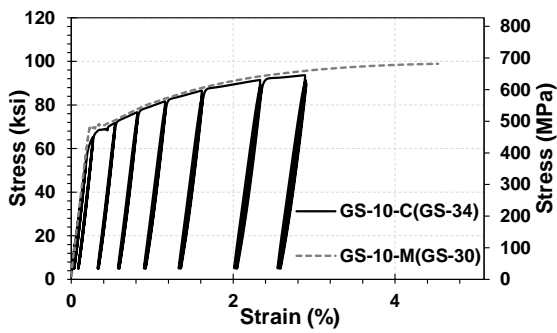


a. Coupler region strains using extensometer displacements

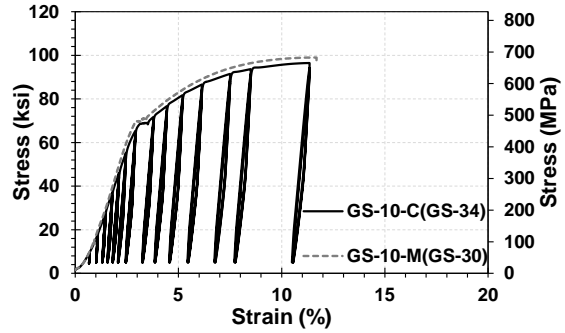


b. Specimen total strains using actuator displacements

Figure 4.57 Cyclic test results for No. 8 (24-mm) grouted sleeve couplers (Dayton Superior)



a. Coupler region strains using extensometer displacements



b. Specimen total strains using actuator displacements

Figure 4.58 Cyclic test results for No. 10 (32-mm) grouted sleeve couplers (Dayton Superior)

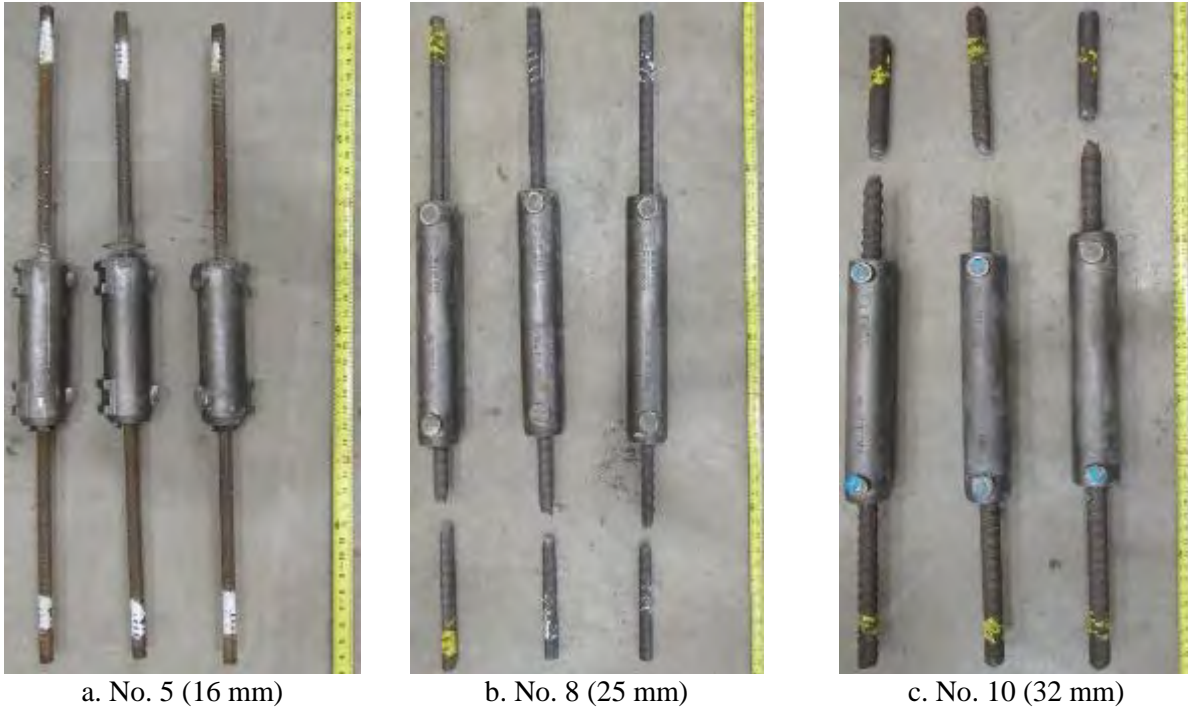


Figure 4.59 Failure of grouted sleeve couplers (Dayton Superior) under cyclic loading

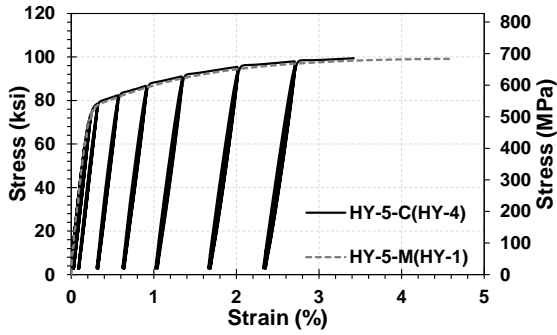
4.4.5 Hybrid Couplers

Two products were categorized as hybrid couplers, and three samples of each product per bar size were cyclically tested to failure. In one of the products, bars were spliced through grouted and threaded mechanisms at the ends of the coupler. In the other hybrid coupler, bars were spliced using threaded mechanism at the middle and the swaged mechanism at the ends.

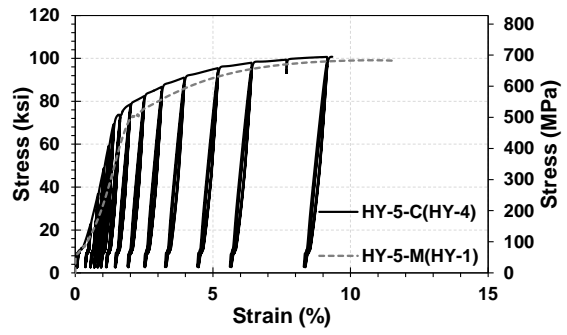
4.4.4.1 Hybrid Couplers (Threaded & Swaged)

Nine threaded-swaged hybrid couplers were tested under the cyclic loading, three samples per bar size. Figures 4.60 to 4.62 show the measured cyclic stress-strain hysteresis for the No. 5 (16-mm), No. 8 (25-mm), and No. 10 (32-mm) threaded-swaged hybrid couplers, respectively. In all cases, the envelope of the splice cyclic behavior was approximately the same as the monotonic behavior. The hysteretic loop was close to what is expected for a steel bar.

Figure 4.63 shows the mode of failure for these samples after completion of the cyclic testing. Bar fractured in all threaded-swaged hybrid couplers outside the coupler region; thus, they are seismic couplers under cyclic loads.

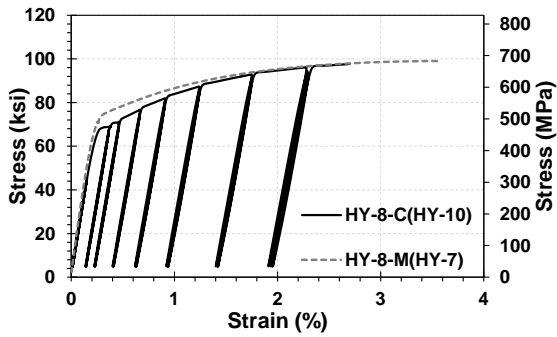


a. Coupler region strains using extensometer displacements

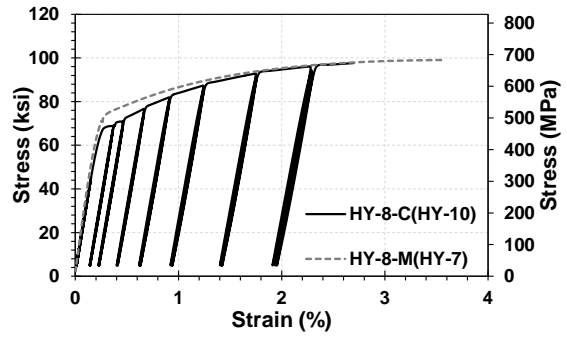


b. Specimen total strains using actuator displacements

Figure 4.60 Cyclic test results for No. 5 (16-mm) threaded-swaged hybrid couplers

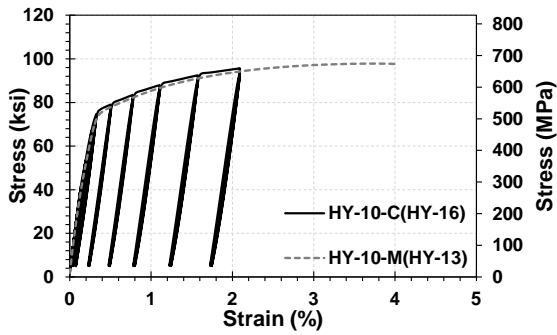


a. Coupler region strains using extensometer displacements

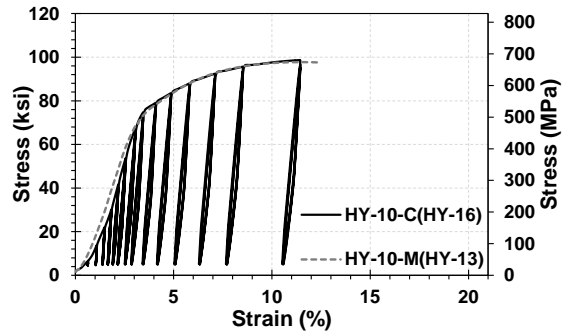


b. Specimen total strains using actuator displacements

Figure 4.61 Cyclic test results for No. 8 (24-mm) threaded-swaged hybrid couplers



a. Coupler region strains using extensometer displacements



b. Specimen total strains using actuator displacements

Figure 4.62 Cyclic test results for No. 10 (32-mm) threaded-swaged hybrid couplers

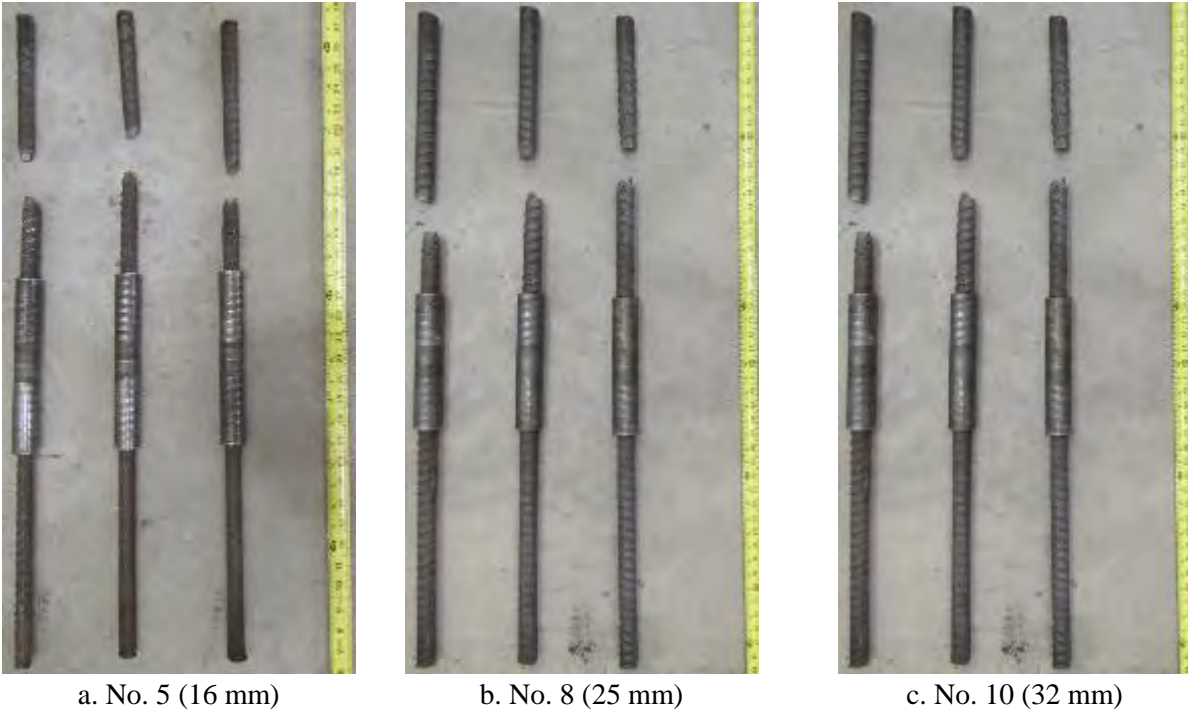
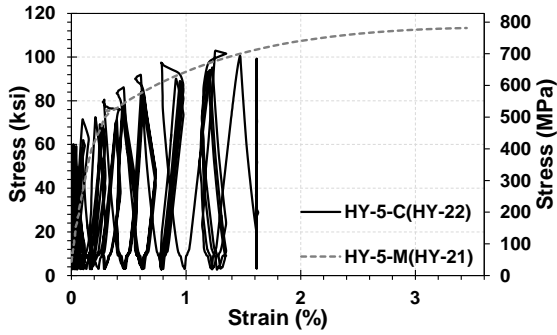


Figure 4.63 Failure of swaged-threaded hybrid couplers under cyclic loading

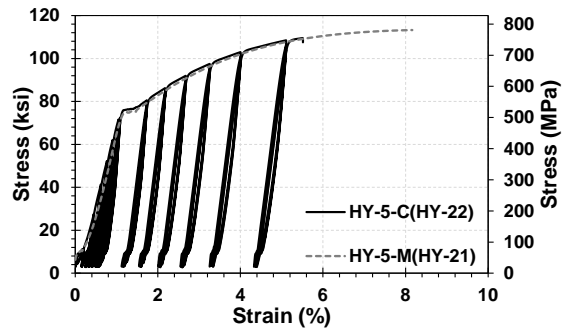
4.4.5.2 Hybrid Couplers (Grouted & Threaded)

Nine grouted-threaded hybrid couplers were tested under the cyclic loading, three samples per bar size. Figures 4.64 to 4.66 show the measured cyclic stress-strain hysteresis for the No. 5 (16 mm), No. 8 (25 mm), and No. 10 (32 mm) grouted-threaded hybrid couplers, respectively. In all cases, the envelope of the splice cyclic behavior was approximately the same as the monotonic behavior. The hysteretic loop was close to what is expected for a steel bar.

Figure 4.67 shows the mode of failure for these samples after completion of the cyclic tests. Except for one No. 10 (32 mm) grouted-threaded hybrid coupler in which bar fractured at the threads, bar fractured in all of the other specimens outside the coupler region. Based on the discussion provided in Section 4.2.5.2, it is concluded that these splice types are seismic couplers under cyclic loads.

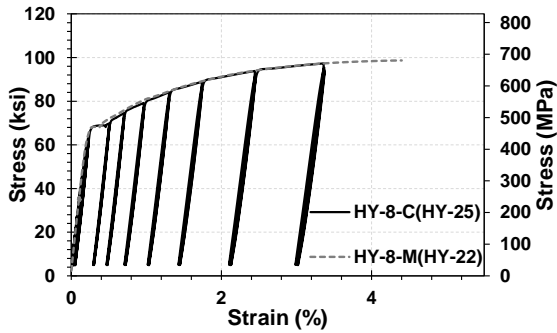


a. Coupler region strains using extensometer displacements

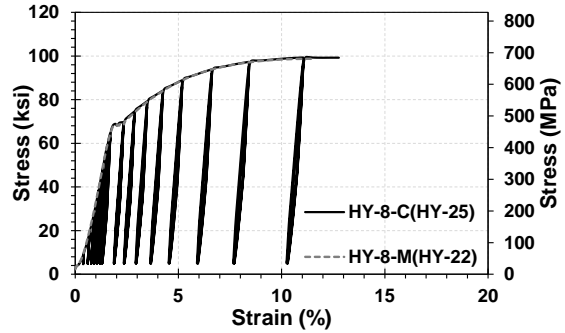


b. Specimen total strains using actuator displacements

Figure 4.64 Cyclic test results for No. 5 (16-mm) grouted-threaded hybrid couplers

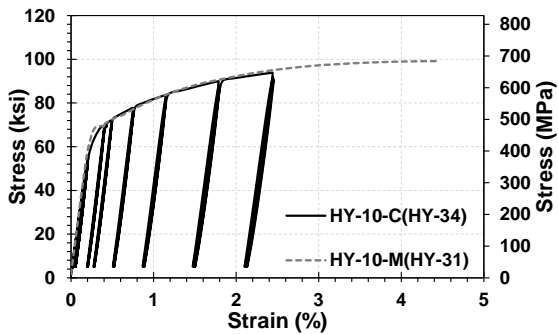


a. Coupler region strains using extensometer displacements

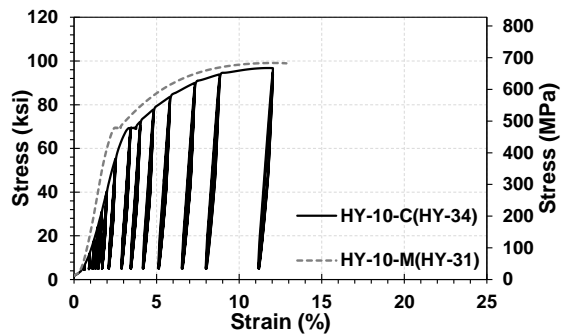


b. Specimen total strains using actuator displacements

Figure 4.65 Cyclic test results for No. 8 (24-mm) grouted-threaded hybrid couplers



a. Coupler region strains using extensometer displacements



b. Specimen total strains using actuator displacements

Figure 4.66 Cyclic test results for No. 10 (32-mm) grouted-threaded hybrid couplers

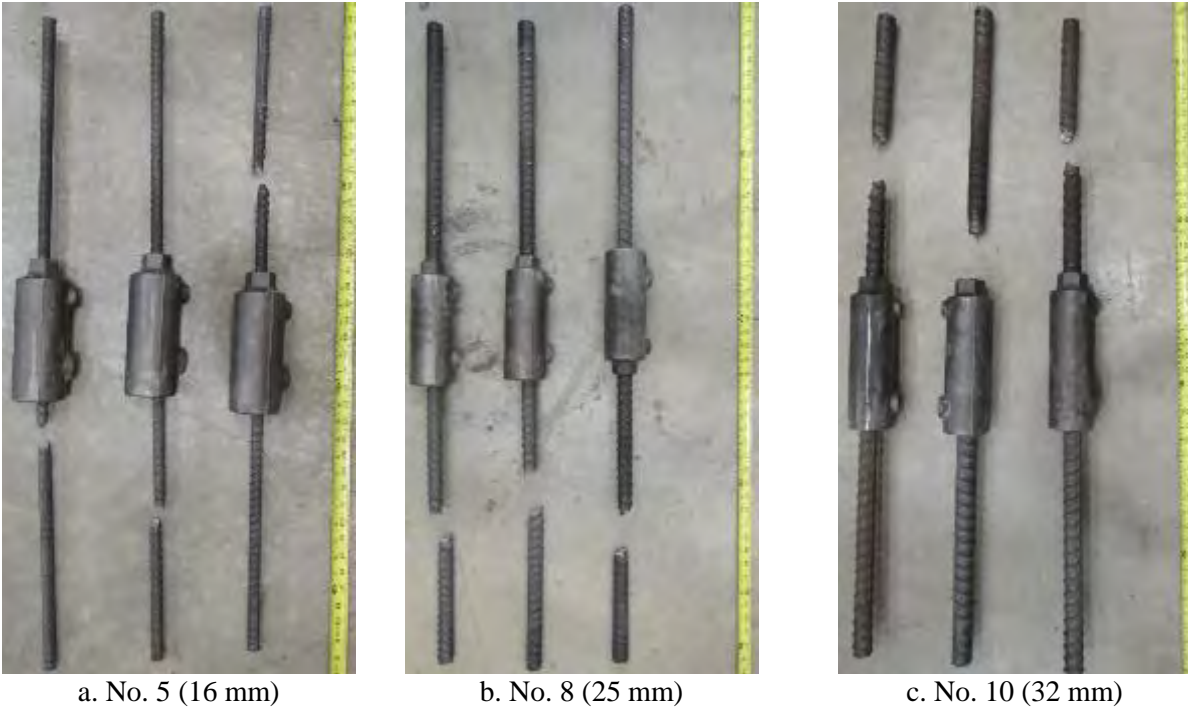


Figure 4.67 Failure of grouted-threaded hybrid couplers under cyclic loading

4.5 Summary of Coupler Cyclic Test Results

Table 4.7 presents a summary of the failure modes for all cyclic tests on couplers. All No. 8 (24 mm) and No. 10 (32 mm) couplers cyclically tested in the present study can be categorized as the seismic couplers. Nevertheless, No. 5 (16-mm) grouted sleeve couplers failed by the bar pullout; thus, they are not seismic couplers.

Comparing the results of the couplers under the monotonic and cyclic loading, it is clear that the performance and failure mode of all coupler types were the same. Therefore, monotonic testing may be sufficient to establish the overall behavior of couplers to be used in the design. Nevertheless, cyclic and dynamic testing of couplers is recommended to comprehensively investigate their performance before any use in the plastic hinge region of columns in high seismic zones.

Table 4.7. Coupler failure modes under cyclic loading

Coupler Type	Size	Failure Mode			Remarks
		Bar Fracture	Bar Pullout	Coupler Failure	
Headed Bar Coupler	No. 5 (16 mm)	XXX			Seismic Coupler
	No. 8 (24 mm)	XXX			Seismic Coupler
	No. 10 (32 mm)	XXX			Seismic Coupler
Swaged Coupler	No. 5 (16 mm)	XXX			Seismic Coupler
	No. 8 (24 mm)	XXX			Seismic Coupler
	No. 10 (32 mm)	XXX			Seismic Coupler
Threaded Coupler (Type A)	No. 5 (16 mm)	XXX			Seismic Coupler
	No. 8 (24 mm)	XXX			Seismic Coupler
	No. 10 (32 mm)	XXX			Seismic Coupler
Threaded Coupler (Type B)	No. 5 (16 mm)	XXX			Seismic Coupler
	No. 8 (24 mm)	XXX			Seismic Coupler
	No. 10 (32 mm)	XXX			Seismic Coupler
Threaded Coupler (Taper)	No. 5 (16 mm)	XXX			Seismic Coupler
	No. 8 (24 mm)	XXX			Seismic Coupler
	No. 10 (32 mm)	XXX			Seismic Coupler
Grouted Coupler (NMB)	No. 5 (16 mm)	X	XX		
	No. 8 (24 mm)	XXX			Seismic Coupler
	No. 10 (32 mm)	XXX			Seismic Coupler
Grouted Coupler (Dayton)	No. 5 (16 mm)		XXX		
	No. 8 (24 mm)	XXX			Seismic Coupler
	No. 10 (32 mm)	XXX			Seismic Coupler
Hybrid Coupler (Threaded and Swaged)	No. 5 (16 mm)	XXX			Seismic Coupler
	No. 8 (24 mm)	XXX			Seismic Coupler
	No. 10 (32 mm)	XXX			Seismic Coupler
Hybrid Coupler (Grouted and Threaded)	No. 5 (16 mm)	XXX			Seismic Coupler
	No. 8 (24 mm)	XXX			Seismic Coupler
	No. 10 (32 mm)	XX		X	Seismic Coupler

X = one sample

4.6 References

- AASHTO SGS. (2011). "AASHTO Guide Specification for LRFD Seismic Bridge Design," 2nd Edition, with 2012, 2014, and 2015 Interim Revisions.
<https://bookstore.transportation.org/item_details.aspx?id=1915>
- ASTM A706. (2009). "Standard specification for Low-Alloy Steel Deformed and Plain Bars for Concrete Reinforcement." West Conshohocken, PA, 6 pp.
- ASTM C109. (2012). "Standard Test Method for Compressive Strength of Hydraulic Cement Mortars (Using 2-in. or [50 mm] cube Specimens)." West Conshohocken, PA.
- Tazarv, M. and Saiidi, M.S. (2016). "Seismic Design of Bridge Columns Incorporating Mechanical Bar Splices in Plastic Hinge Regions," *Engineering Structures*, DOI: 10.1016/j.engstruct.2016.06.041, Vol. 124, pp. 507-520.
- WJE. (2000). "AC133 Cyclic Tests on Splice Sleeve Mechanical Splices for Splice Sleeve North America." Wiss, Janney, Elstner Associates, WJE Report No. 1999.1333.A, 43 pp.

5. ANALYTICAL STUDY ON MECHANICALLY SPLICED BRIDGE COLUMNS

5.1 Introduction

Mechanical properties of nine different coupler products were investigated through tensile testing of more than 160 mechanical bar splices at the Lohr Structures Laboratory at South Dakota State University, and the results were presented in Section 4. Coupler rigid length factor, which is a key parameter to establish the coupler stress-strain behavior, was recommended for the nine coupler products based on the test data. Previous experimental studies (e.g., Haber et al., 2013; Tazarv and Saiidi, 2014; Ameli and Pantelides, 2016) have shown that bar couplers usually reduce the displacement capacity of bridge columns when they are used in plastic hinge regions. This is mainly because the coupler strain capacity is usually less than the unspliced bar strain capacity. In this section, the seismic performance of bridge columns mechanically spliced with each of the nine coupler products tested in the present study is investigated through analytical studies. Specifically, the displacement ductility capacity and the base-shear capacity of mechanically spliced bridge columns are the focus of the study.

A modeling method is presented for mechanically spliced bridge columns, parameters of the analytical study are discussed, and then the results of more than 240 pushover analyses are presented. A summary and conclusions are presented at the end of the section.

5.2 Modeling Method for Mechanically Spliced Bridge Columns

Tazarv and Saiidi (2016) proposed a modeling method for mechanically spliced bridge columns (Figure 5.1). This analytical model was adopted in the present study. Table 5.1 presents the key input of the model. A three-dimensional finite element model was constructed for spliced columns in OpenSees (2016) using three force-based elements and fiber sections. A pedestal (Element 1) was included in the model to monitor the stress-strain behavior of the unspliced bars and to determine the column failure. For a column with couplers at the base, the height of pedestal, H_{sp} , was assumed to be 0.1 in. (2.5 mm). Element 2 is to include the exact length (L_{sp}) and location of the couplers.

Each column section was discretized into 30×10 segments for the core concrete and 10×10 segments for the cover concrete. “Concrete04” and “Concrete01” material models were used for the concrete core and cover fibers, respectively. Concrete04 exhibits an abrupt drop in the stress when the concrete strain reaches the ultimate strain; thus, it is possible to determine the failure of a column when the core concrete fails (a significant reduction in the lateral load carrying capacity of the column). Mander’s model (Mander et al., 1988) was used to calculate the properties of the confined concrete. A uniaxial material model, “ReinforcingSteel,” was used for steel fibers in both spliced (Element 2) and unspliced regions (Elements 1 and 3).

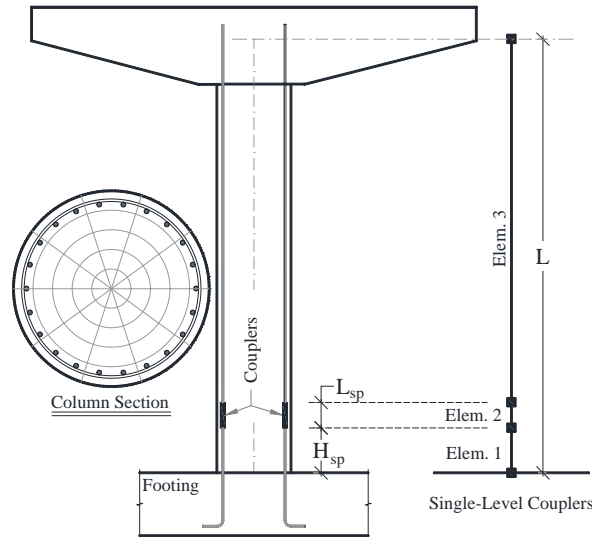


Figure 5.1 Analytical model details for columns with couplers at base

Table 5.1 Modeling method for mechanically spliced bridge columns

General Remarks	
<p>Column Model: Three dimensions with 6 degrees of freedom per node</p> <p>Element Type: “ForceBeamColumn” with 5 integration points for both coupler regions and the remainder of the columns.</p> <p>$P - \Delta$ effects were included, no bond-slip effect was included</p>	<p>Sectional Properties (Fiber Section): Cover Concrete Discretization: 10 radial by 10 circumferential</p> <p>Core Concrete Discretization: 30 radial by 10 circumferential</p>
Column Concrete Fibers	
<p>Application: unconfined concrete Type: “Concrete01” $f'_{cc} = -5000 \text{ psi} (-34.47 \text{ MPa})$ $\epsilon_{cc} = -0.002 \text{ in./in.}$ $f'_{cu} = 0.0 \text{ psi} (0.0 \text{ MPa})$ $\epsilon_{cu} = -0.005 \text{ in./in.}$</p>	<p>Application: confined concrete (based on Mander’s model) Type: “Concrete04” f'_{cc}, ϵ_{cc}, f'_{cu}, & ϵ_{cu} depend on the transverse bar size, type, and spacing, and the clear cover per Mander’s model</p>
Column Steel/Coupler Fibers	
<p>Application: unspliced steel bars Type: “ReinforcingSteel” $f_y = 68.0 \text{ ksi} (468.8 \text{ MPa})$ $f_{su} = 95.0 \text{ ksi} (665.0 \text{ MPa})$ $E_s = 29000 \text{ ksi} (63252 \text{ MPa})$ $E_{sh} = 0.043E_s$ $\epsilon_{sh} = 0.005 \text{ in./in.}$ $\epsilon_{su} = 0.09 \text{ in./in.}$</p>	<p>Application: spliced bars (Element 2) Type: “ReinforcingSteel” $f_y = 68.0 \text{ ksi} (468.8 \text{ MPa})$ $f_{su} = 95.0 \text{ ksi} (665.0 \text{ MPa})$ E_s, E_{sh}, ϵ_{sh}, & ϵ_{su} depend on the type and size of couplers using the model presented in Table 5.2</p>

5.2.1 Expected Mechanical Properties for Couplers

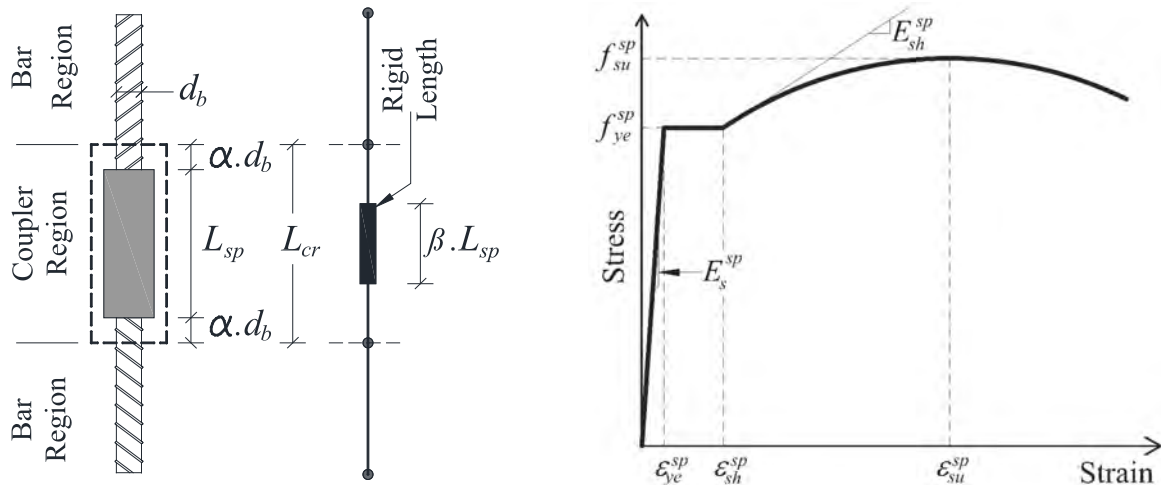
Only seismic couplers should be allowed in bridge columns. Due to a lack of test data, all reinforcement of mechanically spliced bridge columns should conform to the requirements of ASTM A706 Grade 60 (2009) steel bars. Furthermore, current codes only allow ASTM A706 bars for seismic applications (e.g., AASHTO SGS, 2011). Table 5.2 presents the mechanical properties of couplers splicing ASTM A706 Grade 60 steel bars. Figure 5.2 shows the coupler material model parameters. This stress-strain material model, which is genetic and may be used for any seismic coupler, was used in the present study. The rigid length factor (β) for each coupler product and size should be determined through testing. Refer to Section 4 or Section 5.3.2 for the recommended rigid length factors for the nine coupler products tested in the present study.

Table 5.2 Coupler mechanical properties splicing ASTM A706 Grade 60 reinforcing steel bars

Property	Notation	Bar Size	Value/Equation
Expected yield stress (ksi)	f_{ye}^{sp}	#3- #18	68
Expected tensile strength (ksi)	f_{ue}^{sp}	#3- #18	95
Expected yield strain (in./in.)	ϵ_{ye}^{sp}	#3- #18	$0.0023(L_{cr} - \beta L_{sp})/L_{cr}$
Modulus of elasticity (ksi)	E_s^{sp}	#3- #18	$f_{ye}^{sp} / \epsilon_{ye}^{sp}$
Second Modulus of elasticity (ksi)	E_{sh}^{sp}	#3- #18	$0.041E_s^{sp}$
Onset of strain hardening (in./in.) *	ϵ_{sh}^{sp}	#3- #18	$0.005(L_{cr} - \beta L_{sp})/L_{cr}$
Reduced ultimate tensile strain (in./in.)	ϵ_{su}^{sp}	#4- #10	$0.09(L_{cr} - \beta L_{sp})/L_{cr}$
		#11- #18	$0.06(L_{cr} - \beta L_{sp})/L_{cr}$

Note: L_{sp} = coupler length; β = coupler rigid length ratio; L_{cr} = coupler region ($L_{sp} + 2\alpha.d_b$); Alpha should not exceed 2.

*The strain at the onset of strain hardening is reduced compared to AASHTO SGS to improve convergence of analytical models. This change does not affect the seismic design of bridge columns.



a. Couplers parameters (Tazarv & Saiidi, 2016)

b. Couplers stress-strain model

Figure 5.2 Coupler model parameters splicing ASTM A706 Grade 60 reinforcing steel bars

5.3 Parametric Study

A parametric study was conducted to investigate the seismic performance of bridge columns spliced with different coupler products. First, 27 conventional reinforced concrete (RC) columns were designed to cover a practical range of bridge columns. Subsequently, the detailing of these RC columns was modified by incorporating bar couplers at the column base (mechanically spliced columns). Finally, a pushover analysis was performed for each spliced column and compared with the results of its corresponding conventional column.

The column aspect ratio was the ratio of the column height to the column largest side dimension (or diameter). The axial load index was the ratio of the column axial load to the product of the column concrete compressive strength (f'_c) and the column cross-section area (A_g). The displacement capacity was determined at a point where the core concrete failed, the extreme steel bar fractured, or the column lateral load carrying capacity dropped by 15% with respect to the peak lateral strength. The displacement ductility capacity was calculated according to AASHTO SGS (2011). The drift ratio was defined as the ratio of the column lateral displacement to the column height.

5.3.1 Reference Conventional Reinforced Concrete Columns

Tazarv and Saiidi (2016) designed 21 conventional RC columns, which cover a practical range of bridge columns. Six additional RC columns were designed in the present study for completeness. Three column aspect ratios of 4, 6, and 8, three axial load indices of 5, 10, and 15%, and three target displacement ductilities of 3, 5, and 7 were included in the design. Table 5.3 presents the general design parameters of the RC columns and Table 5.4 presents the details of the transverse reinforcement of these columns. All columns had a 4-ft. (1.22-m) diameter, but the column height was varied based on the aspect ratio resulting in columns with a height of 16 ft. (4.88 m), 24 ft. (7.32 m), or 32 ft. (9.75 m).

Table 5.3 RC column general design parameters

Parameter	Value
Column Diameter	4 ft (1.22 m)
Aspect Ratio (AR)	4, 6, 8
Column Length (L)	16 ft (4.88 m), 24 ft (7.32 m) or 32 ft (9.75 m)
Longitudinal Bar	No. 9 (29 mm)
Concrete Compressive Strength, f'_c	5.0 ksi (34.5 MPa)
Axial Load Index ($ALI = P / f'_c \cdot A_g$)	5%, 10%, 15%
Displacement Ductility Capacity (D or μ)	$\mu = \frac{\Delta_u}{\Delta_{yi}}$ where Δ_u : Ultimate Displacement Δ_{yi} : Idealized Yield Displacement

Table 5.4 RC column transverse reinforcement, drift ratio, and displacement ductility capacity

Column ID	Transverse Reinforcement	Drift Ratio (%)	Ductility (μ)
RC-AR4-ALI5-D3	#3 hoops @10 in. ($\rho_s = 0.08\%$)	1.60	3.01
RC-AR4-ALI5-D5	#4 hoops @4 in. ($\rho_s = 0.45\%$)	2.86	4.94
RC-AR4-ALI5-D7	#6 hoops @4 in. ($\rho_s = 1.02\%$)	4.13	7.05
RC-AR4-ALI10-D3	#4 hoops @8 in. ($\rho_s = 0.22\%$)	1.48	2.92
RC-AR4-ALI10-D5	#5 hoops @4 in. ($\rho_s = 0.71\%$)	2.63	4.98
RC-AR4-ALI10-D7	#7 hoops @3.5 in. ($\rho_s = 1.59\%$)	3.88	6.92
RC-AR4-ALI15-D3	#5 hoops @7 in. ($\rho_s = 0.40\%$)	1.45	3.00
RC-AR4-ALI15-D5	#7 hoops @5.5 in. ($\rho_s = 1.01\%$)	2.61	5.04
RC-AR4-ALI15-D7	#8 hoops @3 in. ($\rho_s = 2.43\%$)	3.55	7.11
RC-AR6-ALI5-D3	#3 hoops @10 in. ($\rho_s = 0.10\%$)	2.40	3.16
RC-AR6-ALI5-D5	#4 hoops @4 in. ($\rho_s = 0.45\%$)	4.24	5.12
RC-AR6-ALI5-D7	#5 hoops @3.5 in. ($\rho_s = 0.81\%$)	5.45	7.33
RC-AR6-ALI10-D3	#4 hoops @10 in. ($\rho_s = 0.18\%$)	2.13	3.39
RC-AR6-ALI10-D5	#3 hoops @4 in. ($\rho_s = 0.71\%$)	3.74	5.05
RC-AR6-ALI10-D7	#7 hoops @5 in. ($\rho_s = 1.11\%$)	4.90	6.73
RC-AR6-ALI15-D3	#4 hoops @8 in. ($\rho_s = 0.22\%$)	2.15	2.92
RC-AR6-ALI15-D5	#7 hoops @5 in. ($\rho_s = 1.11\%$)	3.72	4.92
RC-AR6-ALI15-D7	#9 hoops @3 in. ($\rho_s = 2.43\%$)	4.98	6.55
RC-AR8-ALI5-D3	#3 hoops @3 in. ($\rho_s = 0.08\%$)	2.34	3.03
RC-AR8-ALI5-D5	#4 hoops @4 in. ($\rho_s = 0.4\%$)	4.50	5.11
RC-AR8-ALI5-D7	#6 hoops @4 in. ($\rho_s = 1.02\%$)	6.07	7.12
RC-AR8-ALI10-D3	#4 hoops @8 in. ($\rho_s = 0.23\%$)	2.78	3.11
RC-AR8-ALI10-D5	#5 hoops @4 in. ($\rho_s = 0.7\%$)	2.85	5.15
RC-AR8-ALI10-D7	#7 hoops @3 in. ($\rho_s = 1.86\%$)	5.25	7.02
RC-AR8-ALI15-D3	#5 hoops @7 in. ($\rho_s = 0.40\%$)	1.60	3.13
RC-AR8-ALI15-D5	#7 hoops @3 in. ($\rho_s = 1.85\%$)	3.79	5.01
RC-AR8-ALI15-D7	#8 hoops @3 in. ($\rho_s = 2.43\%$)	3.91	6.04

Note: No. 3 bars are 10 mm in diameter, No. 4 bars are 13 mm in diameter, No. 5 bars are 16 mm in diameter, No. 6 bars are 19 mm in diameter, No. 7 bars are 22 mm in diameter, and No. 8 bars are 25.4 mm in diameter; 1 in. is 25.4 mm.

5.3.2 Parameters of Mechanically Spliced Columns

Nine coupler products were tested, and their mechanical properties were established in the previous section. Of those nine, eight products (Table 5.5) were selected to be used in the analytical study to investigate the seismic behavior of mechanically spliced bridge columns. Two threaded coupler products by Dextra were essentially the same and were not repeated herein. In addition to the conventional column variables (27 columns), the length and the rigid length factor for each coupler were varied in the parametric study, resulting in a total of 243 pushover analyses. Note that due to a lack of test data for No. 9 (29-mm) couplers, the rigid length factor and the coupler length for No. 10 bars (32 mm) were utilized in the analysis.

Table 5.5 Coupler products used in analytical study

Coupler Type	Labeled as	Coupler Length, L_{sp} , in.(mm)	Coupler Rigid Length Factor (β)
Headed Reinforcement	HR	3.88 (98.5)	0.55
Threaded (Dextra)	TH	3.06 (77.7)	1.60
Threaded (Erico)	TH (Taper)	4.2 (106.7)	1.05
Swaged (Bar Splice)	SW	9.5 (241.3)	0.95
Grouted Sleeve (NMB)	GS NMB	18 (457)	0.85
Grouted Sleeve (Dayton)	GS Dayton	18 (457)	0.65
Hybrid (Dextra)	HY (Dextra)	10.63 (270)	0.85
Hybrid (Erico)	HY (Erico)	10.75 (273)	0.80

Note: These coupler lengths and rigid length factors are for No. 10 (32-mm) bars.

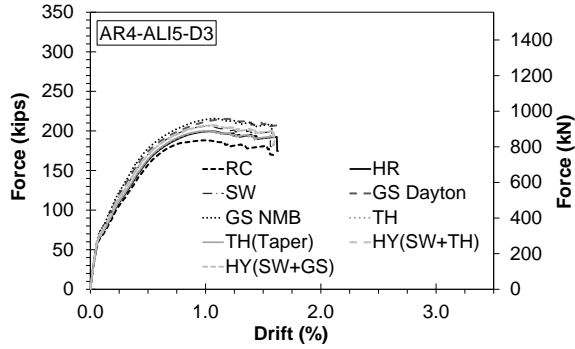
5.4 Parametric Study Results

To better synthesize the effect of couplers on the seismic performance of bridge columns, the pushover analysis results were summarized under low-ductile ($\mu = 3$), medium-ductile ($\mu = 5$), and high-ductile ($\mu = 7$) columns. Two graphs were generated per analysis: one was a regular pushover curve (force-displacement or force-drift), and another was a moment-ductility curve to clearly show the effect of couplers on the moment capacity and displacement ductility capacity of bridge columns.

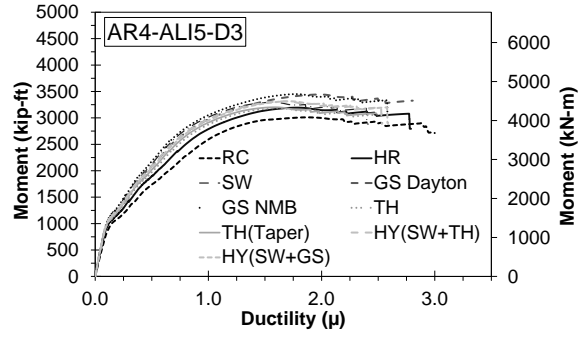
5.4.1 Low-Ductile Columns

Spliced columns with a target displacement ductility of three in their corresponding RC columns were considered as low-ductile columns. Of 243 column models, 81 columns were low ductile. Figures 5.3 to 5.11 show the force-drift and moment-ductility relationships for these columns. The results of the corresponding reference RC columns are included in the graphs with dashed black lines for comparison. It can be seen that the drift capacity and also the displacement ductility capacity of the low-ductile columns were reduced when couplers were used at the column base. For example, the displacement ductility capacity of the spliced AR6-ALI5-D3 columns was reduced between 8% and 22%, compared with that for the reference RC columns. It is clear that longer couplers with higher rigid length factors have a more adverse effect on the column displacement ductility. For example, columns with grouted and swaged couplers exhibited the lowest displacement ductility capacities (e.g., 25% lower than RC using grouted couplers).

Furthermore, it can be inferred that the force or moment capacity of mechanically spliced columns is higher than that in RC columns. For example, grouted coupler columns had 6.6% higher force capacity compared with their reference RC columns. The results also show that couplers did not affect the initial stiffness of the columns. This may be because the coupler length is insignificant compared with the column length; thus, the variations in the splice modulus of elasticity (initial stiffness) do not affect the column overall stiffness.

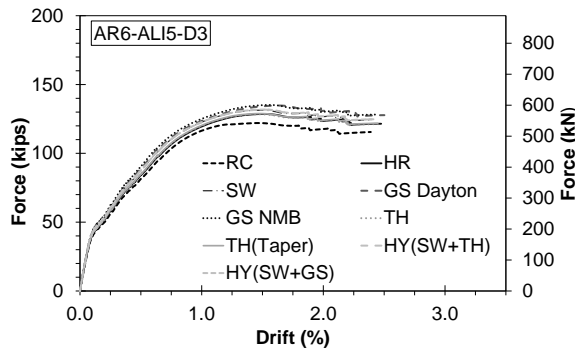


a. Force-drift relationship

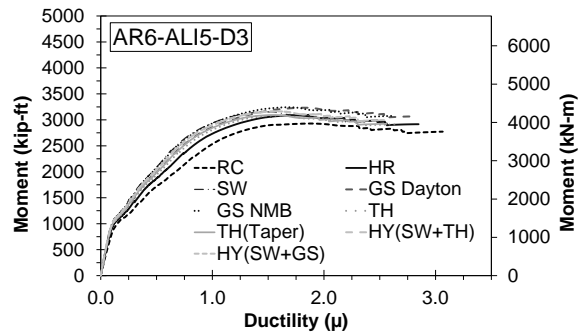


b. Moment-ductility relationship

Figure 5.3 Pushover analysis results for AR4-ALI5-D3

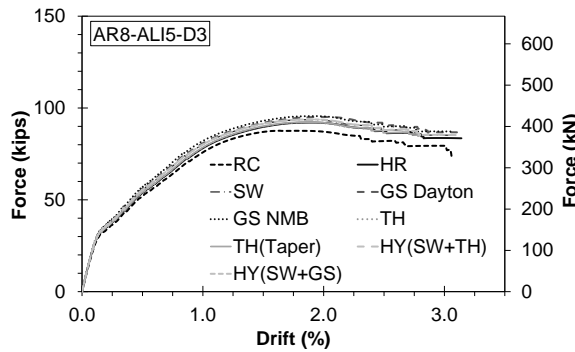


a. Force-drift relationship

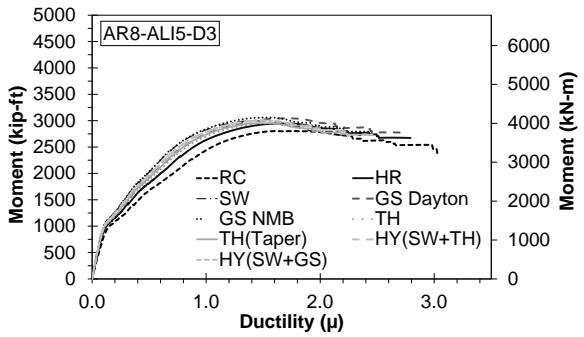


b. Moment-ductility relationship

Figure 5.4 Pushover analysis results for AR6-ALI5-D3

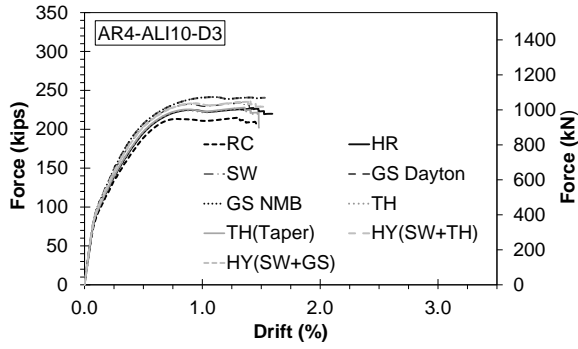


a. Force-drift relationship

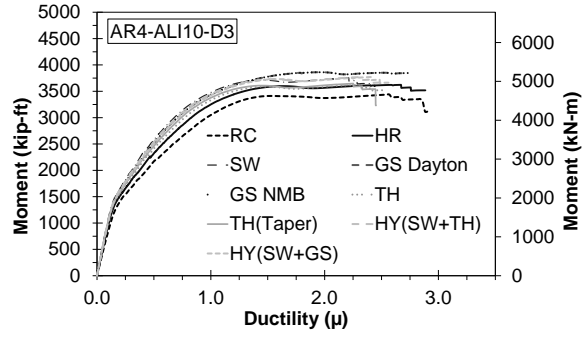


b. Moment-ductility relationship for

Figure 5.5 Pushover analysis results for AR8-ALI5-D3

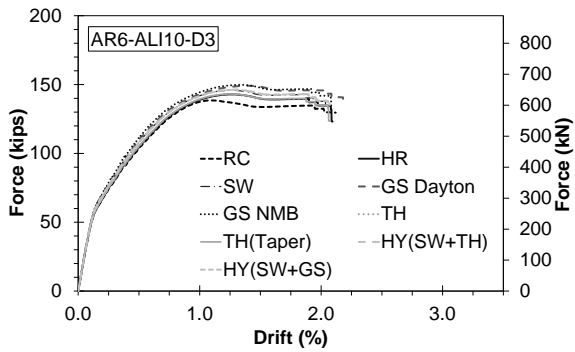


a. Force-drift relationship

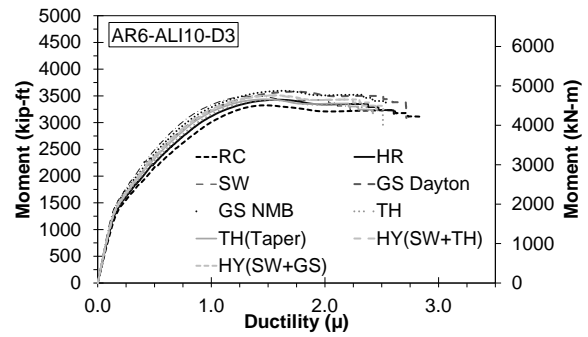


b. Moment-ductility relationship

Figure 5.6 Pushover analysis results for AR4-ALI10-D3

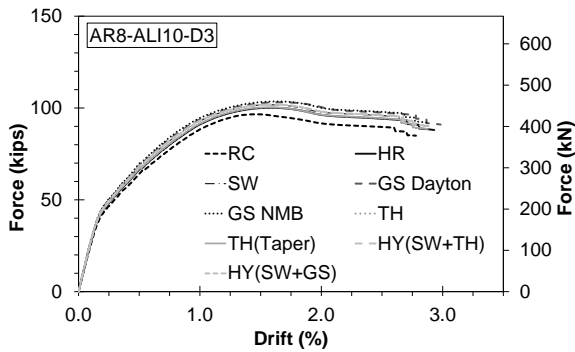


a. Force-drift relationship

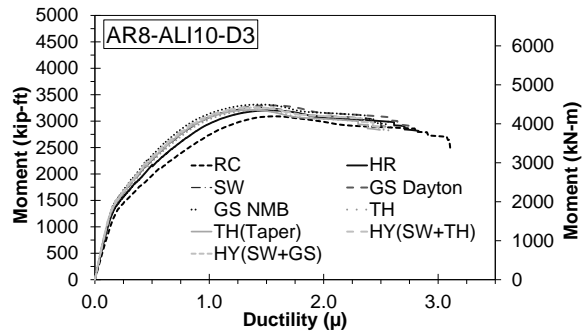


b. Moment-ductility relationship

Figure 5.7 Pushover analysis results for AR6-ALI10-D3

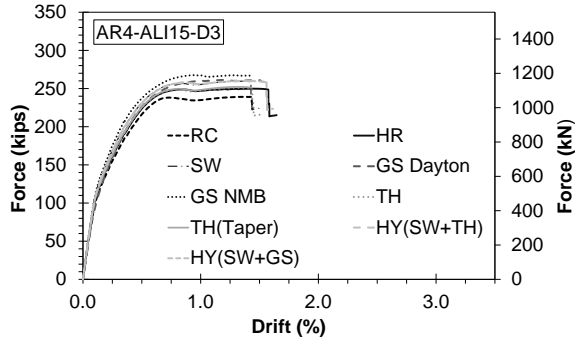


a. Force-drift relationship

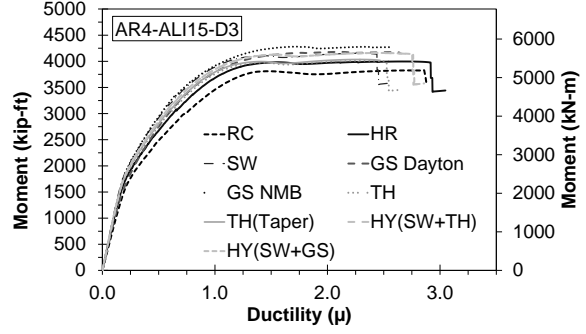


b. Moment-ductility relationship

Figure 5.8 Pushover analysis results for AR8-ALI10-D3

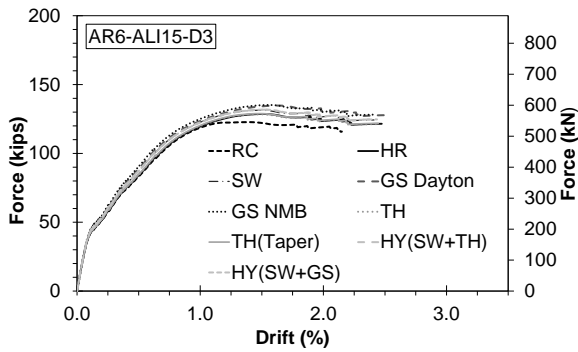


a. Force-drift relationship

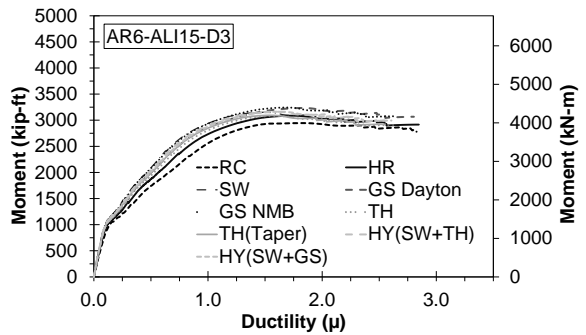


b. Moment-ductility relationship

Figure 5.9 Pushover analysis results for AR4-ALI15-D3

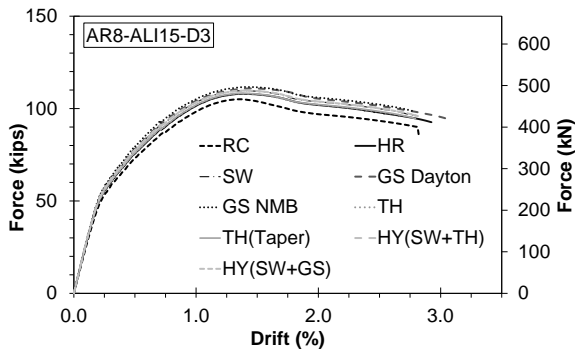


a. Force-drift relationship

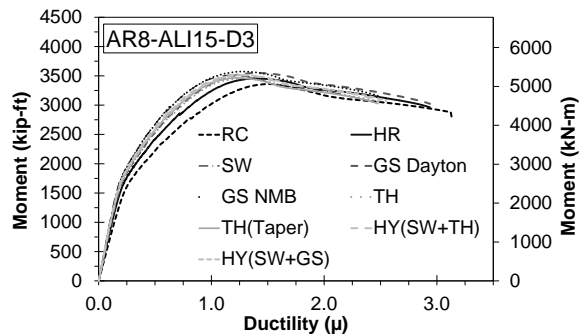


b. Moment-ductility relationship

Figure 5.10 Pushover analysis results for AR6-ALI15-D3



a. Force-drift relationship



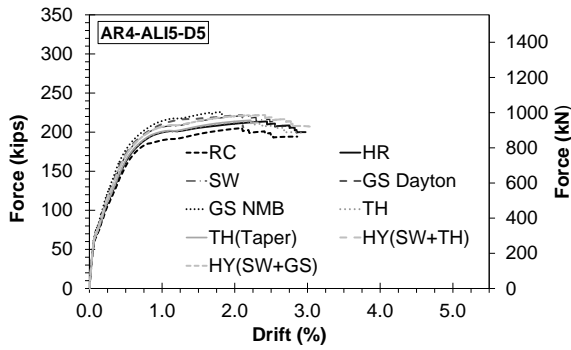
b. Moment-ductility relationship

Figure 5.11 Pushover analysis results for AR8-ALI15-D3

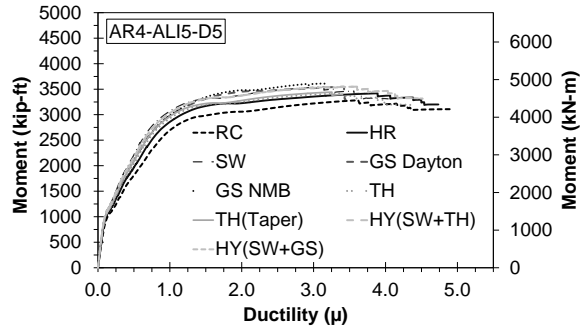
5.4.2 Medium-Ductile Columns

Spliced columns with a target displacement ductility of five in their corresponding RC columns were considered as low-ductile columns. Of 243 column models, 81 columns were medium ductile. Figures 5.12 to 5.20 show the force-drift and moment-ductility relationships for these columns. It can be seen that the drift capacity and the displacement ductility capacity of medium-ductile columns were reduced when couplers were used at the column base. For example, the displacement ductility capacity of the spliced AR6-ALI5-D5 columns was reduced between 5% and 30%, compared with that of the reference RC columns. It is clear that couplers with higher rigid length factors and longer couplers have a more adverse effect on the column displacement ductility. For example, columns with grouted and swaged couplers exhibited the lowest displacement ductility capacities (e.g., 35.8% lower than RC using grouted couplers).

Furthermore, it can be inferred that the force or moment capacity of mechanically spliced columns is higher than that in RC columns. For example, grouted coupler columns had 9.1% higher force capacity compared with their reference columns. The results also show that couplers did not affect the initial stiffness of the medium-ductile columns.

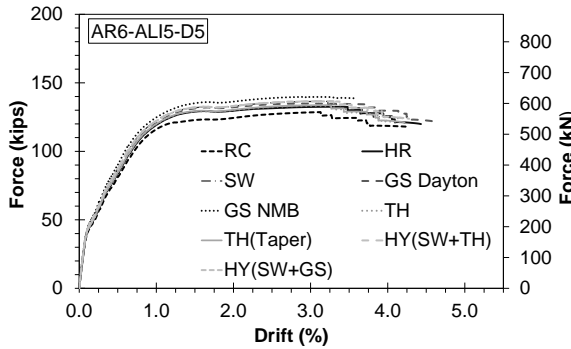


a. Force-drift relationship

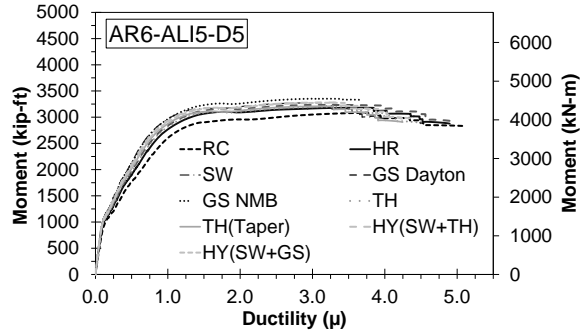


b. Moment-ductility relationship

Figure 5.12 Pushover analysis results for AR4-ALI5-D5

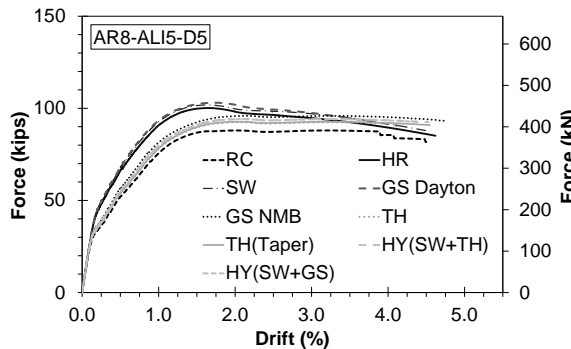


a. Force-drift relationship

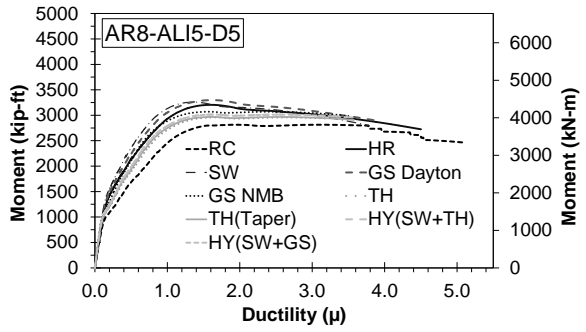


b. Moment-ductility relationship

Figure 5.13 Pushover analysis results for AR6-ALI5-D5

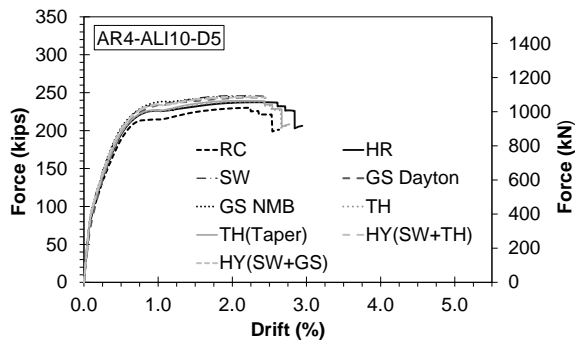


a. Force-drift relationship

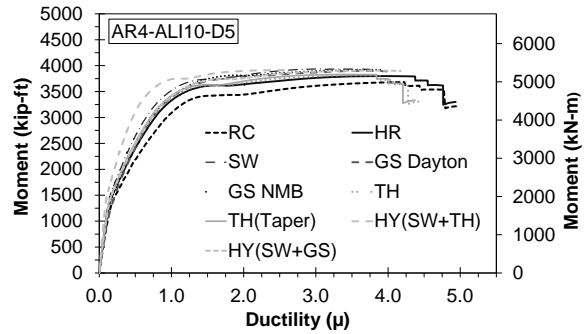


b. Moment-ductility relationship

Figure 5.14 Pushover analysis results for AR8-ALI5-D5

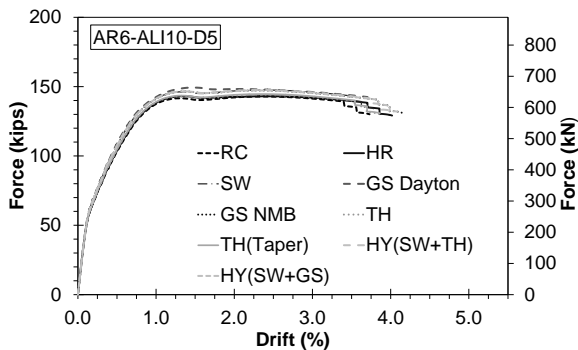


a. Force-drift relationship

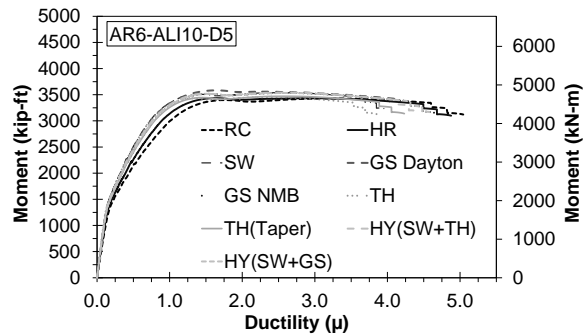


b. Moment-ductility relationship

Figure 5.15 Pushover analysis results for AR4-ALI10-D5

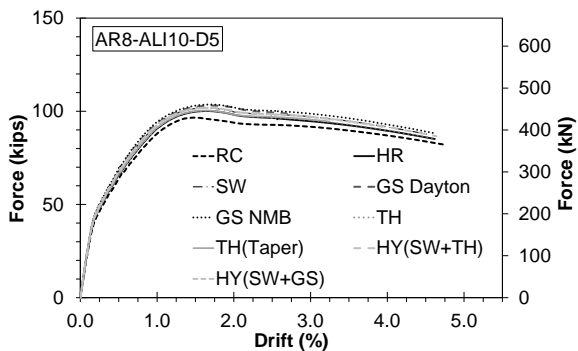


a. Force-drift relationship

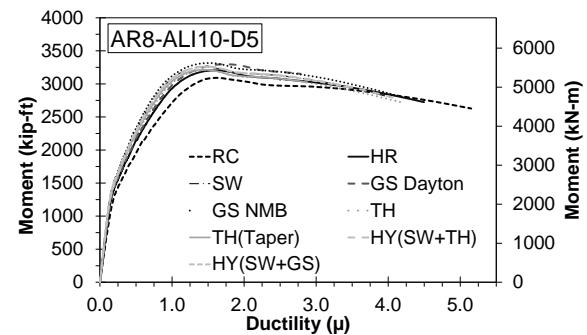


b. Moment-ductility relationship

Figure 5.16 Pushover analysis results for AR6-ALI10-D5

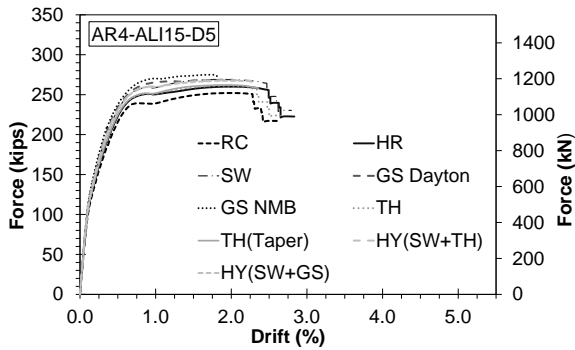


a. Force-drift relationship

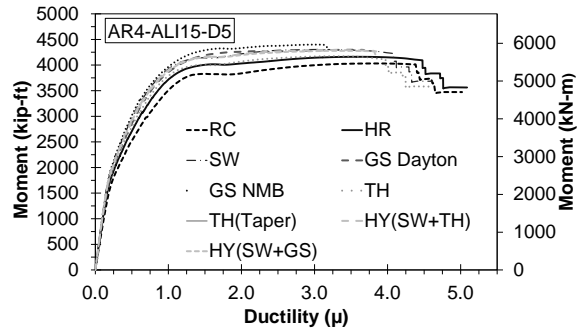


b. Moment-ductility relationship

Figure 5.17 Pushover analysis results for AR8-ALI10-D5

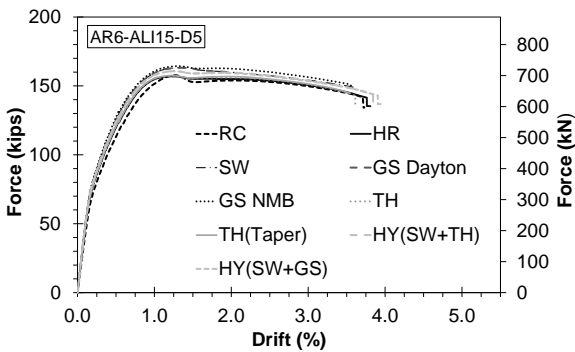


a. Force-drift relationship

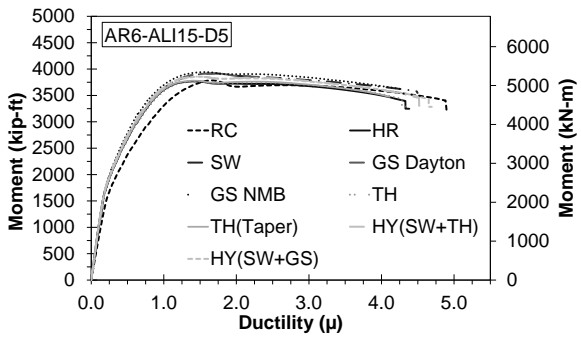


b. Moment-ductility relationship

Figure 5.18 Pushover analysis results for AR4-ALI15-D5

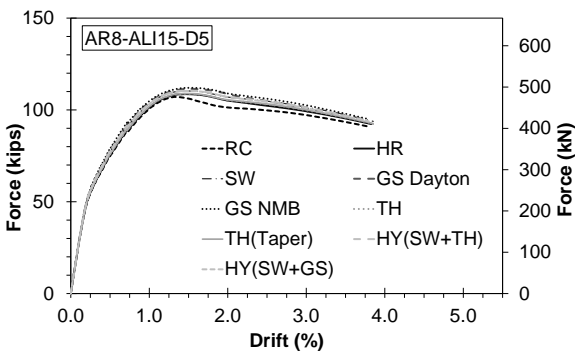


a. Force-drift relationship

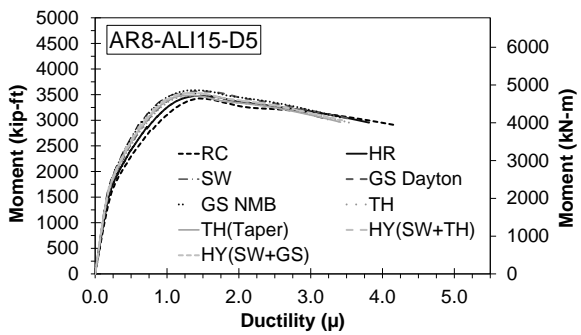


b. Moment-ductility relationship

Figure 5.19 Pushover analysis results for AR6-ALI15-D5



a. Force-drift relationship



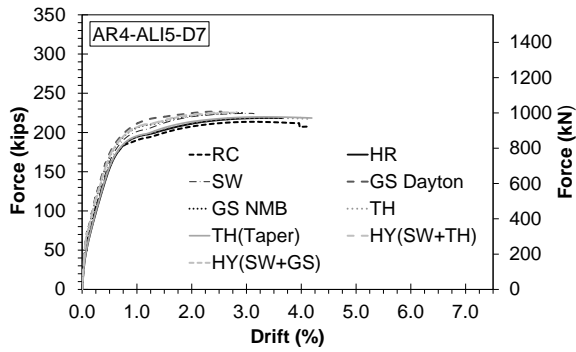
b. Moment-ductility relationship

Figure 5.20 Pushover analysis results for AR8-ALI15-D5

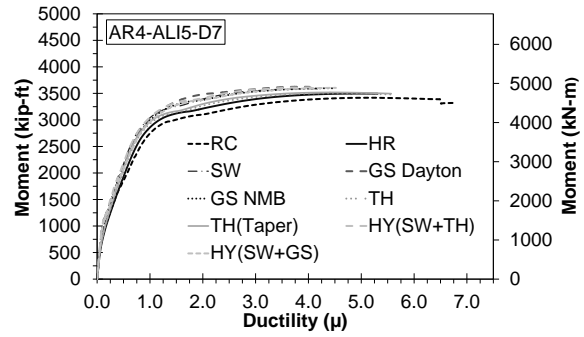
5.4.3 High-Ductile Columns

Of 243 column models, 81 columns were high ductile. Figures 5.21 to 5.29 show the force-drift and moment-ductility relationships for these columns. Similar to what was found for the other spliced columns, the drift capacity and also the displacement ductility capacity of high-ductile columns were reduced when couplers were used at the column base. For example, the displacement ductility capacity of the spliced AR6-ALI5-D7 columns was reduced between 11% and 43%, compared with that of the reference RC columns. Couplers with higher rigid length factors and longer couplers have a more adverse effect on the column displacement ductility. For example, columns with grouted and swaged couplers exhibited the lowest displacement ductility capacities (e.g., 35.8% lower than RC using grouted couplers).

Furthermore, similar to other spliced columns, the force or moment capacity of mechanically spliced columns is higher than that in RC columns. For example, grouted coupler columns had 6.8% higher force capacity compared with their reference columns. The results also show that couplers did not affect the initial stiffness of the high-ductile columns.

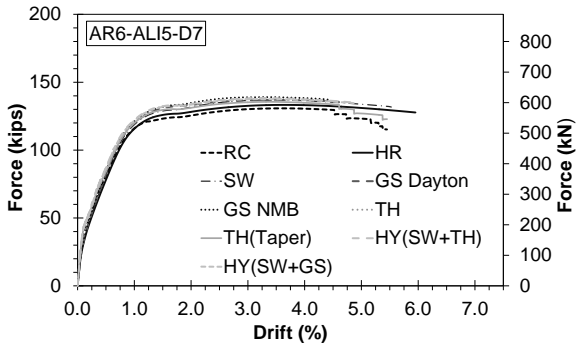


a. Force-drift relationship

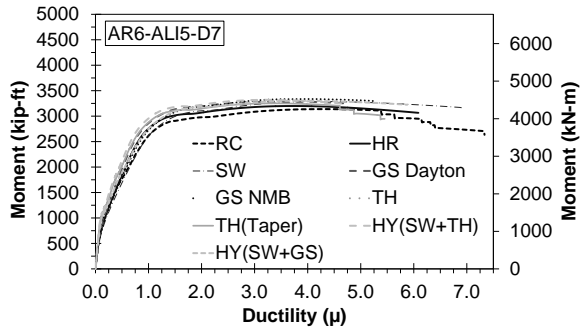


b. Moment-ductility relationship

Figure 5.21 Pushover analysis results for AR4-ALI5-D7

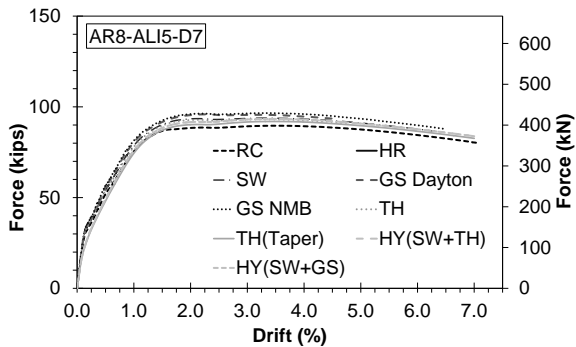


a. Force-drift relationship

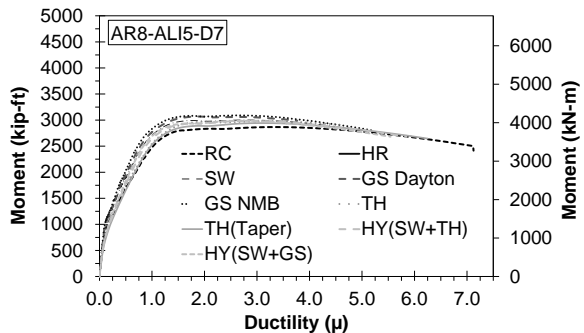


b. Moment-ductility relationship

Figure 5.22 Pushover analysis results for AR6-ALI5-D7

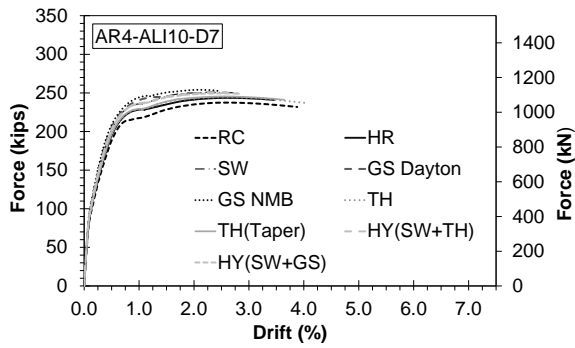


a. Force-drift relationship

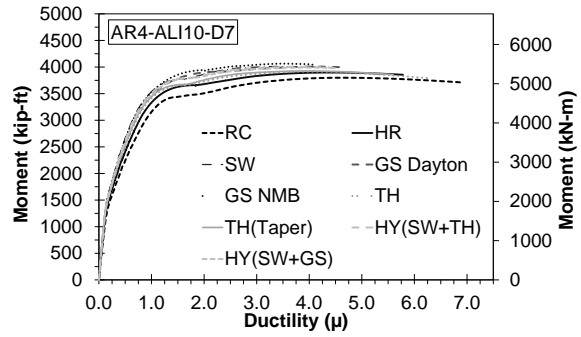


b. Moment-ductility relationship

Figure 5.23 Pushover analysis results for AR8-ALI5-D7

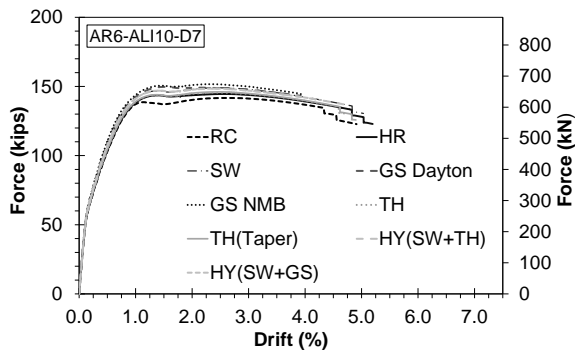


a. Force-drift relationship

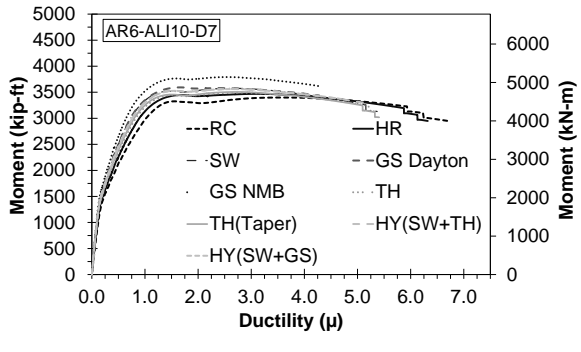


b. Moment-ductility relationship

Figure 5.24 Pushover analysis results for AR4-ALI10-D7

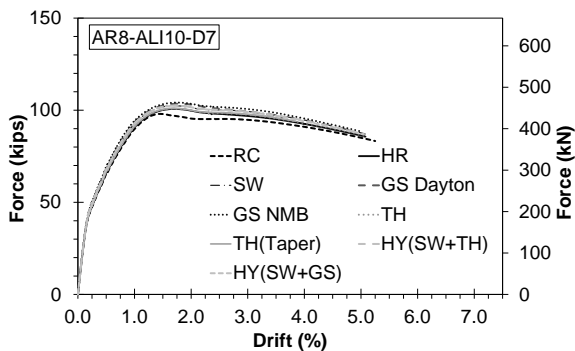


a. Force-drift relationship

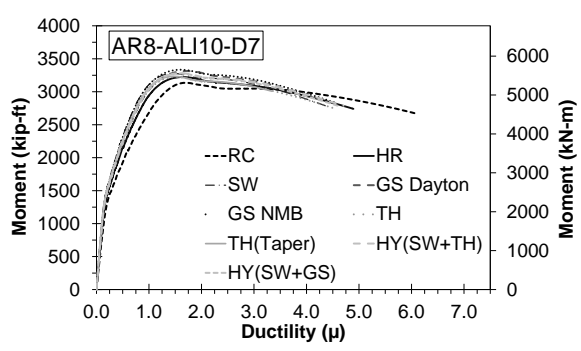


b. Moment-ductility relationship

Figure 5.25 Pushover analysis results for AR6-ALI10-D7

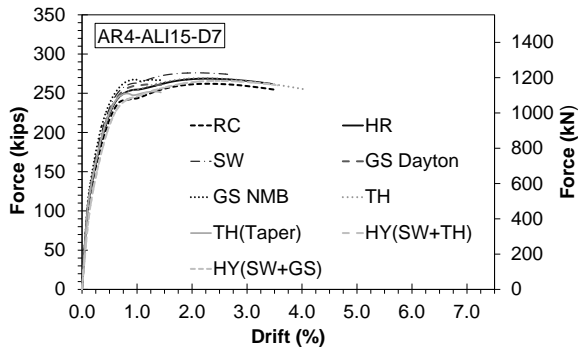


a. Force-drift relationship

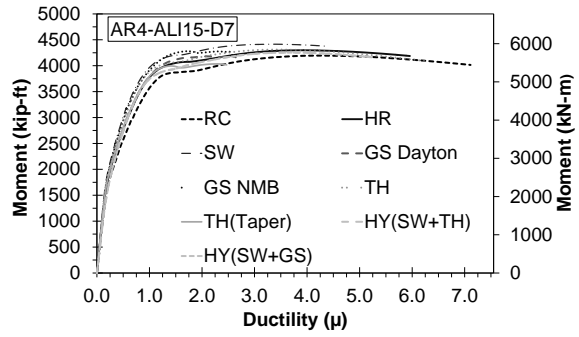


b. Moment-ductility relationship

Figure 5.26 Pushover analysis results for AR8-ALI10-D7

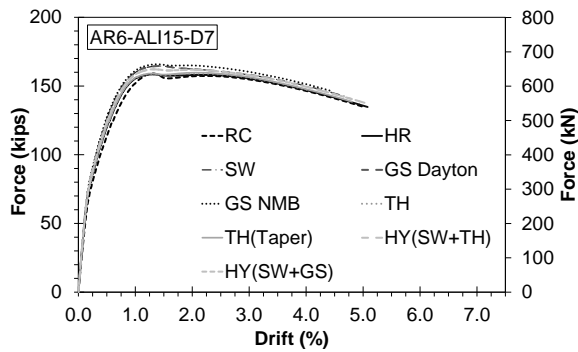


a. Force-drift relationship

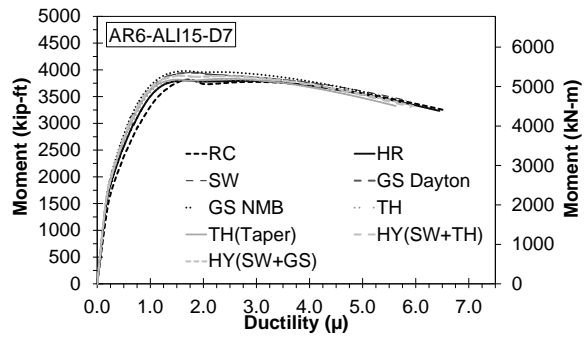


b. Moment-ductility relationship

Figure 5.27 Pushover analysis results for AR4-ALI15-D7

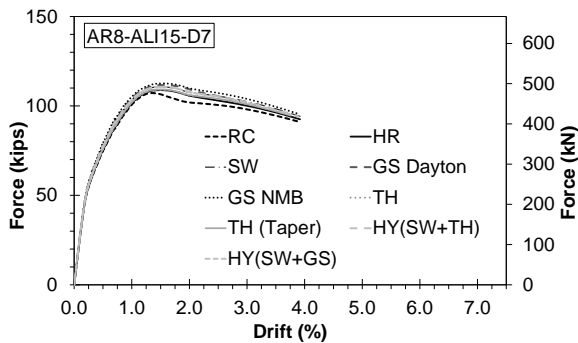


a. Force-drift relationship

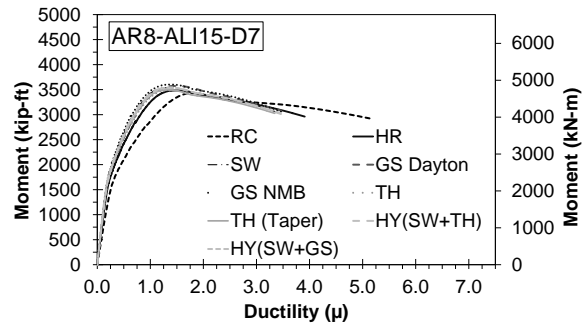


b. Moment-ductility relationship

Figure 5.28 Pushover analysis results for AR6-ALI15-D7



a. Force-drift relationship



b. Moment-ductility relationship

Figure 5.29 Pushover analysis results for AR8-ALI15-D7

5.4.4 Summary of Parametric Study

Table 5.6 presents a summary of the parametric study in which the displacement ductility capacity and the reduction of the displacement ductility capacity of spliced columns compared with their corresponding unspliced columns for all 243 analyses are included. Ductility presented under the second column of the table is for the reference unspliced RC columns.

Even though there are significant variations in the results, the general trend is that mechanically spliced bridge columns with longer and more rigid couplers will exhibit lower displacement ductility capacities. Columns with higher ductilities are affected more when couplers are used in their plastic hinge regions. For example, the lowest displacement ductility capacity in all analyses was for AR8-ALI15-D7 spliced with grouted sleeve couplers (NMB). In this column, the displacement ductility capacity was 43% lower than that of its corresponding RC column. Furthermore, columns spliced with short couplers and low rigidity can show as large displacement capacity as RC columns. One example is AR6-ALI10-D7 spliced with headed reinforcement couplers (HRC), which had only 6% lower displacement ductility capacity compared with its reference RC column.

Table 5.6 Summary of parametric study on mechanically spliced bridge columns

Column ID	Ductility (Ductility Reduction Compared to RC in %)								
	RC	HR $L_{sp} = 3.88$ in. $\beta = 0.55$	TH $L_{sp} = 3.06$ in. $\beta = 1.65$	TH-Taper $L_{sp} = 4.20$ in. $\beta = 1.05$	SW $L_{sp} = 9.50$ in. $\beta = 0.95$	GS-NMB $L_{sp} = 18$ in. $\beta = 0.85$	GS-Dayton $L_{sp} = 18$ in. $\beta = 0.65$	HY-Dextra $L_{sp} = 10.63$ in. $\beta = 0.85$	HY-Erico $L_{sp} = 10.75$ in. $\beta = 0.80$
AR4-ALI5-D3	3.0	2.8 (7.6)	2.6 (15.0)	2.5 (16.9)	2.4 (19.9)	2.6 (14.0)	2.6 (6.6)	2.5 (15.6)	2.6 (14.0)
AR4-ALI5-D5	4.9	4.9 (0.2)	4.4 (10.8)	4.2 (14.6)	4.0 (18.2)	3.2 (36.0)	3.4 (30.4)	4.5 (8.5)	4.5 (8.7)
AR4-ALI5-D7	7.0	5.3 (24.8)	6.2 (12.2)	5.6 (21.1)	4.2 (40.7)	4.5 (36.4)	4.0 (42.8)	4.1 (41.4)	4.5 (35.7)
AR4-ALI10-D3	2.9	2.9 (1.0)	2.5 (13.7)	2.5 (16.1)	2.3 (21.6)	2.7 (6.2)	2.7 (6.2)	2.5 (13.7)	2.6 (11.3)
AR4-ALI10-D5	5.0	5.0 (0.0)	4.5 (10.7)	4.4 (12.3)	3.8 (24.7)	3.9 (20.9)	4.0 (20.1)	2.6 (47.6)	4.0 (19.9)
AR4-ALI10-D7	6.9	5.8 (16.4)	6.3 (9.0)	5.6 (18.6)	4.3 (38.3)	4.1 (41.3)	4.6 (33.4)	4.4 (35.8)	4.6 (34.0)
AR4-ALI15-D3	3.0	2.9 (4.0)	2.7 (11.7)	2.6 (13.3)	2.6 (15.0)	2.6 (14.3)	2.7 (11.7)	2.9 (4.7)	2.9 (4.3)
AR4-ALI15-D5	5.0	4.9 (2.1)	4.6 (9.5)	4.5 (10.3)	4.6 (8.5)	3.2 (37.1)	3.7 (26.6)	3.9 (23.4)	3.9 (22.8)
AR4-ALI15-D7	7.1	6.0 (16.3)	5.0 (29.8)	6.7 (5.5)	5.1 (28.1)	4.6 (34.9)	4.9 (30.9)	4.1 (42.1)	5.3 (25.5)
AR6-ALI5-D3	3.1	2.9 (8.5)	2.6 (15.3)	2.6 (17.8)	2.4 (22.3)	2.6 (16.9)	2.8 (10.1)	2.6 (18.2)	2.6 (18.2)
AR6-ALI5-D5	5.1	4.9 (4.5)	4.5 (11.9)	4.3 (17.0)	4.1 (19.9)	3.7 (28.1)	5.0 (3.3)	4.2 (17.2)	4.4 (14.3)
AR6-ALI5-D7	7.3	6.5 (11.6)	4.8 (34.7)	6.2 (15.8)	5.0 (31.8)	4.3 (41.2)	4.8 (34.7)	4.7 (35.5)	5.1 (31.0)
AR6-ALI10-D3	3.3	2.8 (14.0)	2.6 (21.9)	2.5 (24.0)	2.3 (29.2)	2.5 (22.8)	2.8 (16.4)	2.5 (24.3)	2.5 (22.8)
AR6-ALI10-D5	5.1	4.9 (3.7)	4.3 (14.4)	4.2 (16.9)	4.0 (20.7)	4.7 (7.8)	4.5 (10.2)	4.5 (11.6)	4.7 (8.0)
AR6-ALI10-D7	6.7	6.3 (6.1)	5.8 (14.3)	5.6 (16.8)	5.4 (20.2)	4.9 (26.9)	4.8 (28.1)	5.2 (23.0)	4.7 (29.6)
AR6-ALI15-D3	2.9	2.8 (3.1)	2.6 (9.6)	2.6 (12.7)	2.4 (17.1)	2.6 (10.3)	2.9 (2.1)	2.6 (12.7)	2.6 (10.6)
AR6-ALI15-D5	4.9	4.8 (2.2)	4.3 (11.8)	4.3 (13.4)	4.6 (6.3)	4.3 (13.4)	4.0 (17.7)	4.6 (7.1)	4.7 (4.5)
AR6-ALI15-D7	6.6	6.4 (1.7)	6.0 (8.2)	5.9 (10.2)	5.9 (10.7)	5.4 (18.3)	4.3 (34.5)	6.0 (8.4)	6.0 (8.1)
AR8-ALI5-D3	3.0	2.8 (7.9)	2.6 (14.5)	2.5 (17.5)	2.4 (22.4)	2.5 (19.1)	2.7 (10.9)	2.5 (18.2)	2.5 (18.2)
AR8-ALI5-D5	5.1	4.5 (11.9)	5.3 (-2.7)	5.1 (0.8)	3.8 (26.0)	4.5 (11.7)	4.3 (16.4)	5.2 (-1.0)	3.5 (32.3)
AR8-ALI5-D7	7.1	4.3 (40.2)	6.1 (14.5)	6.3 (12.2)	5.3 (26.1)	5.2 (27.4)	5.0 (30.2)	5.8 (18.0)	5.5 (22.2)
AR8-ALI10-D3	3.1	2.8 (8.7)	2.6 (17.1)	2.5 (19.7)	2.6 (15.8)	2.6 (17.7)	2.8 (11.3)	2.5 (19.7)	2.5 (18.1)
AR8-ALI10-D5	5.2	4.5 (12.8)	4.2 (19.0)	4.3 (17.3)	4.4 (15.3)	4.1 (19.6)	4.3 (17.1)	4.1 (19.6)	4.0 (22.1)
AR8-ALI10-D7	7.0	4.8 (31.2)	4.6 (35.2)	4.4 (36.9)	4.5 (35.3)	4.6 (35.2)	4.5 (35.3)	4.7 (33.0)	4.6 (34.6)
AR8-ALI15-D3	3.1	2.9 (6.2)	2.6 (18.3)	2.5 (20.8)	2.4 (25.0)	2.5 (20.2)	2.9 (6.2)	2.5 (20.5)	2.6 (18.6)
AR8-ALI15-D5	5.1	3.8 (25.0)	3.5 (30.5)	3.4 (32.9)	3.3 (35.8)	3.4 (32.5)	3.5 (30.5)	3.4 (33.5)	3.4 (32.5)
AR8-ALI15-D7	6.0	3.9 (35.4)	3.6 (40.1)	3.6 (40.7)	3.5 (42.4)	3.5 (42.7)	3.7 (38.9)	3.5 (42.7)	3.5 (41.9)

Note: "AR" refers to the aspect ratio, "ALI" refers to the column axial load index, "D" refers to the displacement ductility capacity, "RC" refers to the reference columns, "HR" refers to the headed reinforcement couplers, " L_{sp} " is the coupler length, " β " is the coupler rigid length factor, "TH" refers to the threaded couplers, "SW" refers to the swaged couplers, "GS" refers to the grouted couplers, and "HY" refers to the hybrid couplers; 1 in. = 25.4 mm.

5.5 Summary

A parametric study was performed to investigate the seismic performance of bridge columns utilizing mechanical bar splices. A total of 243 pushover analyses were performed on 27 columns spliced with eight different coupler products. The following conclusions can be drawn based on the pushover analysis.

- Columns incorporating mechanical bar splices will usually show lower displacement ductility capacities compared with conventional RC columns.
- The parametric study showed that the coupler length and its rigid length factor significantly affect the displacement ductility capacity of mechanically spliced columns. Long couplers with a high rigid length factor may decrease the displacement ductility capacity by 43%.
- The lateral load carrying capacity of mechanically spliced bridge columns are slightly higher than that of conventional columns (no more than 10%).

5.6 References

- AASHTO SGS. (2011). "AASHTO Guide Specifications for LRFD Seismic Bridge Design," Washington, DC: American Association of State Highway and Transportation Officials.
- ASTM A706/A706M-09b. (2009). "Standard Specification for LowAlloy Steel Deformed and Plain Bars for Concrete Reinforcement," ASTM International, West Conshohocken, PA.
- Ameli, M.J. and. Pantelides, C.P. (2016). "Seismic Analysis of Precast Concrete Bridge Columns Connected with Grouted Splice Sleeve Connectors," *Journal of Structural Engineering*, ASCE, Vol. 143, No. 2, 13 pp.
- Mander, J.B., Priestly, M.J.N., and Park, R. (1988). "Theoretical Stress-Strain Model for Confined Concrete," *Journal of Structural Engineering*, ASCE, Vol 114, No. 8, pp. 1804-1826.
- Haber, Z.B., Saiidi, M.S., and Sanders, D.H. (2013). "Precast Column Footing Connections for Accelerated Bridge Construction in Seismic Zones." Rep. No. CCEER 13-08 Center for Civil Engineering Earthquake Research, Dept. of Civil and Environmental Engineering, Univ. of Nevada, Reno. NV.
- OpenSees. (2016). "Open System for Earthquake Engineering Simulations," Version 2.4.1, Berkeley, CA, Available online: <<http://opensees.berkeley.edu>>.
- Tazarv, M. and Saiidi, M.S. (2016). "Seismic Design of Bridge Columns Incorporating Mechanical Bar Splices in Plastic Hinge Regions," *Engineering Structures*, DOI: 10.1016/j.engstruct.2016.06.041, Vol. 124, pp. 507-520.
- Tazarv, M., and Saiidi, M.S. (2014). "Next Generation of Bridge Columns for Accelerated Bridge Construction in High Seismic Zones," Center for Civil Engineering Earthquake Research, University of Nevada, Reno, NV, CCEER Report No. 14-06, 400 pp.

6. MECHANICAL BAR SPLICES FOR ACCELERATED CONSTRUCTION OF BRIDGE COLUMNS

6.1 Introduction

Mechanical bar splices, which are commonly referred to as bar couplers, can be incorporated in bridge columns to accelerate construction. For accelerated bridge construction (ABC), couplers most likely will be used at the ends of precast columns either inside the column or in the column adjoining member. In either case, couplers might affect the column seismic performance by mainly reducing the displacement capacity.

Not all mechanical bar splices can be used in bridge columns since they may prematurely fail. The current specifications ban the use of couplers in column plastic hinge regions. Nevertheless, establishing a standard testing method for couplers, providing acceptance criteria for couplers, and quantifying coupler effects on the column behavior may relax this ban and may allow deployment of mechanically spliced precast columns in high seismic regions.

Based on the findings of the present study and the review of the literature, acceptance criteria, a material model, and standard testing methods are proposed for mechanical bar splices.

6.2 Proposed Acceptance Criteria for Mechanical Bar Splices

Current U.S. bridge design codes specify certain limitations for mechanical bar splices mainly for use in non-critical sections, or in bridge columns located in low seismic zones. AASHTO LRFD Bridge Design Specifications (AASHTO LRFD) (2013) categorize couplers as “full-mechanical connection” when they resist at least a stress of 1.25 times the specified yield strength of the spliced bar. AASHTO LRFD also specifies the total slip of a bar within the splice following the California Department of Transportation (Caltrans) Seismic Design Criteria (SDC). The AASHTO Guide Specifications for LRFD Seismic Bridge Design (AASHTO SGS) (2011) do not allow the use of full-mechanical connections in the plastic hinge of bridge columns located in seismic design categories of C and D.

To consider the use of mechanical bar splices in column plastic hinges, new acceptance criteria that reflect column seismic loading are needed to determine the suitability of these splices. To facilitate certification of existing and new splices for seismic application, the acceptance criteria will need to be universal, encompassing various couplers with a variety of characteristics.

6.2.1 General Requirements

Based on available information, the following minimum acceptance criteria for couplers in column plastic hinges are proposed:

1. The total length of a mechanical bar splice (L_{sp}) shall not exceed 15 times the diameter of the smaller of the two spliced bars in columns.
2. A spliced bar shall fracture outside the coupler region with a strength of at least 95% of the ultimate tensile strength of its reference unspliced bar regardless of the loading type (monolithic, cyclic, or dynamic). The coupler region length is defined as $L_{cr} = L_{sp} + 2 \alpha d_b$, where α is a variable limited to 2 (Figure 6.1), and d_b is the diameter of the larger spliced bar. Only ASTM A706 Grade 60 reinforcing steel bars shall be used for seismic applications.

Couplers that meet both requirements are referred to as “seismic mechanical bar splices” or seismic couplers in the present document.

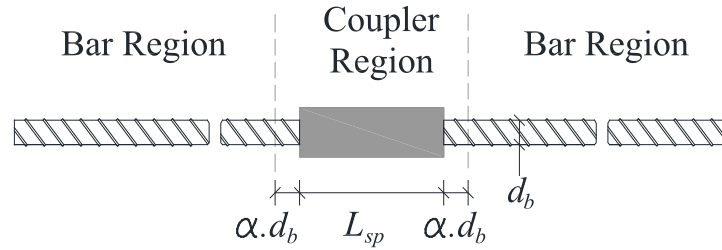


Figure 6.1 Coupler and bar regions

The coupler length limitation is meant to minimize adverse effects of a coupler on the rotational capacity of the structural member due to possible reduction in the plastic hinge length. Another reason for the limit on the coupler length is that test data are available only for columns with a coupler length of $15d_b$ or less. The literature review confirmed that bridge columns incorporating couplers that cannot develop the full stress and strain capacity of the spliced bars fail prematurely. Therefore, only couplers in which the bar fracture is outside the coupler region are acceptable. AASHTO SGS presents the expected mechanical properties for ASTM A706 reinforcing steel bars. These requirements were adopted in the present study. Other types of steel bars shall not be used as longitudinal reinforcement in bridge columns in moderate and high seismic zones. The 95% strength requirement guarantees that a seismic coupler is achieving large strains with sufficient strength.

6.3 Proposed Material Model for Mechanical Bar Splices

When a spliced bar is in tension (Figure 6.2a), it can be assumed that a portion of the coupler (βL_{sp}) is rigid, thus does not contribute to the elongation of the coupler region. L_{sp} is the coupler length and β is defined as the “coupler rigid length factor,” and is determined from tensile testing of a spliced bar. This factor is affected by the deformation of the coupler region that includes elongation of the spliced portion of the bar within the coupler, the coupler elongation, and the bar slippage. The reduction in the total elongation of the splice results in smaller overall strains for the coupler region compared with those measured in the bar alone (Figure 6.2b). Therefore, the coupler region strain (ε_{sp}) can be estimated as

$$\frac{\varepsilon_{sp}}{\varepsilon_s} = \frac{L_{cr} - \beta L_{sp}}{L_{cr}} \quad (\text{Eq. 6.1})$$

where ε_s is the strain of an unspliced bar.

The coupler axial stiffness may vary depending on the anchoring mechanism. For example, the size of threads and the bearing strength of threads in threaded couplers, or the bond strength between the sleeve and the grout, controls the axial stiffness of the coupler. Another example is the extent of penetration of screws into the spliced bars and the strength of screws in shear-screw couplers. The coupler rigid length factor ranges theoretically from 0.0 to 1.0. As an example, Figure 6.3 shows coupler region stress-strain relationships for a coupler rigid length factor of 0.25 and 0.75 for a No. 10 (32 mm) ASTM A706 Grade 60 bar.

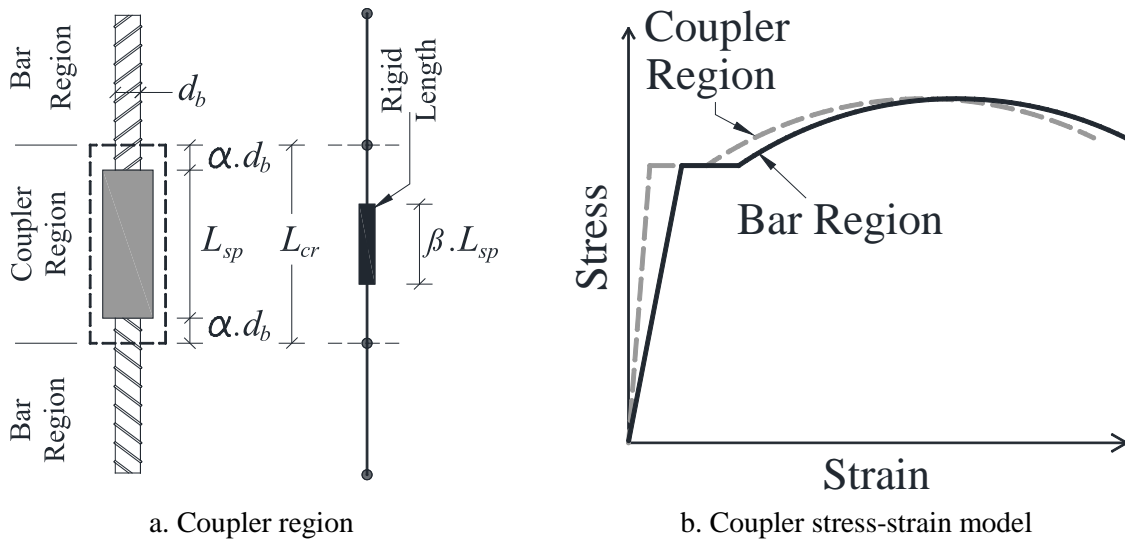


Figure 6.2 Generic stress-strain model for mechanical bar splices (Tazarv and Saïdi, 2016)

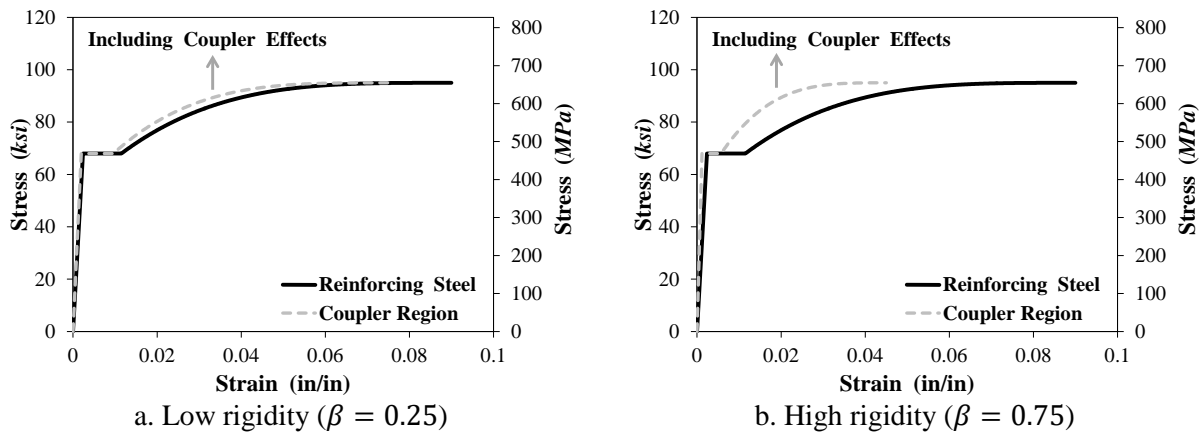


Figure 6.3 Stress-strain relationships for mechanically spliced No. 10 (32 mm) bars

Mechanical bar couplers that meet the proposed minimum requirements do not alter the strength of spliced bars since the strength of the connection is controlled by the strength of the spliced bars. Couplers that do not exhibit fracture outside the coupler region are not acceptable. Examples include fracture of bars within the coupler due to stress concentration under the screws in a shear-screw coupler, bar pullout in a grouted coupler, thread failure in a threaded coupler, and bar fracture inside the coupler region. In summary, mechanical bar couplers do not increase the strength beyond the strength of the spliced bars; thus, no adjustment in the overstrength factor beyond that required in AASHTO SGS is expected for this type of connections.

6.4 Proposed Method of Testing for Mechanical Bar Splices

California Test 670 (2004) and ASTM A1034 (2016) present testing procedures for reinforcing steel bar mechanical splices. Since the ASTM standard provides neither a modeling method for couplers nor any acceptance criteria, the California Test method was adopted in the present study. However, further modifications were made to accommodate the requirements presented in the previous sections for

couplers. For example, the California test procedure only allows testing of couplers with a length of $10d_b$ or less. This limitation is removed in the present document.

6.4.1 Scope

This test method presents monotonic, cyclic, and dynamic testing procedures for the determination of mechanical properties of mechanical bar splices for incorporation in the plastic hinge region of ductile members such as bridge columns. The proposed testing methods can be used for spliced bars conforming to either ASTM A706 or ASTM A615. Recall, however, that A615 bars are excluded from use in the plastic hinge regions of columns in SDC C and D.

6.4.2 Referenced Documents

- ASTM A370 / A370M – Test Methods and Definitions for Mechanical Testing of Steel Products
- ASTM A615 / A615M – Specifications for Deformed and Plain Carbon-Steel Bars for Concrete Reinforcement
- ASTM A706 / A706M – Low-Alloy Steel Deformed and Plain Bars for Concrete Reinforcement
- ASTM E4 – Practices for Force Verification of Testing Machines
- ASTM E8 / E8M – Test Methods for Tension Testing of Metallic Materials
- ASTM E83 – Practice for Verification and Classification of Extensometer Systems
- ASTM E2309 / E2309M – Practices for Verification of Displacement Measuring Systems and Devices Used in Material Testing Machines

6.4.3 Apparatus

- 1) Testing Machines – Tensile testing machines shall conform to the requirements of ASTM E4. Components of testing machines, such as grips, measurement devices, and calibration of the machines, shall conform to the requirements of ASTM E8 and ASTM A370.
- 2) Displacement Measuring Devices – Displacement measuring devices, such as dial indicators and LVDTs, shall conform to the requirements of Class-A ASTM E2309.
- 3) Extensometers – Extensometers used in strain measurement shall conform to the requirements of ASTM E83. Use Class B2 or better extensometers.
- 4) Caliper – A calibrated caliper with an accuracy of 0.001 *in.* or better.

6.4.4 Definitions

Bar Region – A length of the spliced bar outside the coupler region (Figure 6.4) that is utilized for the strain measurement of spliced bars.

Coupler Region – A length consisting of the total length of the coupler (L_{sp}) plus α times the diameter of the larger spliced bar (or $\alpha \cdot d_b$) on each end of the coupler (Figure 6.4). Alpha shall not exceed two.

Coupler Rigid Length factor (β) – A factor that represents the rigidity of a coupler, which depends on the anchoring mechanism of the coupler and includes the effect of coupler elongation, bar elongation inside the coupler, and the slippage of the spliced bars inside the coupler.

Fracture – Physical rupture or breaking of bars or couplers.

Lot – a lot includes a 150 count, or a fraction thereof, of the same type of either reinforcing bars or mechanical bar splices for each bar size and bar deformation pattern.

Mechanical Bar Splices – Mechanical devices that are used to connect two reinforcing bars. The term “coupler” is frequently used for mechanical bar splices.

Plastic Range – A strain range between the yield and the ultimate points in the stress-strain relationship of a reinforcing bar.

Samples – Reinforcing bars from the same lot.

Seismic Splices – Couplers that are not longer than $15d_b$ and exhibit bar fracture outside the coupler region with a strength that is at least 95% of the tensile strength of a corresponding “unspliced specimen,” as defined below. All the spliced specimens shall meet these requirements to be considered a “seismic coupler”.

Spliced Specimen – A specimen including a coupler and two spliced bars connected to the coupler.

Strain – The ratio of the elongation of the test specimen within an initial gauge length (measuring region) to the initial gauge length.

Stress – The ratio of the applied load to the sample nominal cross-section area.

Ultimate Strain – The strain at the peak tensile stress.

Ultimate Strength – The peak tensile stress.

Unspliced Specimen – A single-bar specimen used to determine benchmark mechanical properties of bars.

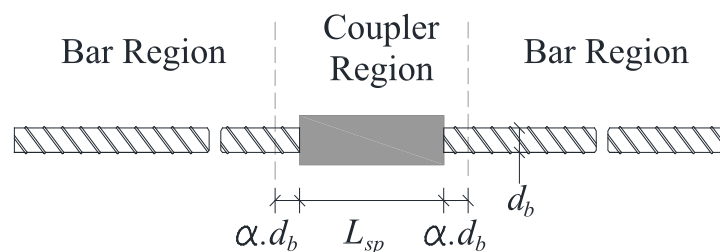


Figure 6.4 Coupler and bar regions

6.4.5 Physical Properties and Preparation

Each test sample shall conform to the following requirements:

- 1) **Sample length:** For No. 9 (29-mm) bars and smaller, sample length must be at least 5 ft. (1.52 m). For No. 10 (32-mm) bars and larger, sample length must be at least 7.5 ft. (2.29 m). The unspliced and spliced specimens for each test shall be taken from the same lot. It is highly recommended to take each set of the unspliced and spliced specimens from the same sample (bar).
- 2) **Spliced specimen length:** The lab may shorten, machine, or otherwise alter the submitted sample length to meet the configuration of its testing equipment. The minimum length of the spliced specimen between the grips of the tensile testing machine shall be $L_{sp} + 16d_b$, where L_{sp} is the coupler length and d_b is the nominal bar diameter of the larger spliced bar. The center of the coupler shall be located at the center of the test specimen.

- 3) Alignment: The alignment along the test sample must be straight to within 0.5 in. (12.7 mm) along any 3 ft. (914 mm) of the length of the sample.

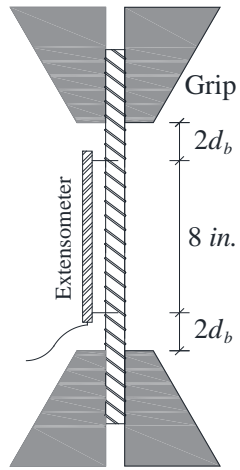
6.4.6 Monotonic Test

Monotonic tensile testing of unspliced and spliced specimens is required for each bar size and shall be performed according to ASTM A370. A minimum of four samples shall be tested for each lot.

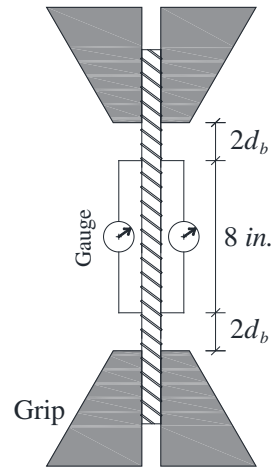
Steps for tensile testing of an **unspliced specimen** are as follows:

- 1) Apply an axial tensile load to the unspliced specimen to fracture.
- 2) Full stress-strain relationship can be obtained using continuous measurement (e.g., 8-in. extensometer or two high-resolution LVDTs and data acquisition system) (Figure 6.5a) or discontinuous measurement (dial or digital indicators) (Figure 6.5b). Steps for the discontinuous method are:
 - a. Measure the initial gauge length using a caliper. The greater of $5d_b$ and 8 in. is recommended as the gauge length.
 - b. Mount the unspliced specimen in the tensile test machine.
 - c. Attach two displacement measuring devices so their indicators are 180° apart.
 - d. Once the setup is completed, stress the unspliced specimen to 3,000 psi (20 MPa) then zero out the indicators.
 - e. Apply an axial stress of 30,000 psi (200 MPa). Maintain this stress until a stable reading is obtained from both indicators. Record the two indicator readings then take the average of the two readings. Increase the stress to 90% the nominal yield strength and record the average of the two indicator readings.
 - f. After the two initial readings in the elastic range, more frequent readings are needed to properly capture the plastic range of the stress-strain diagram. At least 10 data points are needed in the plastic range. The appropriate readings (force in the plastic range) may be obtained when the indicators show values corresponding to strains equal to 0.005, 0.01, 0.02, 0.03, 0.04, 0.05, 0.06, 0.07, 0.08, 0.09, and 0.01 in./in. Readings with an interval of 0.01 in./in. should be continued until the bar fractures.
- 3) Remove the displacement measuring devices.
- 4) Report the full stress-strain relationship for the unspliced specimen (Figure 6.6a).

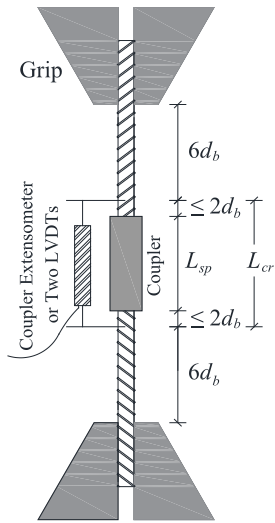
NOTE – For an unspliced specimen, the measurement is valid only when the bar fractures within the instrumented gauge length.



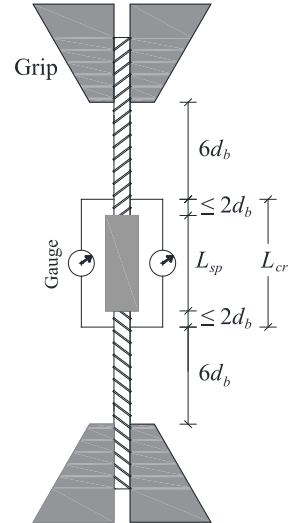
(a) Unspliced specimen – continuous reading



(b) Unspliced specimen – discontinuous reading



(c) Spliced specimen - continuous reading



(d) Spliced specimen - discontinuous reading

Figure 6.5 Test setup and minimum length requirements for unspliced and spliced specimens

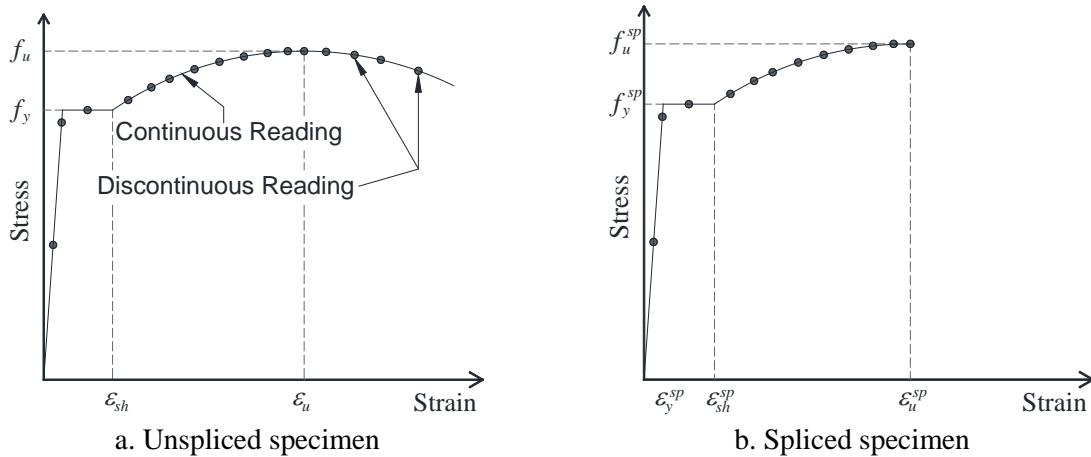


Figure 6.6 Measured stress-strain relationships for unspliced and spliced specimens

Steps for tensile testing of a **spliced specimen** are as follows:

- 1) Apply an axial tensile load to the spliced specimen to fracture. The prior-to-yielding strain rate specified in ASTM E8 is recommended for testing the spliced specimens.
- 2) Full stress-strain relationship can be obtained using continuous measurement (e.g., a coupler extensometer or two high-resolution LVDTs and data acquisition system) (Figure 6.5c) or discontinuous measurement (dial or digital indicators) (Figure 6.5d). Steps for the discontinuous method are:
 - a. Measure the initial gauge length using a caliper. The gauge length shall be taken as $L_{cr} = L_{sp} + 2\alpha d_b$, where α shall not exceed two.
 - b. Mount the spliced specimen in the tensile test machine as shown in Figure 6.5d.
 - c. Attach two displacement measuring devices so their indicators are 180° apart.
 - d. Once the setup is complete, stress the smaller spliced specimen to 3,000 psi (20 MPa) in the bar then zero out both indicators.
 - e. Apply an axial stress of 30,000 psi (200 MPa) in the smaller spliced bar. Maintain this stress until a stable reading is obtained from both indicators. Record the two dial indicator readings, then take the average of the two readings. Increase the stress to 90% the nominal yield strength of the smaller spliced bars and record the average of the two indicator readings.
 - f. After two initial readings in the elastic range, more frequent readings are needed for the plastic range of the stress-strain diagram. At least 10 data points are needed in the plastic range. The appropriate readings (force in the plastic range) may be obtained when the indicators show values corresponding to strains equal to 0.005, 0.01, 0.015, 0.02, 0.025, 0.03, 0.035, 0.04, 0.045, 0.05, and 0.055 in./in. Readings with an interval of 0.005 in./in. should be continued until the bar fractures.
- 3) Remove the displacement measuring devices.
- 4) Report the mode of failure (bar fracture, bar pullout, or coupler failure) and the location of the failure.
- 5) report the full stress-strain relationship for the spliced specimen (Figure 6.6b).
- 6) Superimpose the stress-strain relationship of the spliced specimen with that measured for the unspliced specimen (Figure 6.7). At a stress (f_i) greater than the measured f_y , draw a horizontal line on the stress-strain graph then obtain the spliced and unspliced strains associated with f_i . Calculate

$$\beta_i = \left(1 - \frac{\varepsilon_{sp}^i}{\varepsilon_s^i}\right) \left(\frac{L_{cr}}{L_{sp}}\right) \quad (\text{Eq. 6.2})$$

Repeat this process for at least five stress levels using data obtained in Step 2f with the last point being where $f_i = f_u$. Calculate the coupler rigid length factor as

$$\beta = \max\left(\frac{1}{N} \sum \beta_i, \beta_u\right) \quad (\text{Eq. 6.3})$$

where N is the number of the data points, and β_u is the rigid length factor calculated based on the strain at the peak stress ($i = u$ in Eq. 6.2). Round up the calculated coupler rigid length factor to the nearest 0.05 (e.g., 0.76 will be 0.80). The calculated coupler rigid length shall be limited between zero and one ($0.0 \leq \beta \leq 1.0$).

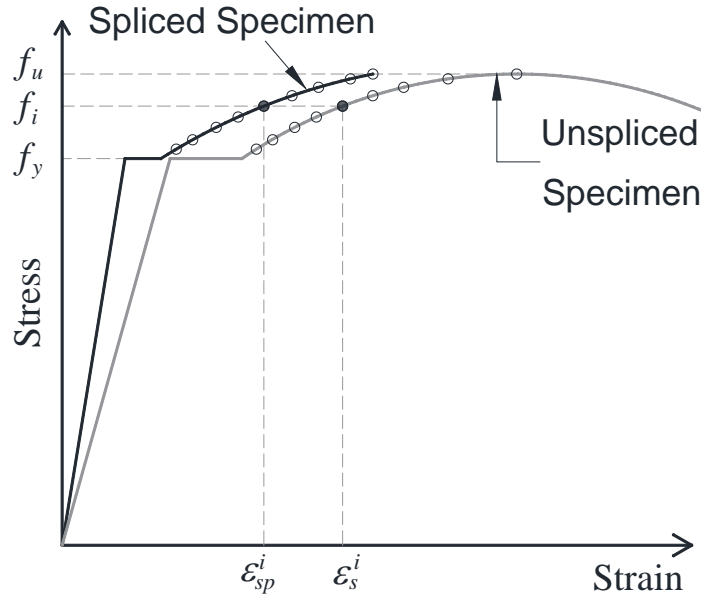


Figure 6.7 Calculation of coupler rigid length factor based on stress-strain relationships

- 7) Report all β_i , β_u , and β . The design value for the coupler rigid length factor may be taken as the average for all four the test specimens.

NOTE – When the testing facility allows continuous measurement with multiple channels using a data acquisition system, the unspliced bar stress-strain relationship may be measured during the testing of a spliced sample. A pair of extensometers, one for each potential bar fracture zone outside the coupler region, may be used for this purpose. In this case, the ratio of the coupler region strain to the bar region strain can be directly calculated using the continuous dataset, but utilizing the strain data from the extensometer in which the spliced bar fractures. Subsequently, the coupler rigid length factor can be calculated according to Eq. 6.2 and then Eq. 6.3.

- 8) Report whether or not the coupler meets the requirements of the seismic coupler under monotonic loading.

NOTE – For a spliced specimen, the strain measurement is valid only when the bar fractures outside the coupler region and outside the grip. Another spliced specimen may be tested if the splice is potentially a seismic coupler to obtain reliable strain data. Beta should be reported only for a seismic coupler. Couplers that do not meet the seismic coupler requirements shall not be used for ductile members.

6.4.7 Cyclic Test

Cyclic tensile testing of spliced specimens is required for product verification of a new coupler or that which has not been tested according to the cyclic test procedure presented herein. A minimum of four samples shall be tested for each lot. Continuous measurement, as explained in the previous section, is recommended. A cycle in this document refers to a half-cycle and consists of applying tensile axial loading to the specimen to a target stress or strain and unloading to zero force (or a small tensile force to prevent bar buckling).

For cyclic testing:

- 1) Cyclically load the spliced specimen to strains corresponding to stresses of 10%, 30%, 50%, 70%, 80%, 90%, and 100% of the ultimate strength (f_u) of the spliced bar. Repeat each cycle of loading four times. Use a constant rate of prior-to-yielding or post-yielding specified in ASTM E8.

NOTE I – To avoid buckling of the test sample under accidental compressive loads, the tensile stress on the unloading branch of each cycle does not need to be less than 3,000 psi (20 MPa) in the larger of the spliced bar.

NOTE II – Measured stress-strain data from a spliced specimen with the same coupler type, bar size, and reinforcement properties tested under monotonic loading may be used to determine the strains corresponding to the target cyclic stresses.

- 2) Report the mode of failure (bar fracture, bar pullout, or coupler failure) and the location of the failure. If continuous measurement is utilized, report the cyclic stress-strain graphs for the spliced specimens.
- 3) Report whether or not the coupler meets the requirements of the seismic coupler under cyclic loading.

6.4.8 Dynamic Test

Dynamic tensile testing of spliced specimens is required for product verification of a new coupler or that which has not been tested according to the dynamic test procedure presented herein. A minimum of four samples shall be tested for each lot. Continuous measurement, as explained in previous sections, should be used to collect dynamic data.

For dynamic testing:

- 1) Load the spliced specimen with a strain rate of 30,000 micro-strain/sec (3.0%/sec) to fracture. The strain rate may be converted to head displacement rate using a length equal to the grip-to-grip clear distance minus βL_{sp} . An error of up to 25% between the target and the achieved strain or displacement rate shall be allowed.
- 2) Report the mode of failure (bar fracture, bar pullout, or coupler failure) and the location of the failure. Report the stress-strain graphs for both spliced and unspliced specimens.
- 3) Report whether or not the coupler meets the requirements of the seismic coupler under dynamic loading.

NOTE – The proposed strain rate to simulate seismic loadings is based on data collected from several studies on bars and couplers (e.g., DesRoches et al., 2004; Haber et al., 2015, NCHRP 12-105), and large-scale shake-table column/bent tests (Laplace et al., 2002; Nada et al., 2003; Johnson et al., 2005, Phan et al., 2005; Brown and Saiidi, 2009; Zaghi and Saiidi, 2010; Mehraein and Saiidi, 2016).

6.4.9 Report

The lab staff shall develop a “test report,” which will include the items specified in the present document for each loading type.

6.4.10 Hazards

The test samples are heavy and may contain sharp edges or burrs. Sample fracture may involve brittle fractures and ejection of sample fragments. Use appropriate safety measures.

6.4.11 Safety

The user of this test method must establish appropriate safety and health practices and determine the applicability of regulatory limitations prior to use. Prior to handling, testing, or disposing of any materials, testers must be knowledgeable about safe laboratory practices, hazards and exposure, chemical procurement and storage, and personal protective apparel and equipment.

6.5 Summary

Current acceptance criteria for bar couplers do not ensure satisfactory performance of bar couplers in bridge columns under seismic loads because these criteria were developed against the backdrop of the current ban on couplers in plastic hinges. Therefore, new criteria were needed and proposed in this document. Acceptance criteria for seismic couplers, including monotonic, cyclic, and dynamic testing procedures, were specified to evaluate the suitability of couplers for seismic applications. A stress-strain model for use in analytical studies of columns with bar couplers was also presented.

6.6 References

- AASHTO LRFD. (2013). “AASHTO LRFD Bridge Design Specifications,” Washington, DC: American Association of State Highway and Transportation Officials.
- AASHTO SGS. (2011). “AASHTO Guide Specifications for LRFD Seismic Bridge Design,” Washington, DC: American Association of State Highway and Transportation Officials.
- ASTM A1034/A1034M-10a. (2015). “Standard Test Methods for Testing Mechanical Splices for Steel Reinforcing Bars,” West Conshohocken, PA, 5 pp.
- ASTM A370/A370M-15. (2015). “Standard Test Methods and Definitions for Mechanical Testing of Steel Products,” West Conshohocken, PA, 50 pp.
- ASTM A615/A615M-16. (2016). “Standard Specification for Deformed and Plain Carbon-Steel Bars for Concrete Reinforcement,” West Conshohocken, PA, 8 pp.
- ASTM A706/A706M-16. (2016). “Standard Specification for Low-Alloy Steel Deformed and Plain Bars for Concrete Reinforcement,” West Conshohocken, PA, 7 pp.
- ASTM E4. (2015) “Standard Practices for Force Verification of Testing Machines,” West Conshohocken, PA, 11 pp.
- ASTM E8/E8M-15a. (2015). “Standard Test Methods for Tension Testing of Metallic Materials,” West Conshohocken, PA, 29 pp.

- ASTM E83-10a. (2010). "Practice for Verification and Classification of Extensometer Systems," West Conshohocken, PA, 14 pp.
- ASTM E2309/E2309M. (2016). "Practices for Verification of Displacement Measuring Systems and Devices Used in Material Testing Machines," West Conshohocken, PA, 8 pp.
- Brown, A. and Saiidi, M.S. (2009). "Investigation of Near-Fault Ground Motion Effects on Substandard Bridge Columns and Bents," Center for Civil Engineering Earthquake Research, Department of Civil and Environmental Engineering, University of Nevada, Reno, Nevada, Report No. CCEER-09-1, July.
- California Test 670. (2004). "Method of Tests for Mechanical and Welded Reinforcing Steel Splices," Sacramento, CA, California Department of Transportation, 13 pp.
- Caltrans. (2013). "Seismic Design Criteria (SDC)," version 6.7. Sacramento, CA: California Department of Transportation.
- DesRoches, R., McCormick, J., Delemont, M. (2004). "Cyclic Properties of Superelastic Shape Memory Alloy Wires and Bars," *Journal of Structural Engineering, ASCE*, Vol. 130, No. 1, pp. 38-46.
- Haber, Z.H., Saiidi, M.S., and Sanders, D.H. (2015). "Behavior and Simplified Modeling of Mechanical Reinforcing Bar Splices," *ACI Structural Journal*, Vol. 112, No. 2, pp. 179-188.
- Johnson, N., Saiidi, M.S., and Sanders, D. (2006). "Large-Scale Experimental and Analytical Seismic Studies of a Two-Span Reinforced Concrete Bridge System," Center for Civil Engineering Earthquake Research, Department of Civil and Environmental Engineering, University of Nevada, Reno, NV, Report No. CCEER-06-02, March.
- Laplace, P., Sanders, D., and Saiidi, M.S. (2001). "Experimental Study and Analysis of Retrofitted Flexure and Shear Dominated Circular Reinforced Concrete Bridge Columns Subjected to Shake Table Excitation," Center for Civil Engineering Earthquake Research, Department of Civil and Environmental Engineering, University of Nevada, Reno, NV, Report No. CCEER-01-6, June.
- Mehraein, M., and Saiidi, M.S. (2016). "Seismic Performance of Bridge Column-Pile-Shaft Pin Connections for Application in Accelerated Bridge Construction," Center for Civil Engineering Earthquake Research, Department Of Civil and Environmental Engineering, University of Nevada, Reno, NV, Report No. CCEER-16-01, May.
- Nada, H., D. Sanders, D., and Saiidi, M.S. (2003). "Seismic Performance of RC Bridge Frames with Architectural-Flared Columns," Center for Civil Engineering Earthquake Research, Department of Civil and Environmental Engineering, University of Nevada, Reno, NV, Report No. CCEER 03-3, January.
- Phan, V., Saiidi, M.S., and Anderson, J. (2005) "Near Fault (Near Field) Ground Motions Effects on Reinforced Concrete Bridge Columns," Center for Civil Engineering Earthquake Research, Department of Civil and Environmental Engineering, University of Nevada, Reno, NV, Report No. CCEER-05-7, August.
- Tazarv, M. and Saiidi, M.S. (2015). "Design and Construction of Bridge Columns Incorporating Mechanical Bar Splices in Plastic Hinge Zones," Center For Civil Engineering Earthquake Research, Department of Civil and Environmental Engineering, University of Nevada, Reno, NV, Report No. CCEER-15-07, 149 pp.

Tazarv, M. and Saiidi, M.S. (2016) “Seismic Design of Bridge Columns Incorporating Mechanical Bar Splices in Plastic Hinge Regions,” *Engineering Structures*, DOI: 10.1016/j.engstruct.2016.06.041, Vol. 124, pp. 507-520.

Zaghi, A. E., and Saiidi, M.S. (2010). “Seismic Design of Pipe-Pin Connections in Concrete Bridges,” Center for Civil Engineering Earthquake Research, Department of Civil and Environmental Engineering, University of Nevada, Reno, NV, Report No. CCEER-10-01, January.

6.7 Appendix

Photographs of different strain measuring devices for mechanical bar splices are presented in Figure 6.8.



(a) Device with dial indicators (California Test 670)



(b) Device with extensometer (Haber et al., 2015)



(c) Device with two LVDTs (NCHRP 12-105)



(b) Device with coupler extensometer

Figure 6.8 Different strain measuring devices for mechanical bar splices

7. SUMMARY AND CONCLUSIONS

7.1 Summary

Mechanical bar splices can be used in bridges to connect precast columns to adjacent members. Nevertheless, current seismic codes prohibit the use of bar couplers in the plastic hinge region of columns in high seismic zones. This is because the behavior of couplers is largely unknown at the component level and also when they are used in bridge columns. The main objective of the present study was to establish the behavior of mechanical bar splices suited for bridge columns through experimental and analytical studies. Nine different coupler products were selected for testing, and more than 160 mechanical bar splices were tested to failure under monotonic and cyclic loading. Three bar sizes, No. 5 (16 mm), No. 8 (25 mm), and No. 10 (32 mm), were included in the test matrix. A coupler material model and acceptance criteria were selected from the literature and then the behavior of the nine coupler products was established through experiments. The first-of-its-kind and unified database on the properties of bar couplers was developed and “seismic” and “non-seismic” couplers were identified. Furthermore, more than 240 pushover analyses were performed on bridge columns incorporating couplers, which their behavior was established in the experimental program of the study.

7.2 Conclusions

The following conclusions can be drawn based on the experimental and analytical studies:

- The test data showed that the coupler length, size, and type significantly affect the coupler performance. The general trend was that longer couplers exhibited lower strain capacities compared with shorter couplers. Couplers with higher rigid length factors showed the lowest strain capacities.
- The coupler acceptance criteria and the coupler stress-strain model proposed by Tazarv and Saiidi (2016) were found viable to identify couplers that are suited for bridge columns. These couplers were labeled as seismic couplers.
- The test data showed that monotonic testing is sufficient to establish a coupler behavior using only one parameter, “coupler rigid length factor.” No significant change was seen in the behavior of couplers under monotonic and cyclic loads. Nevertheless, the cyclic loading is needed to verify the coupler performance under simulated seismic actions.
- Consistent results can be achieved using the proposed standard testing method for couplers.
- The parametric study showed that the size, type, and length of couplers can significantly affect the ductility of bridge columns. Longer couplers and couplers with higher rigid length factors may reduce the column displacement ductility capacity by 43%.
- The analytical study showed that the lateral load carrying capacity of mechanically spliced bridge columns are slightly higher than that for conventional RC columns (no more than 10%).

APPENDIX A. CALTRANS AUTHORIZED LIST OF COUPLERS

A current list of mechanical bar splices authorized by Caltrans (not for use in plastic hinge regions of bridge columns but in non-critical sections and members) can be found at:

http://www.dot.ca.gov/hq/esc/approved_products_list/pdf/steel_reinforcing_couplers_backup.pdf